nature metabolism

Article

https://doi.org/10.1038/s42255-023-00803-0

# SIRT2 regulates extracellular vesicle-mediated liver–bone communication

In the format provided by the authors and unedited

**Figure.1a** Western blot analysis of SIRT2 protein expression in primary hepatocytes of aged female and male mice

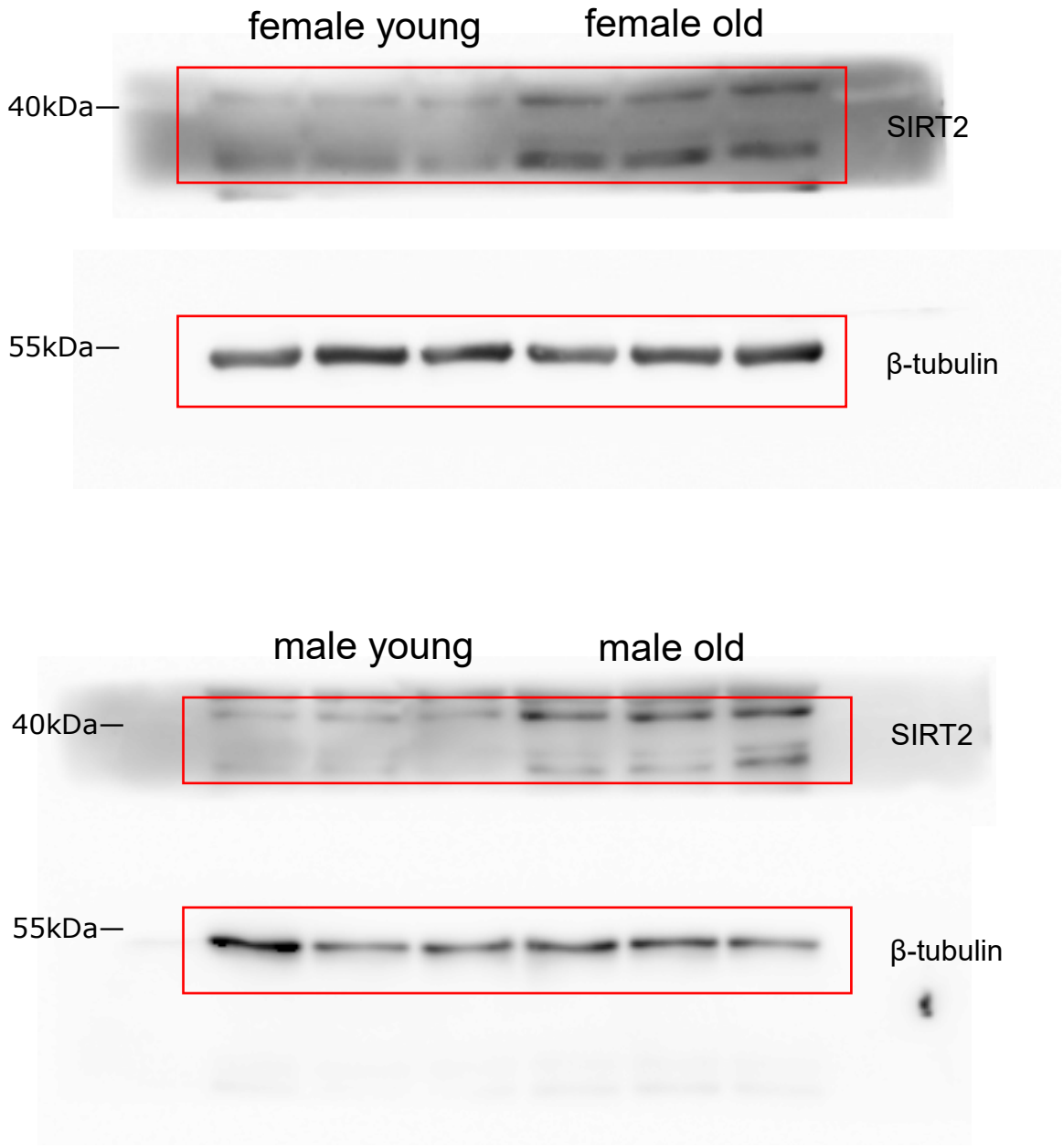

**Figure.1c** IHC images of SIRT2 protein expression in liver tissues from young and aged mice

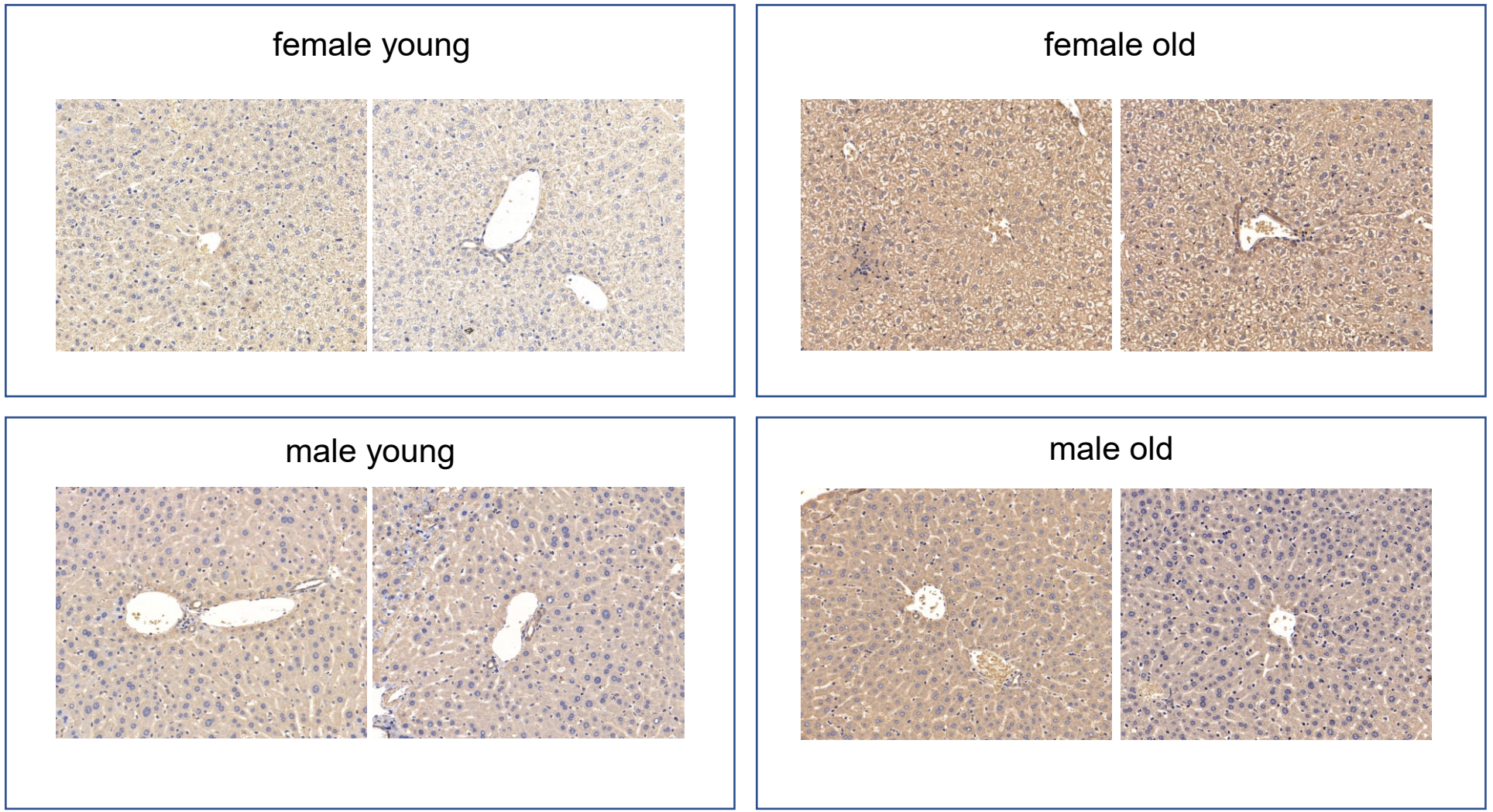

**Figure.1e**

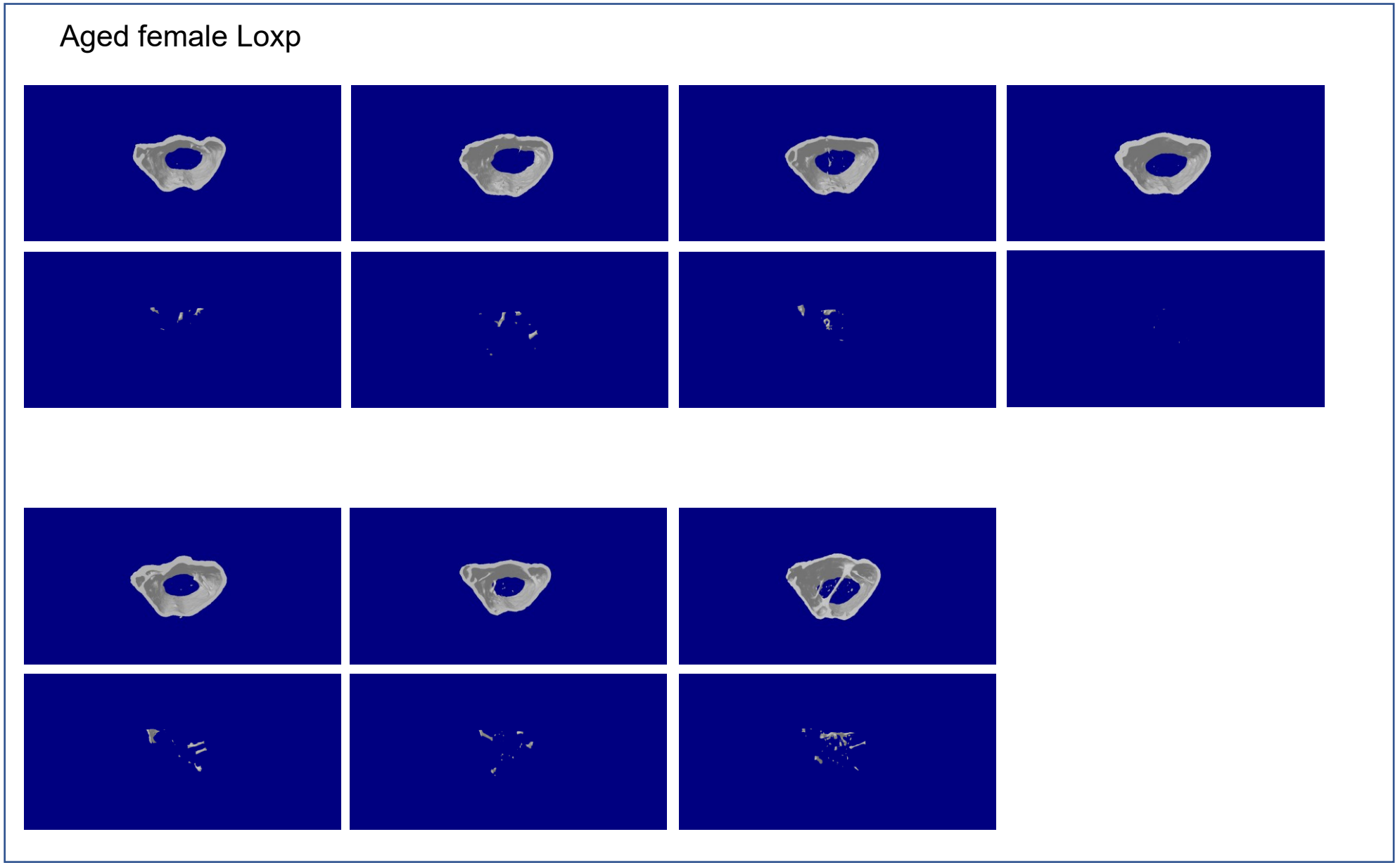

**Figure.1e**

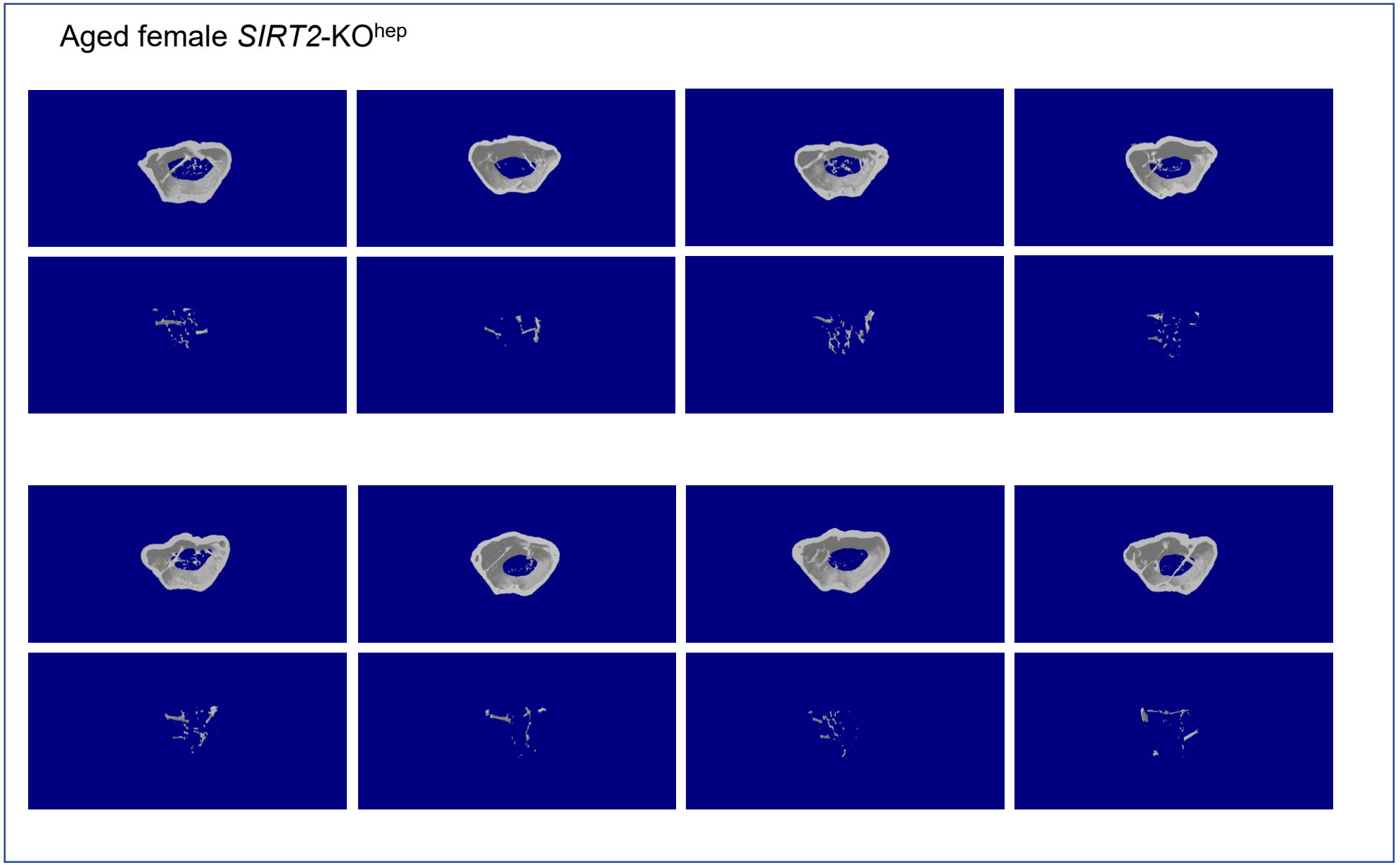

**Figure.1g**

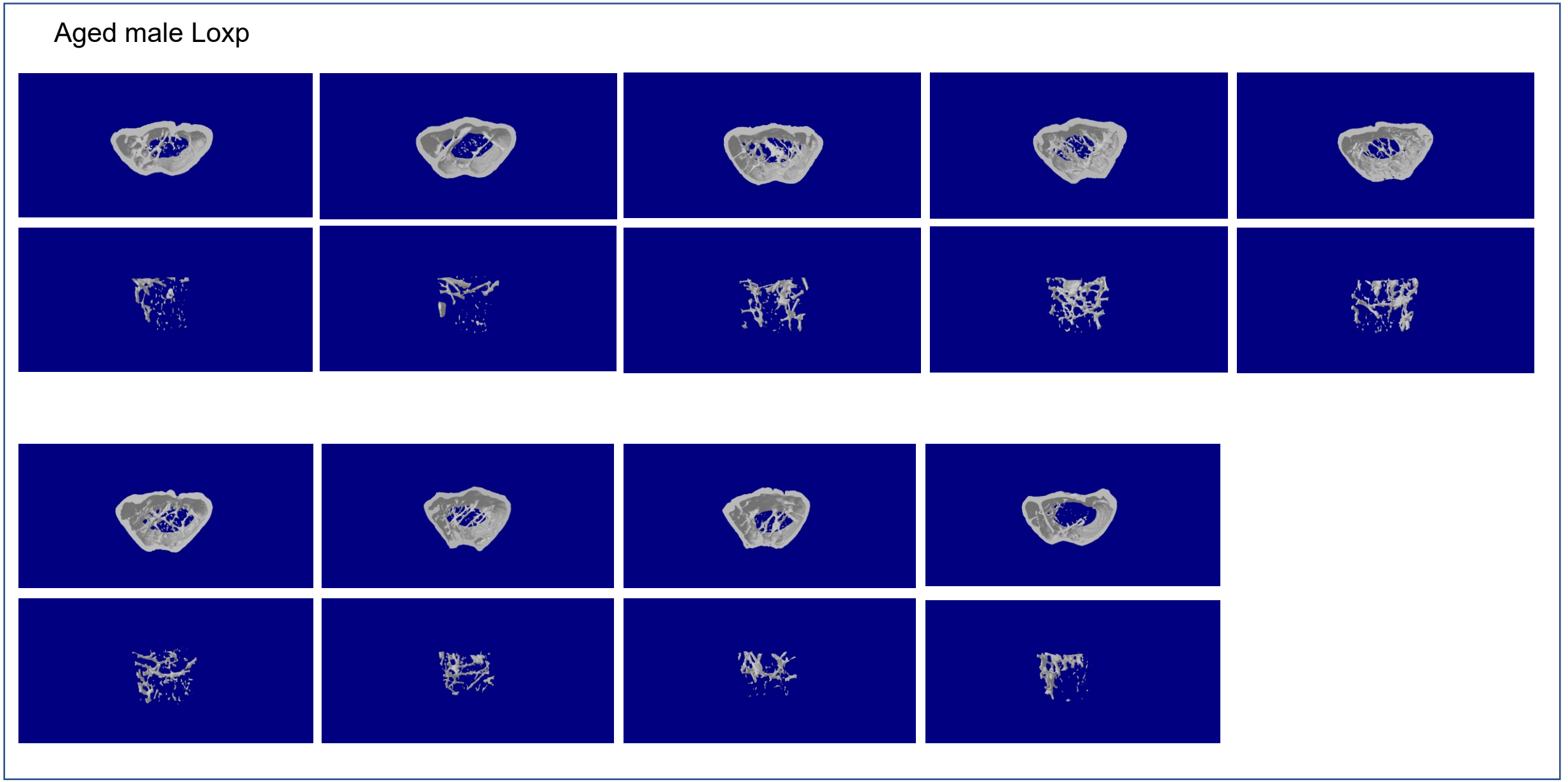

**Figure.1g**

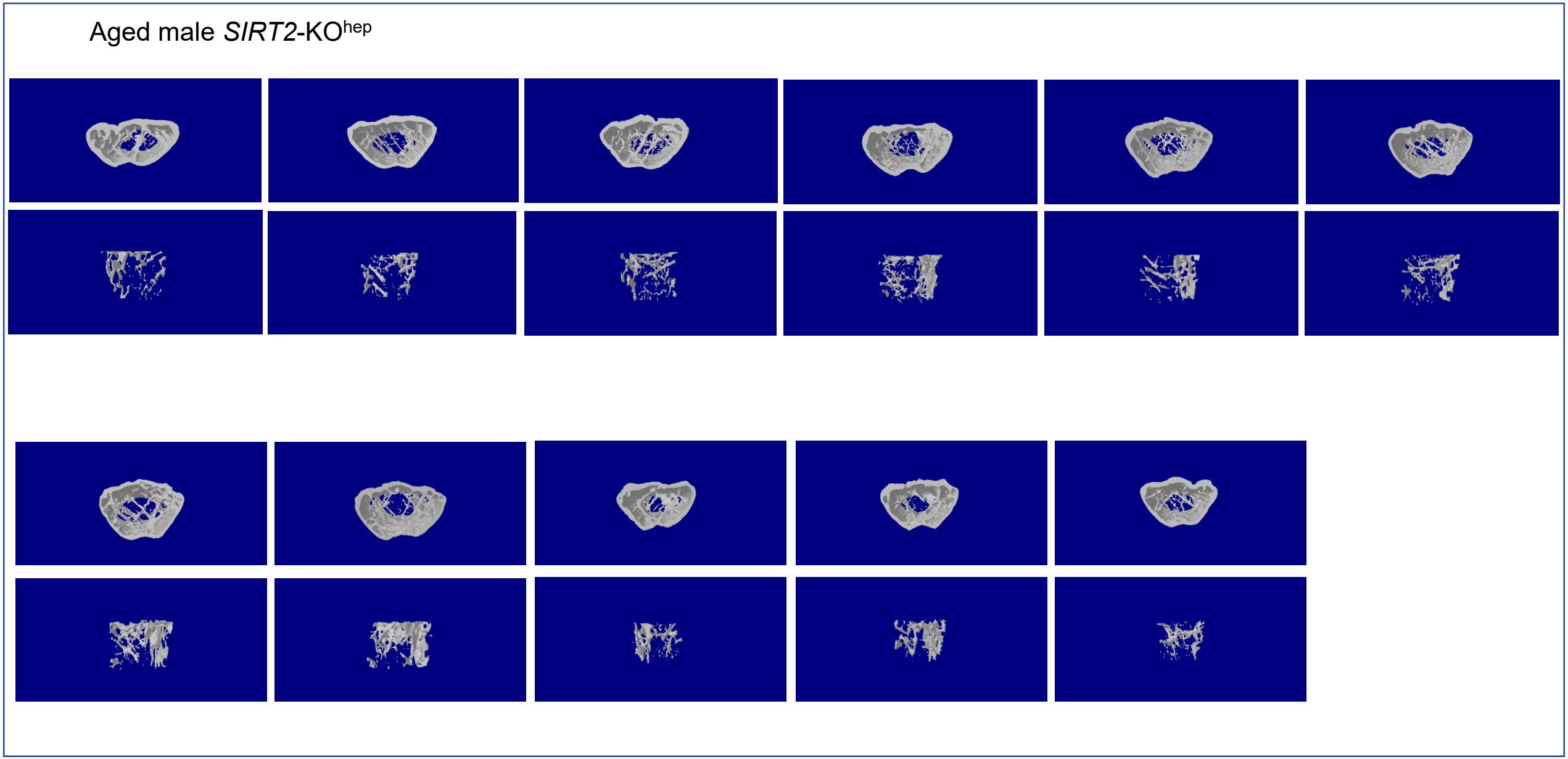

**Figure.1k** TRAP staining on paraffin-embedded femur sections in aged mice

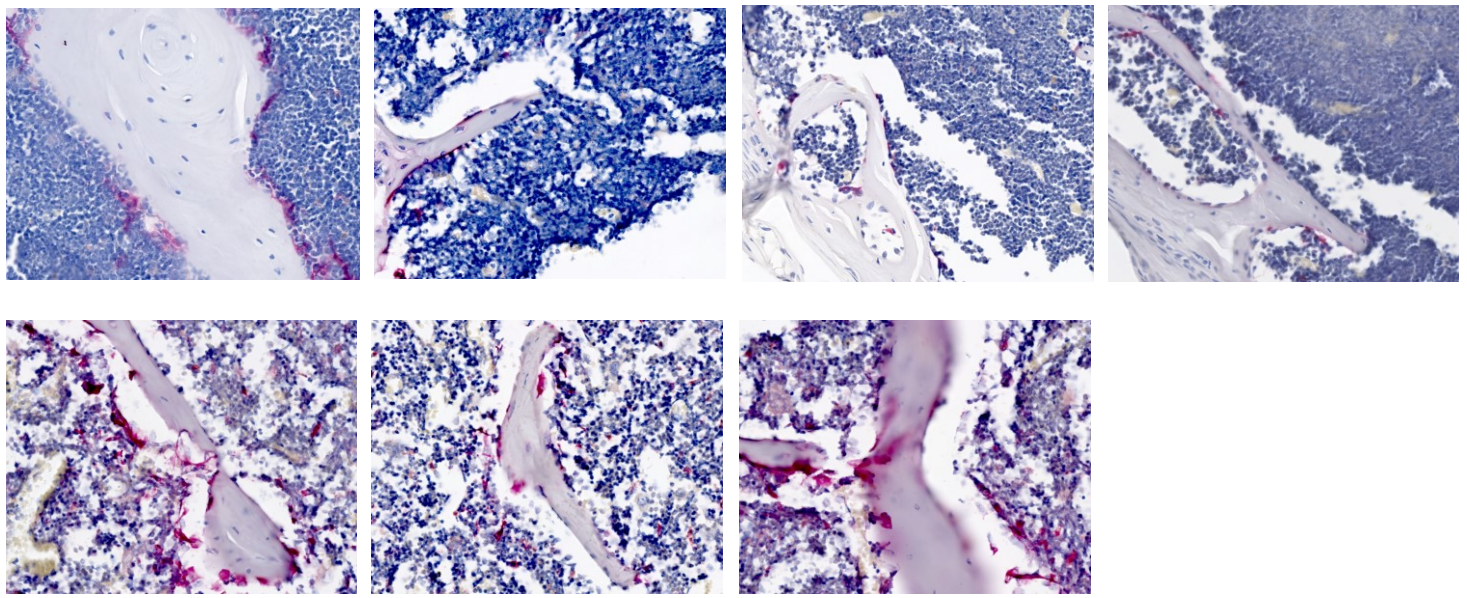


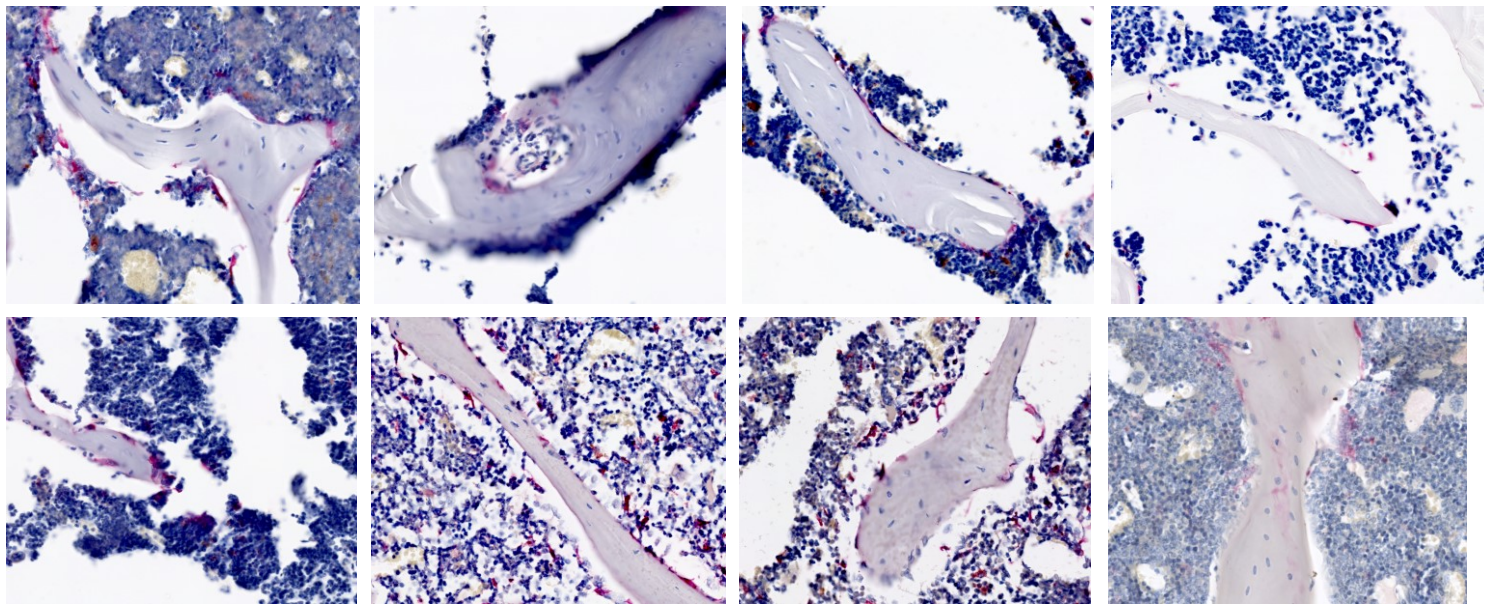

**Figure.1m** TRAP staining on paraffin-embedded femur sections in aged mice

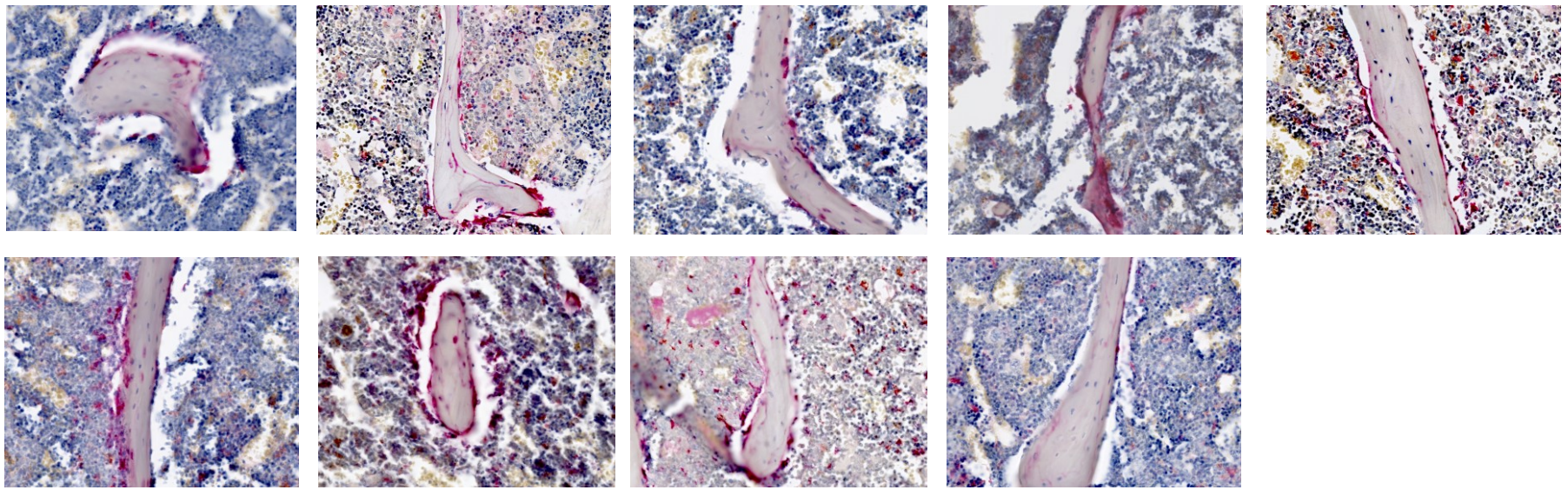


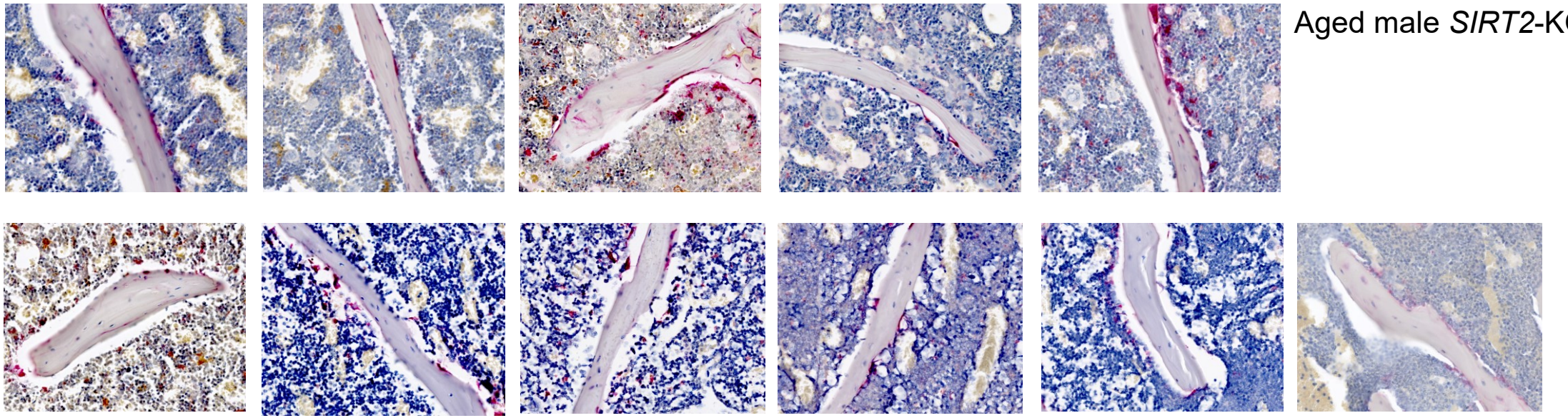

**Figure.2a** TRAP staining images of osteoclasts administered with the plasma of aged mice

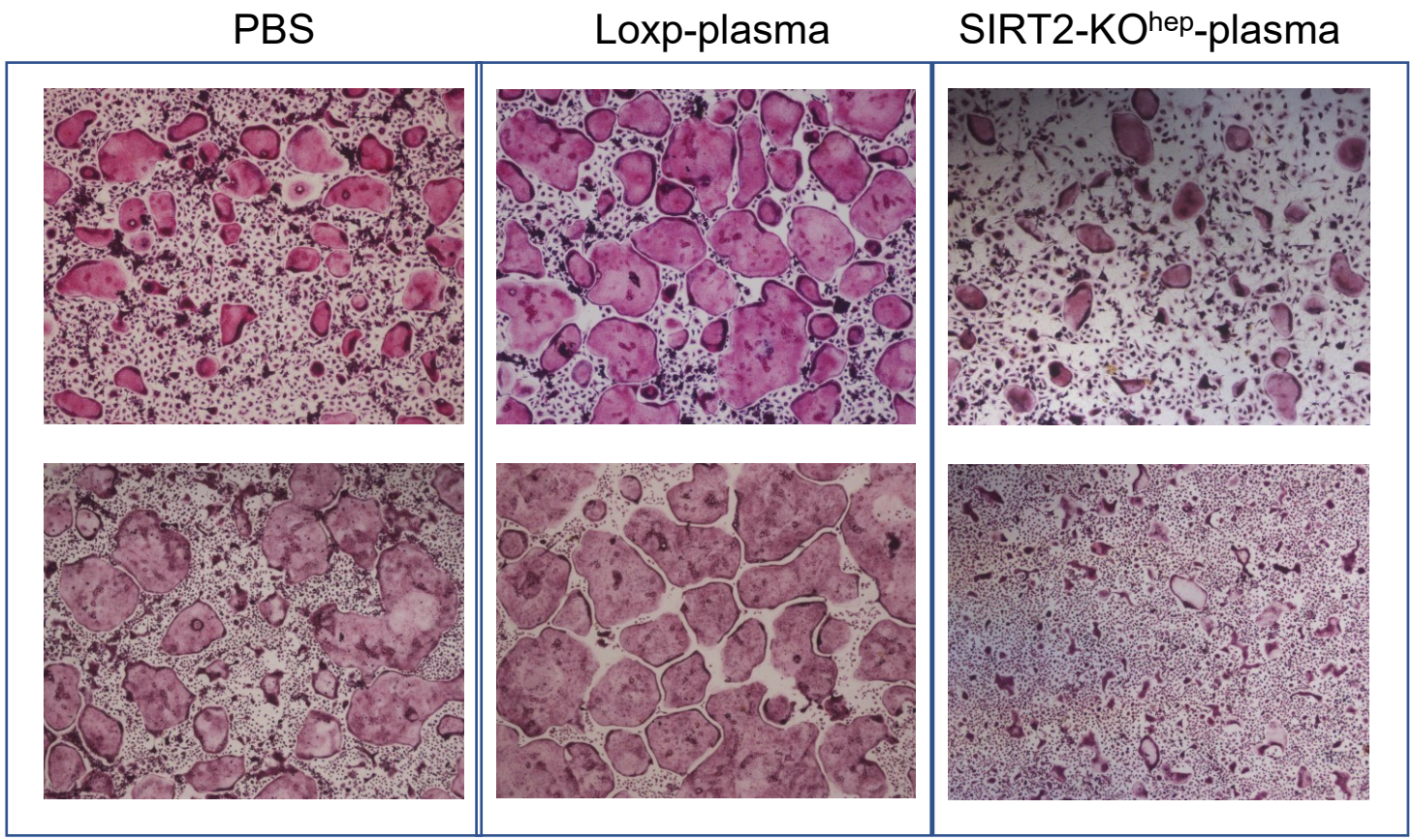

**Figure.2e** TRAP staining images of osteoclasts treated with the sEVs derived from LoxP or SIRT2-KOhep plasma

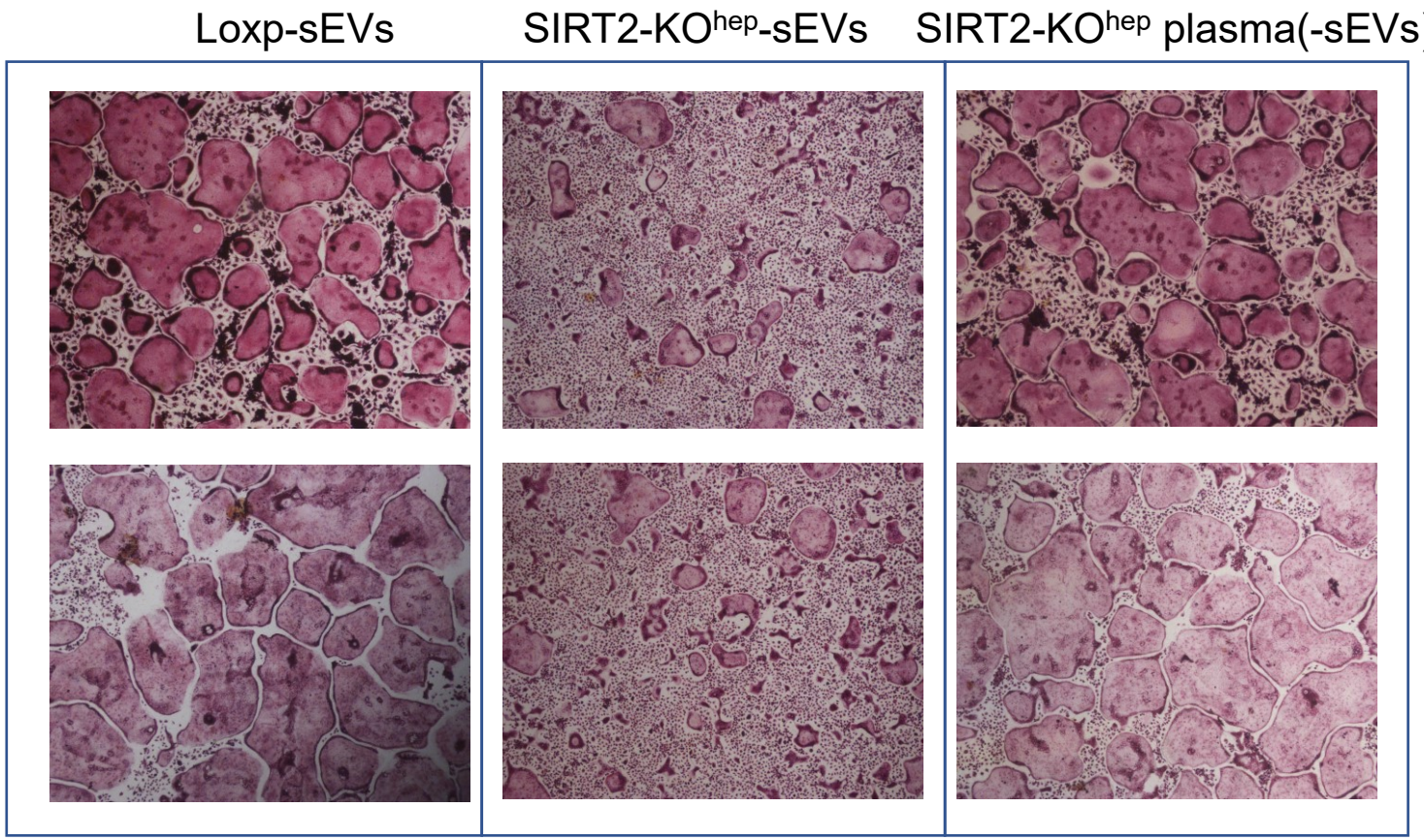

**Figure.2i** TRAP staining of osteoclasts treated with sEVs derived from the medium of the primary hepatocytes of aged female mice

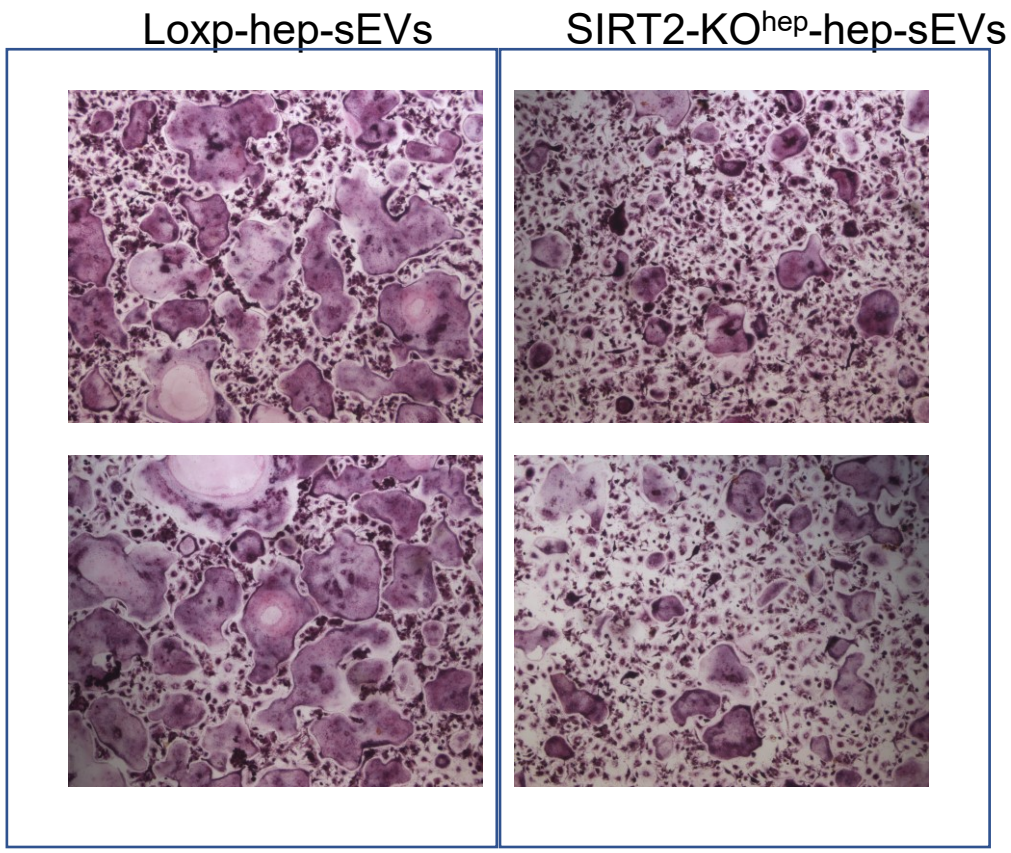

**Figure.2l** TRAP staining of osteoclasts treated with sEVs derived from the medium of the primary hepatocytes of aged male mice

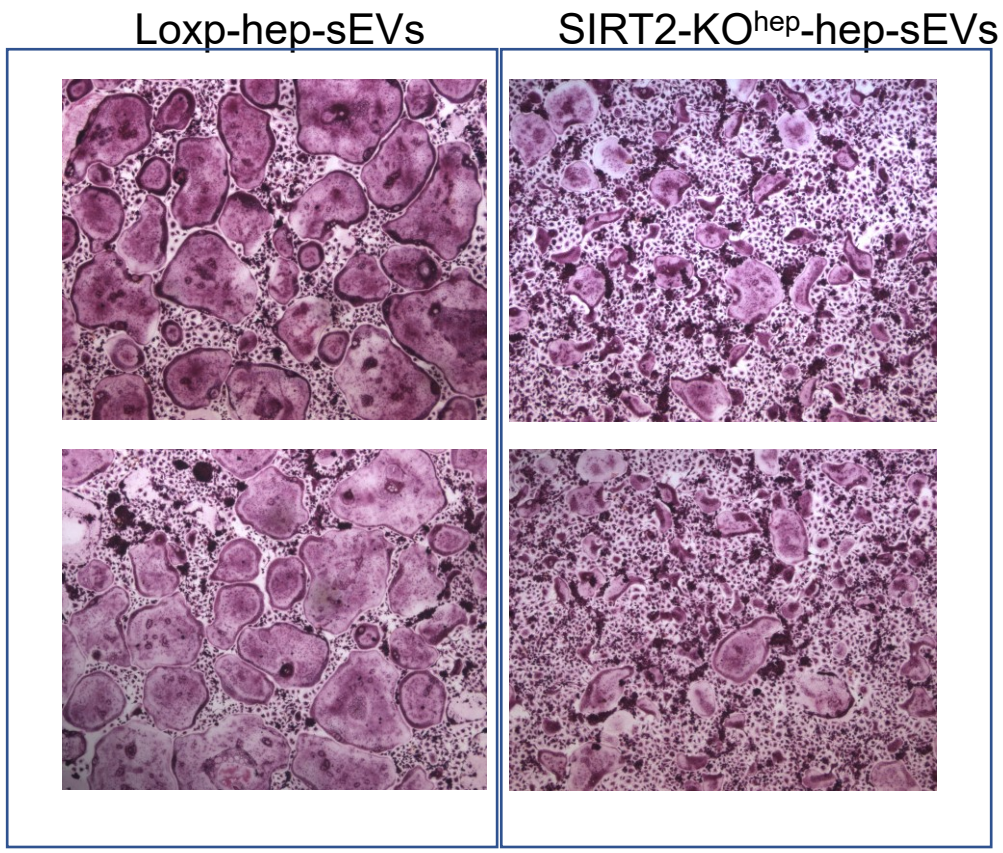

**Figure.3e** immunofluorescence images of murine femurs in aged mice

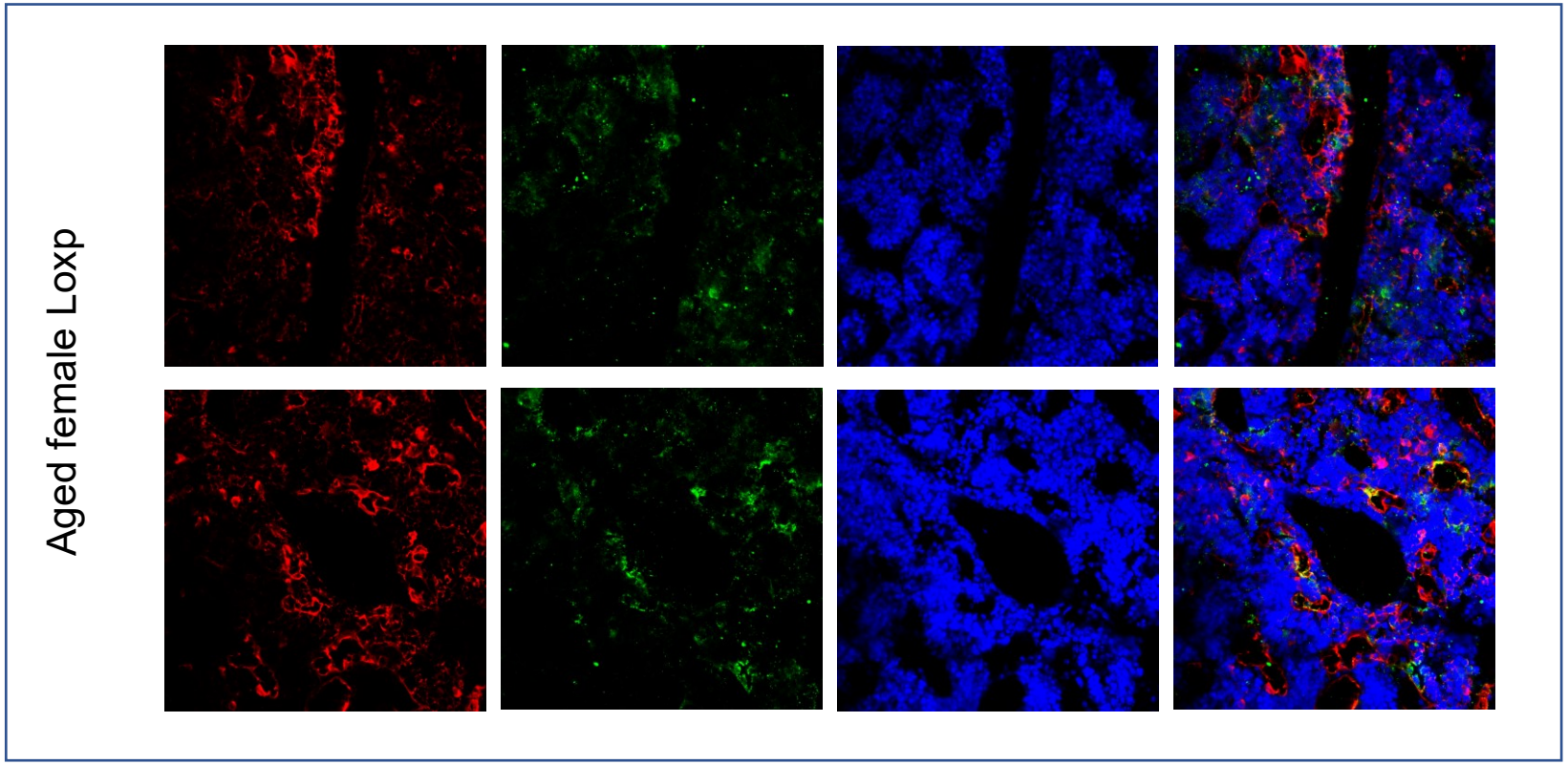

**Figure.3e** immunofluorescence images of murine femurs in aged mice

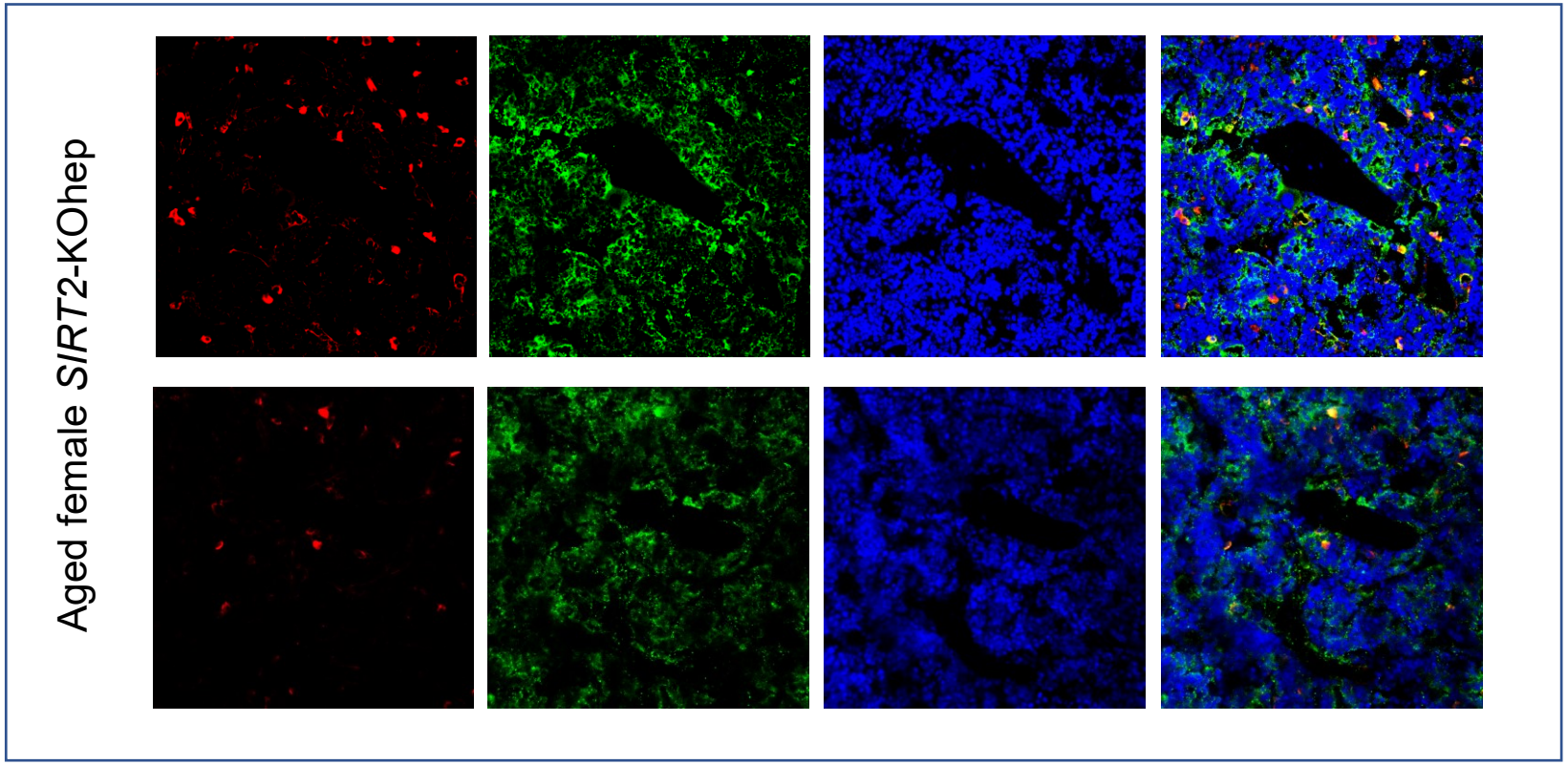

**Figure.3g** immunofluorescence images of murine femurs in aged mice

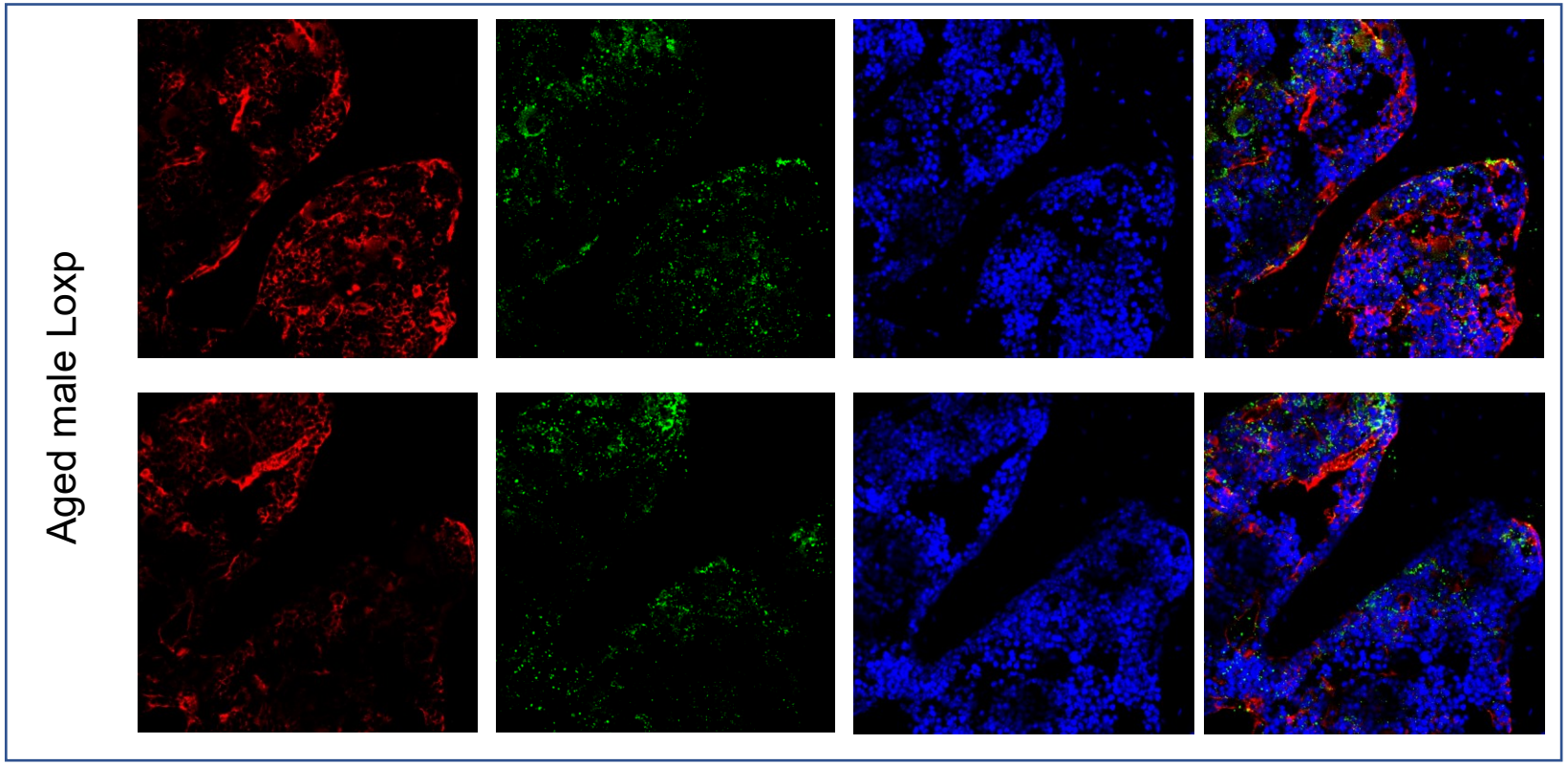

**Figure.3g** immunofluorescence images of murine femurs in aged mice

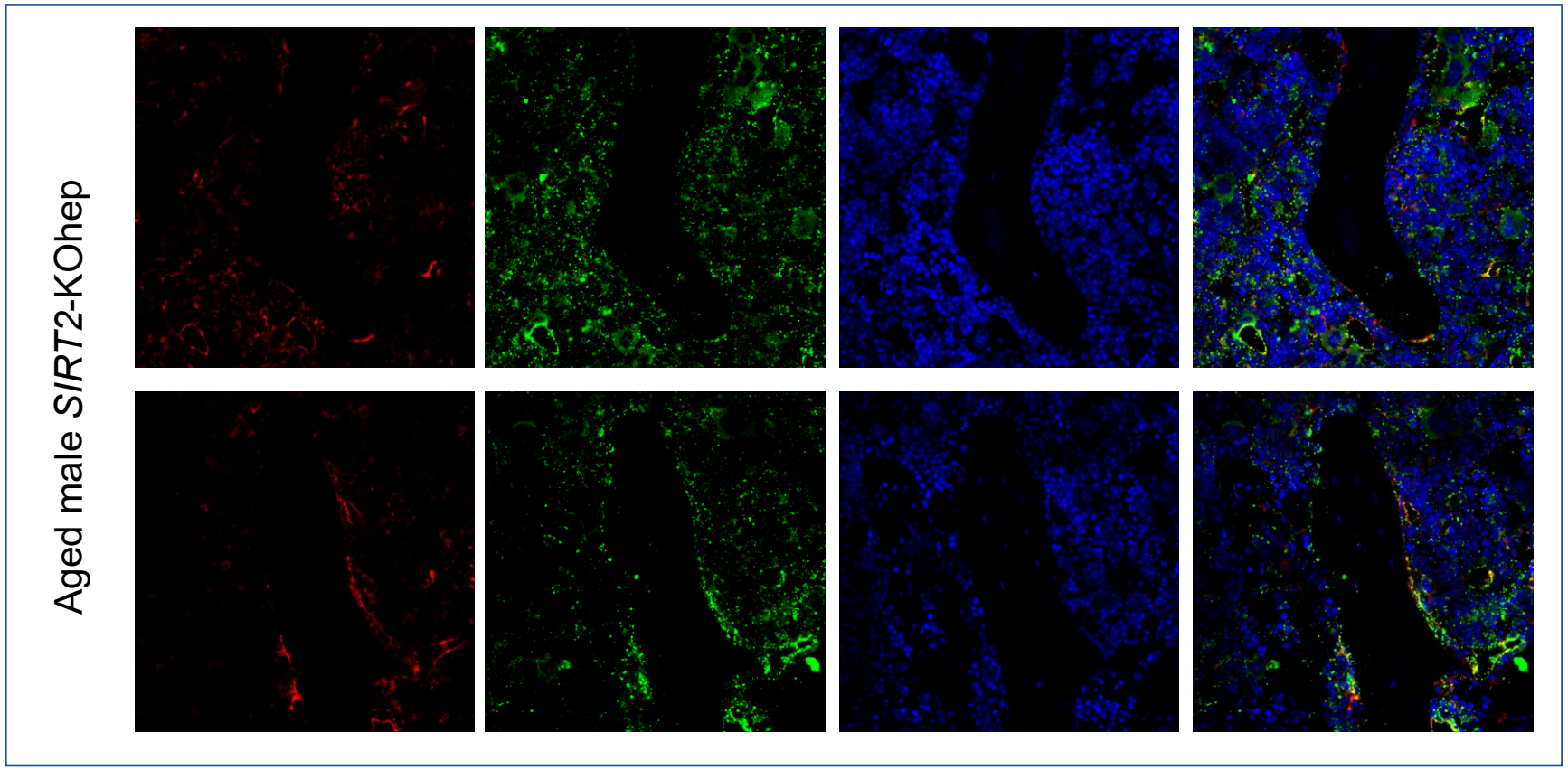

Figure.3m

sham Loxp-ctrl

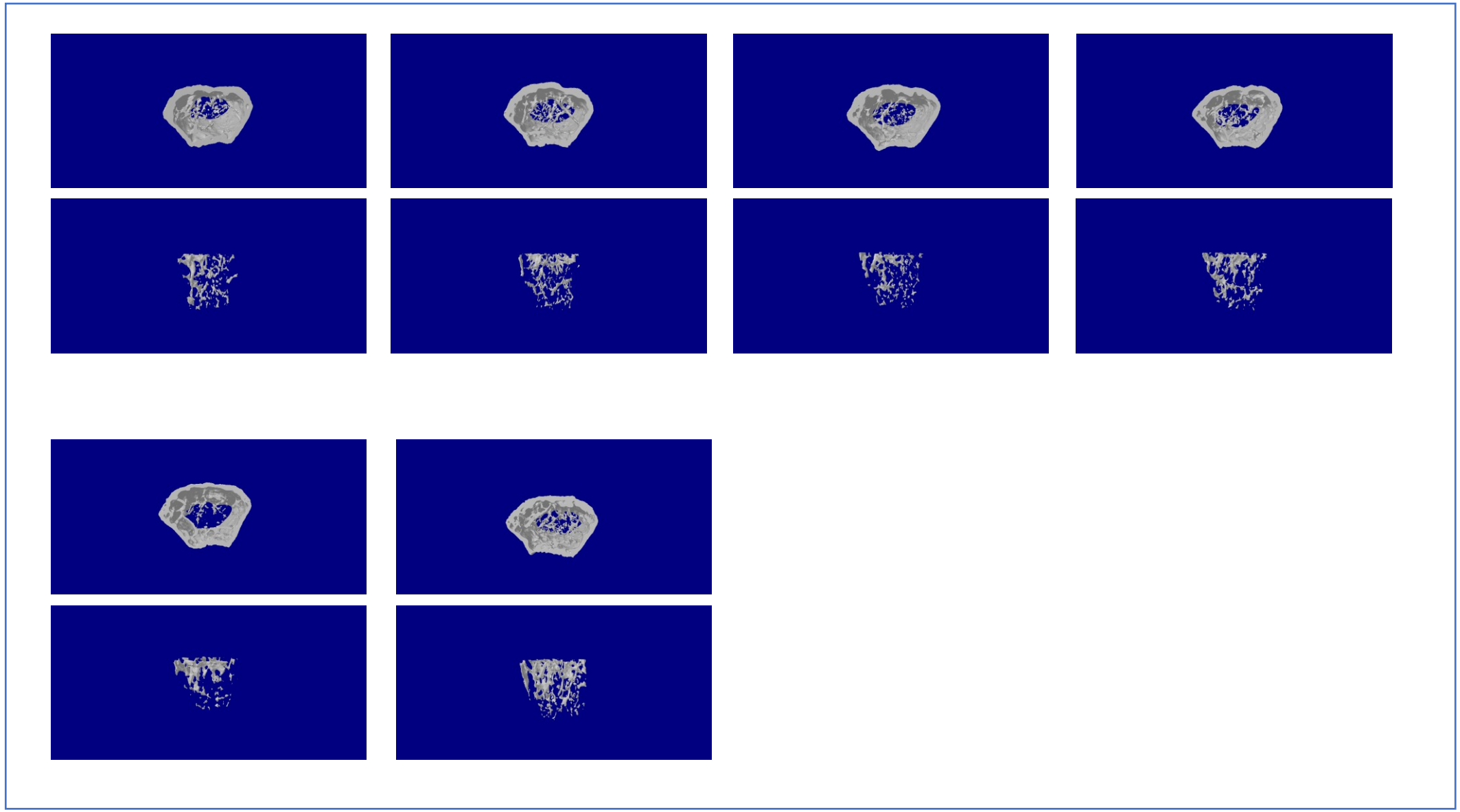

Figure.3m

sham SIRT2-KO$^{hep}$-ctrl

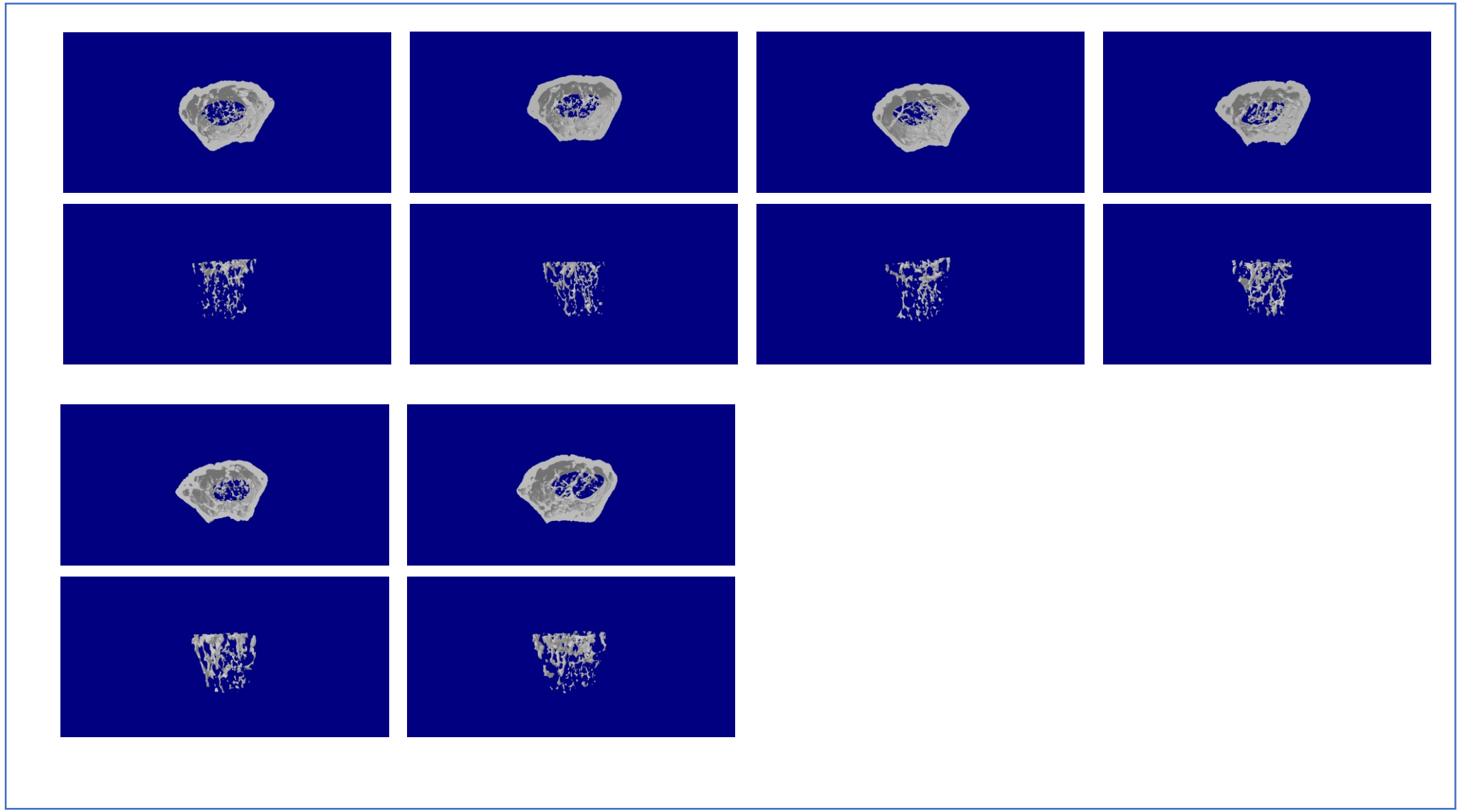

Figure.3m

OVX Loxp-ctrl

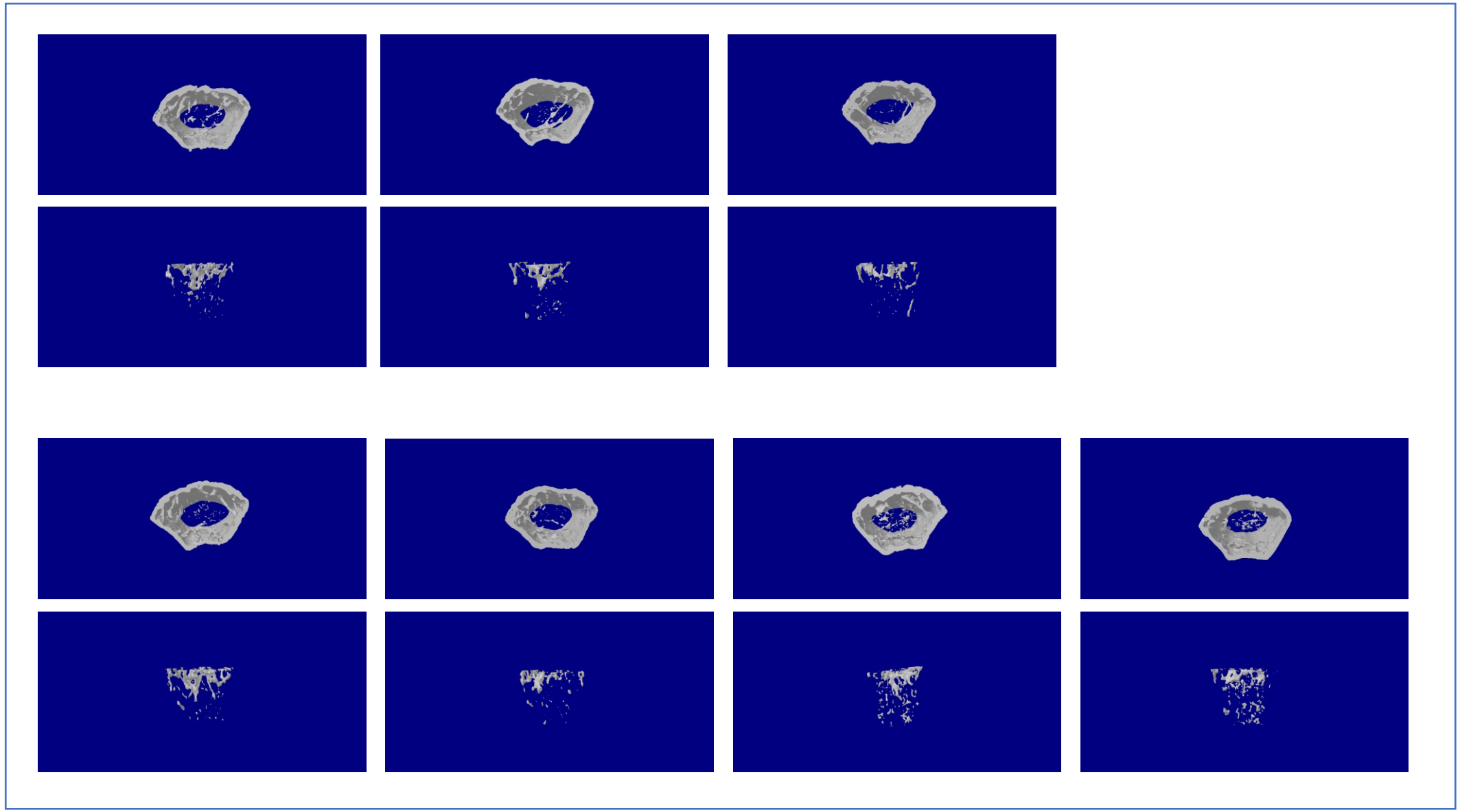

Figure.3m

## OVX SIRT2-KO$^{hep}$-ctrl

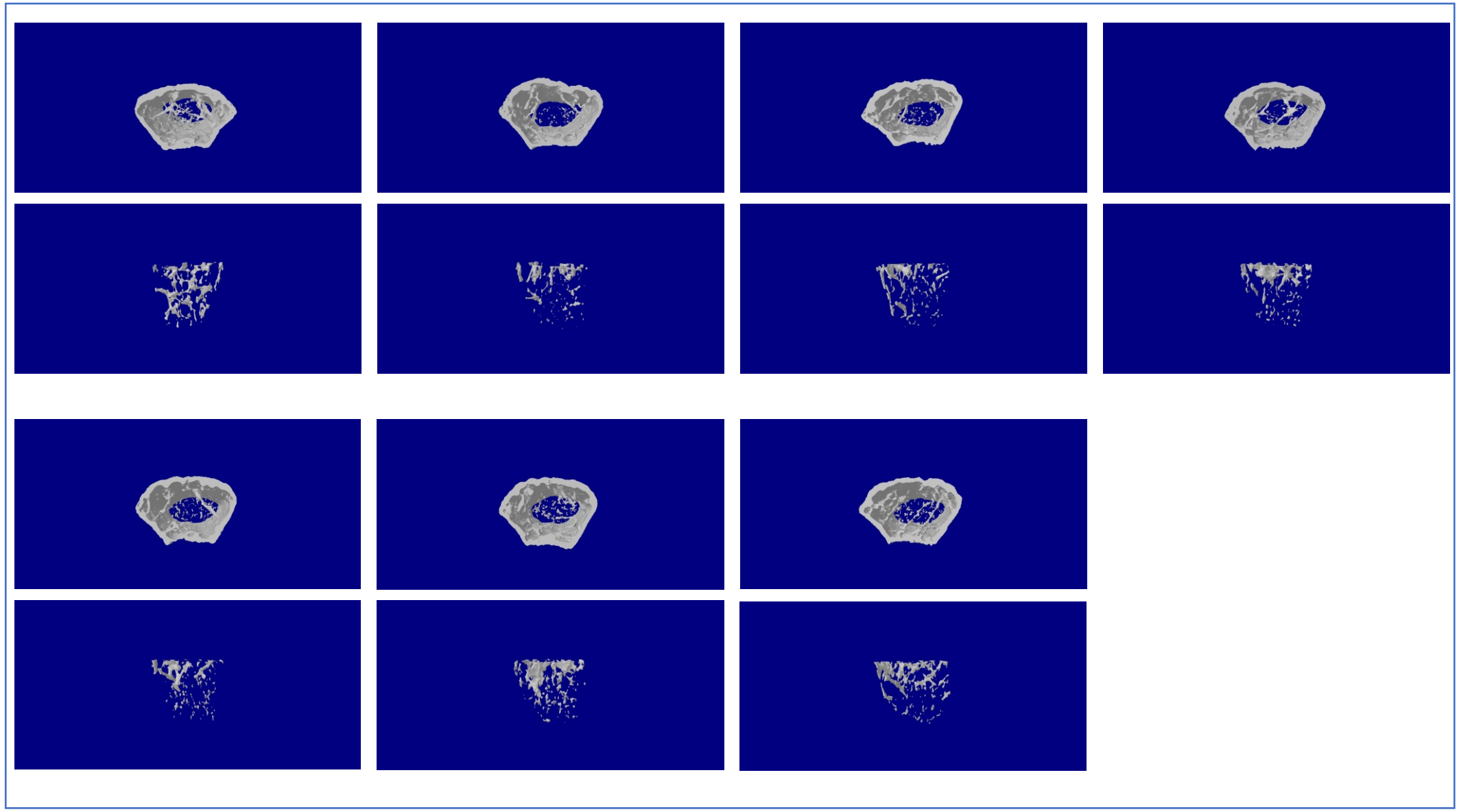

Figure.3m

OVX SIRT2-KO$^{hep}$-shLRG1

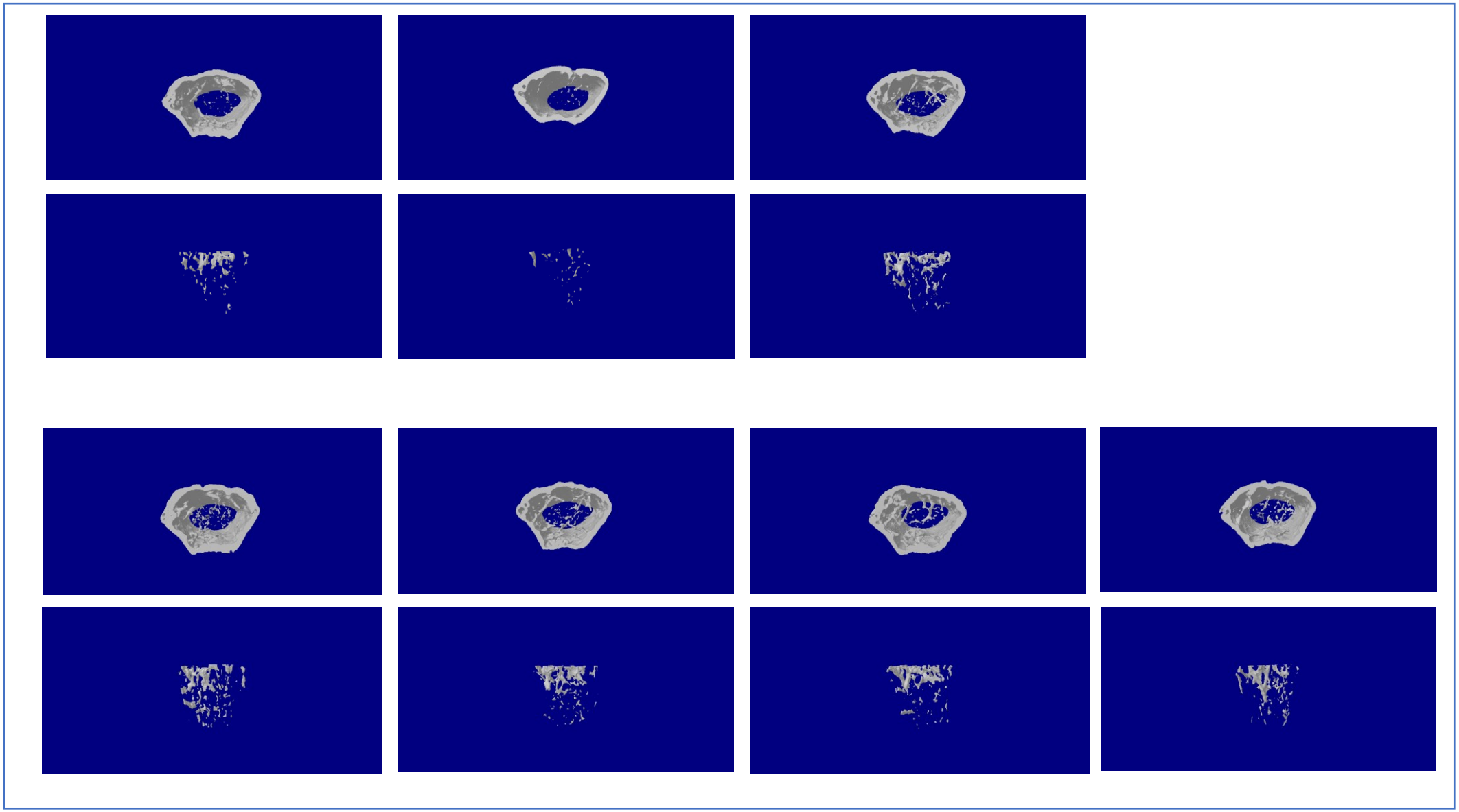

**Figure.4b** TRAP staining of osteoclasts treated with sEVs from AML-12 cells

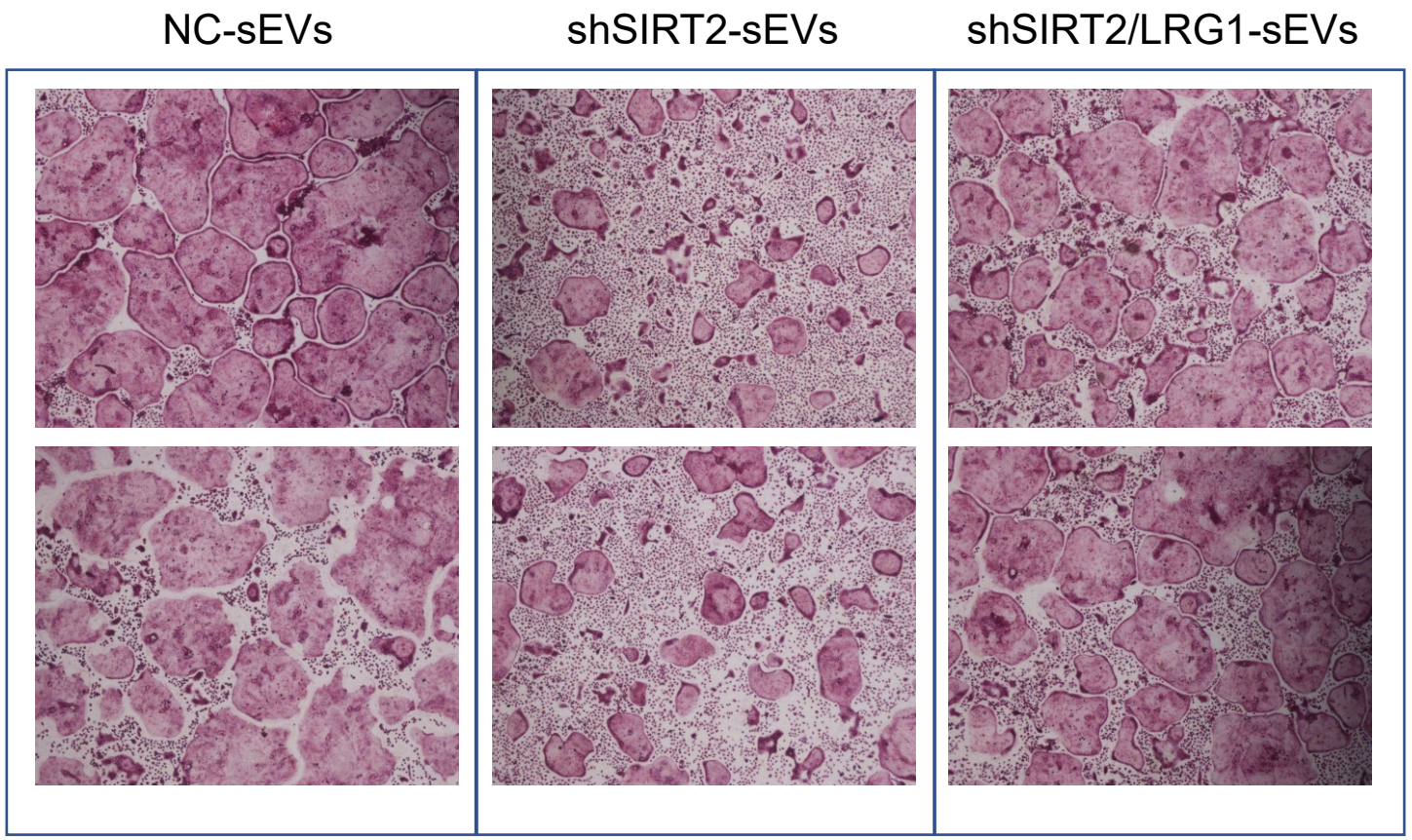

Figure.4h

sham NC-sEVs

Figure.4h

OVX NC-sEVs

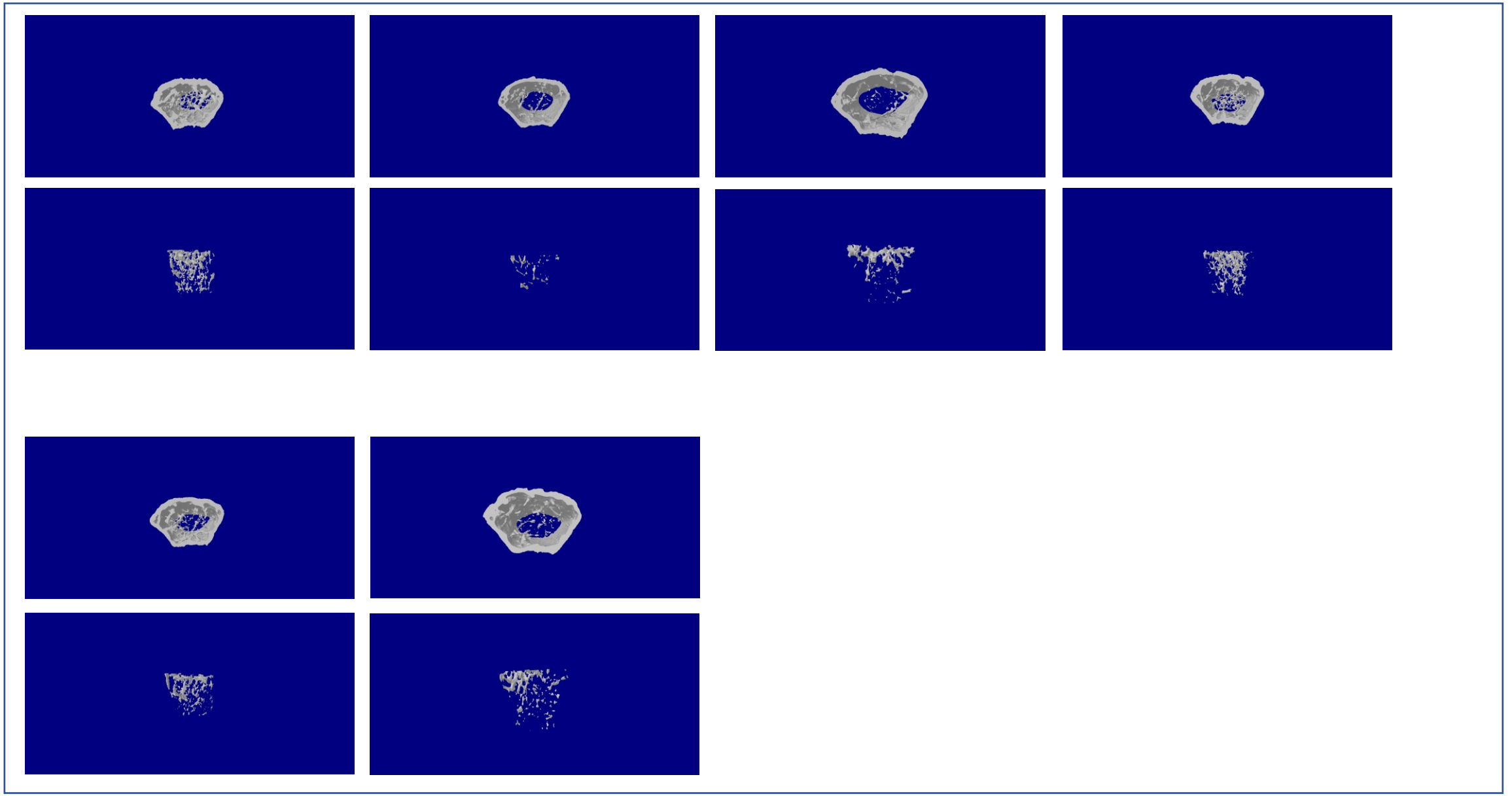

Figure.4h

OVX shSIRT2-sEVs

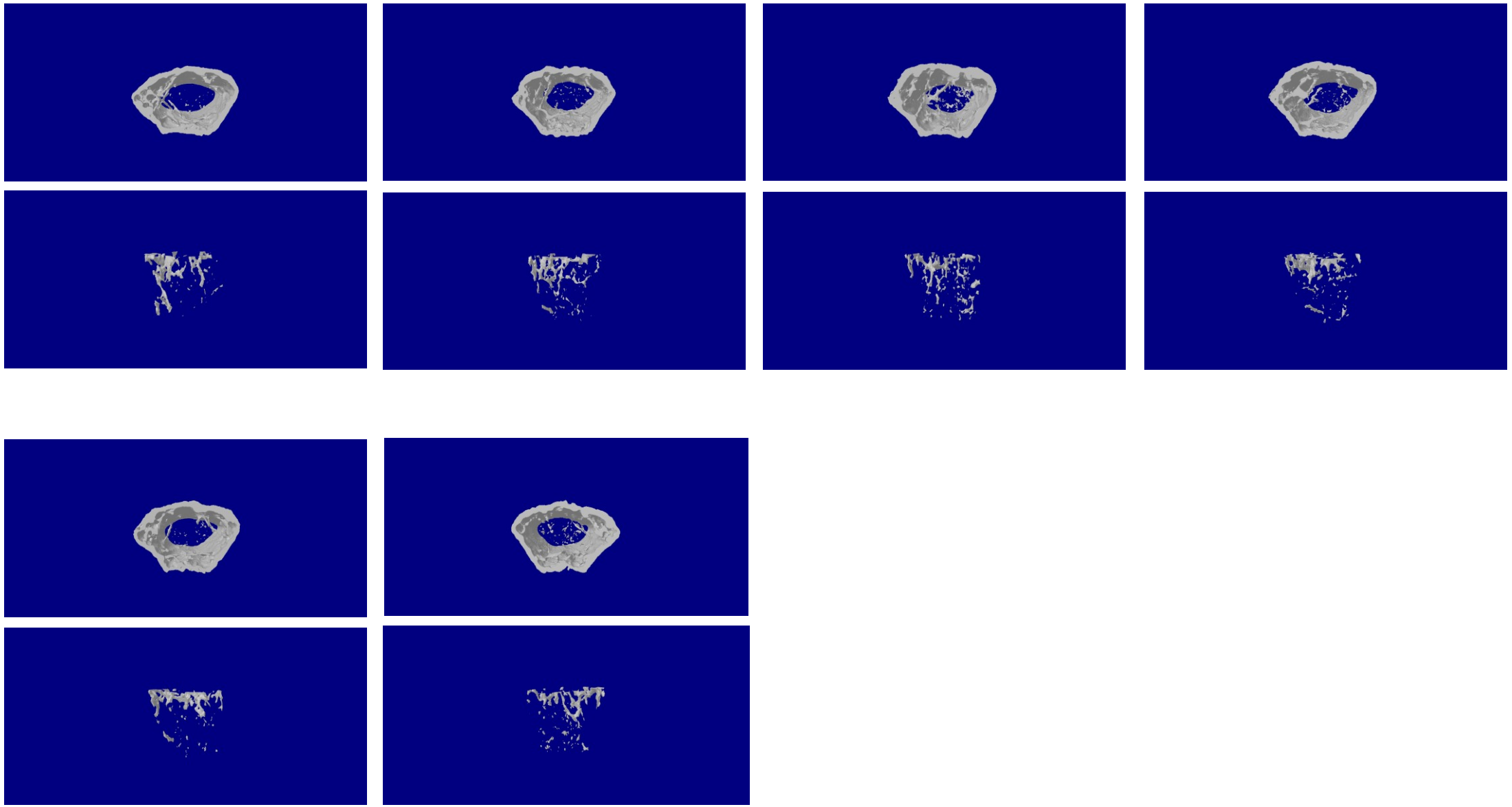

Figure.4h

OVX shSIRT2-shLRG1-sEVs

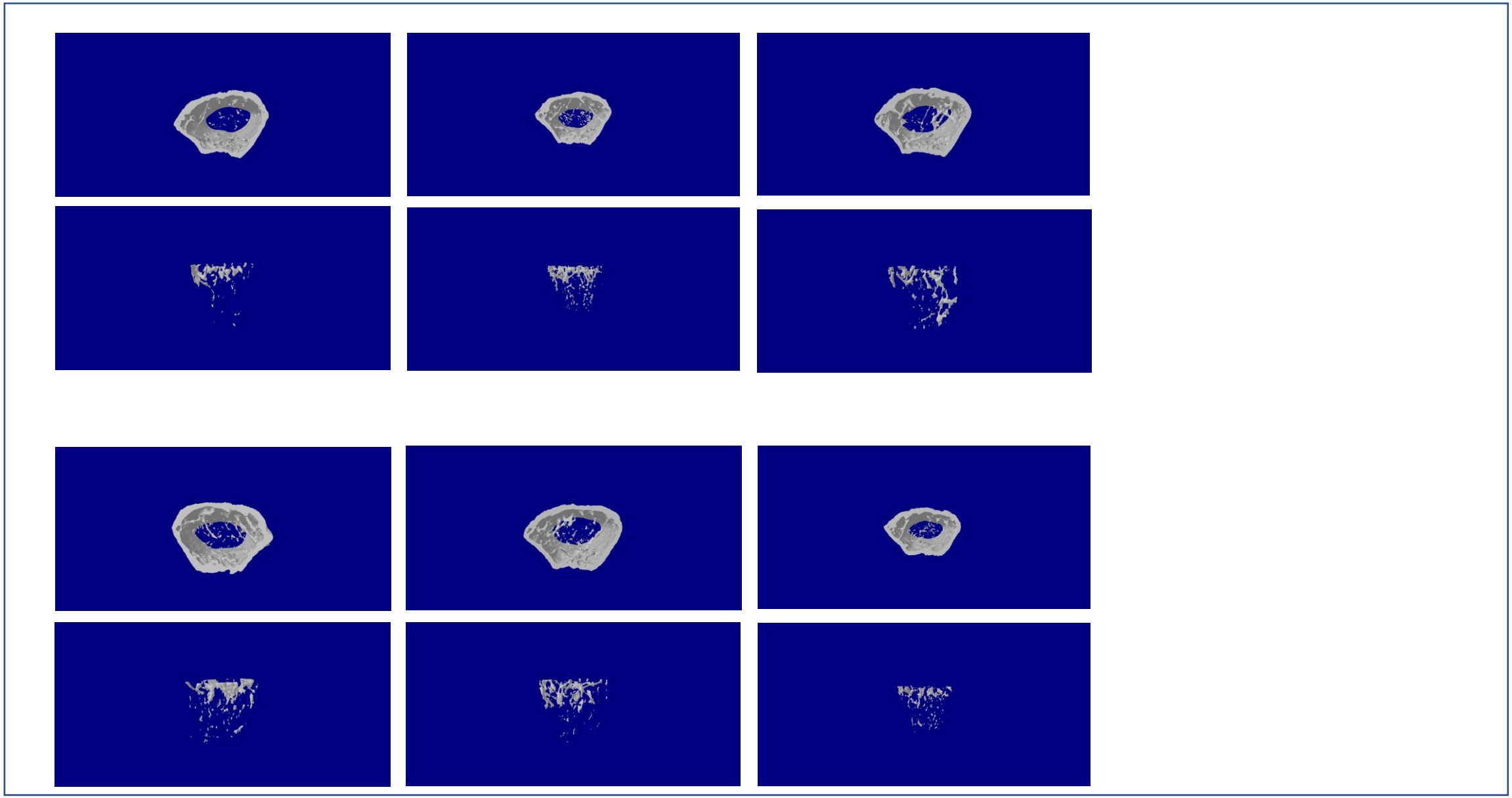

Figure.4h

OVX LRG1-sEVs

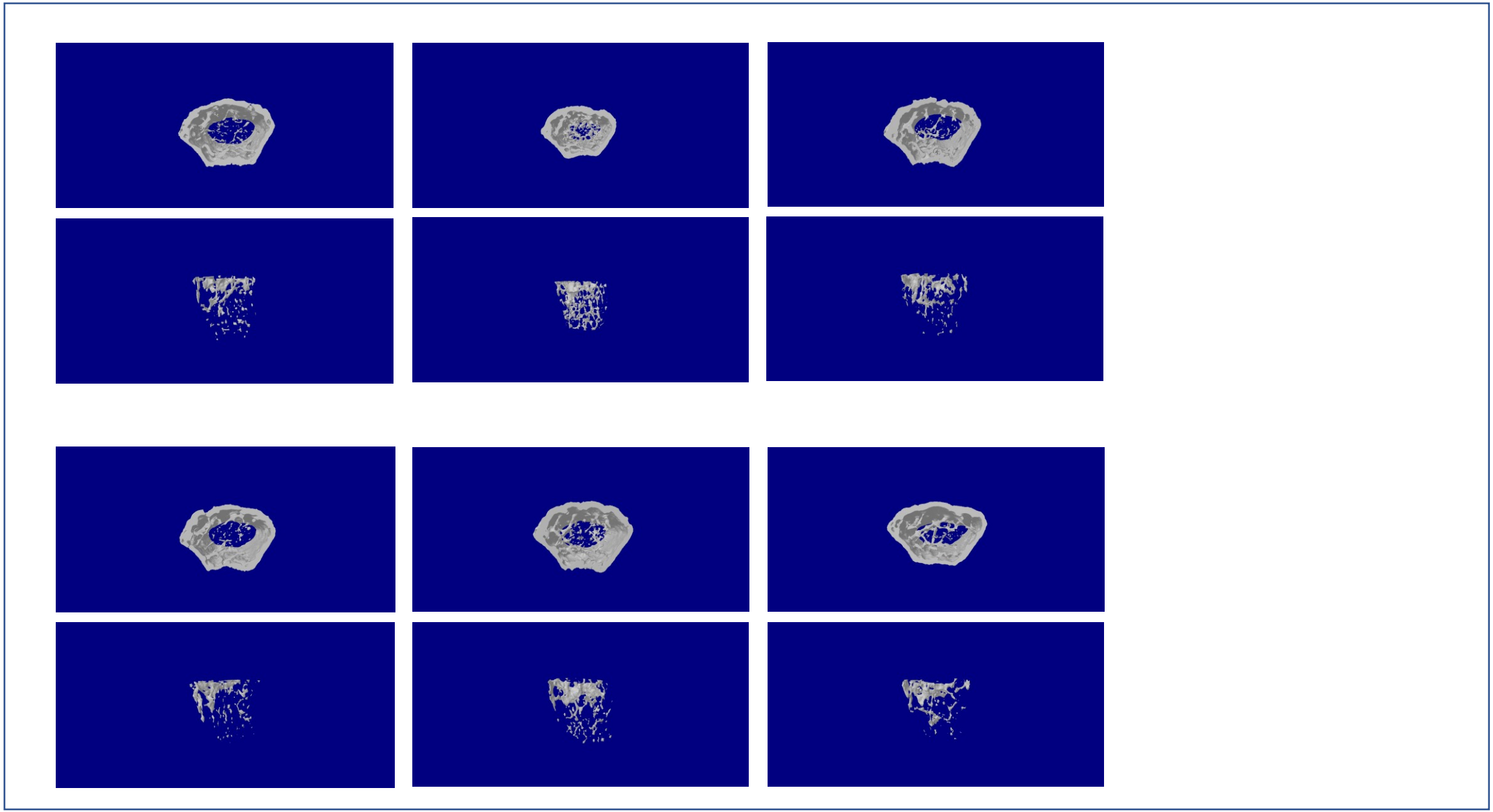

**Figure.4k** TRAP staining on paraffin-embedded femur sections in each group after corresponding sEVs treatment

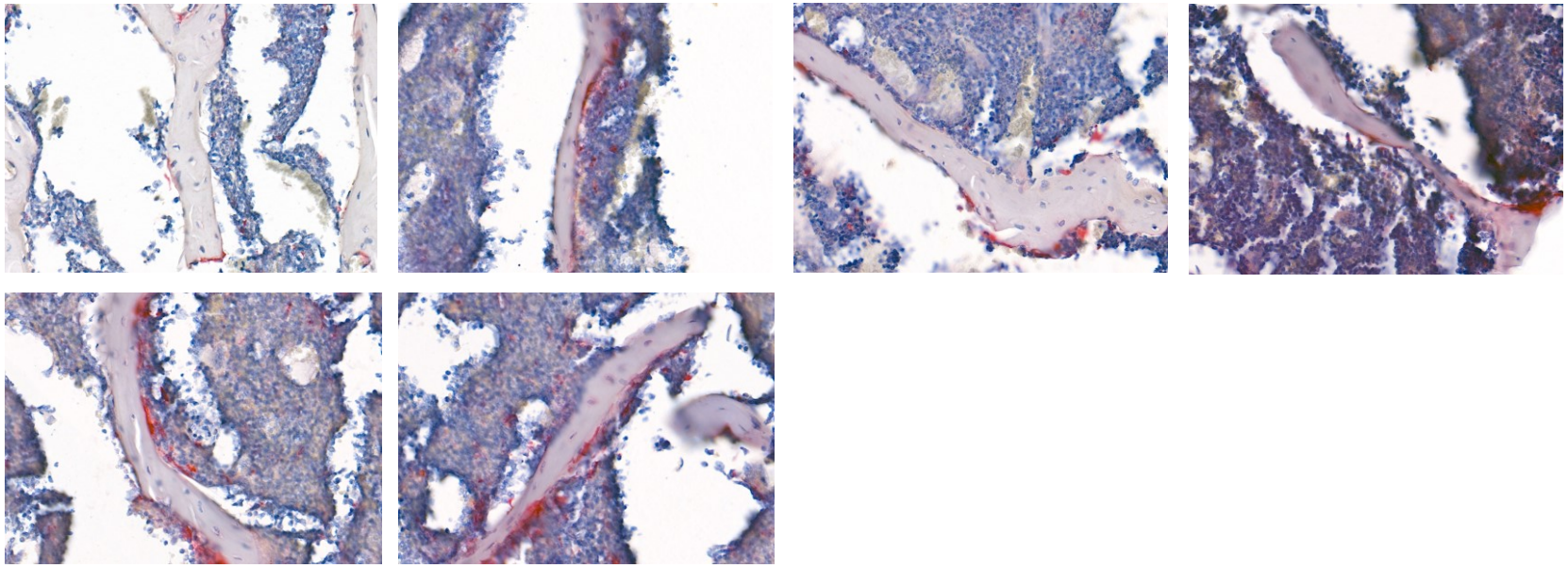


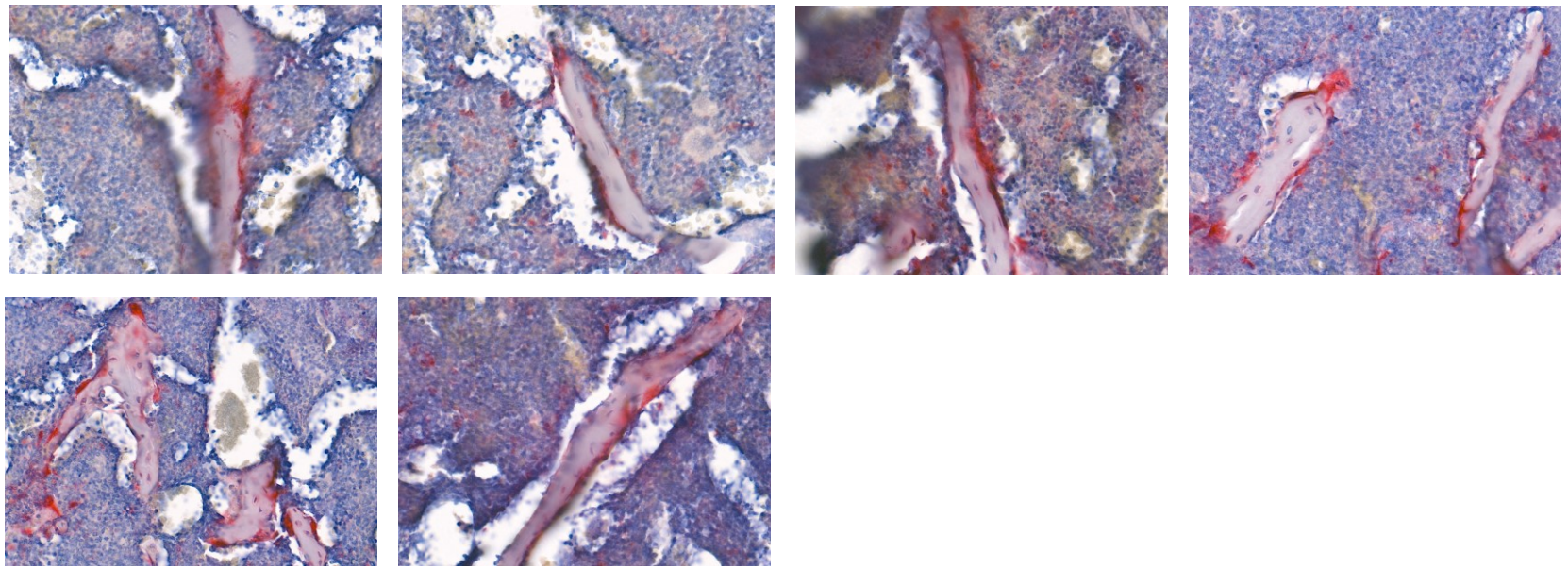

**Figure.4k** TRAP staining on paraffin-embedded femur sections in each group after corresponding sEVs treatment

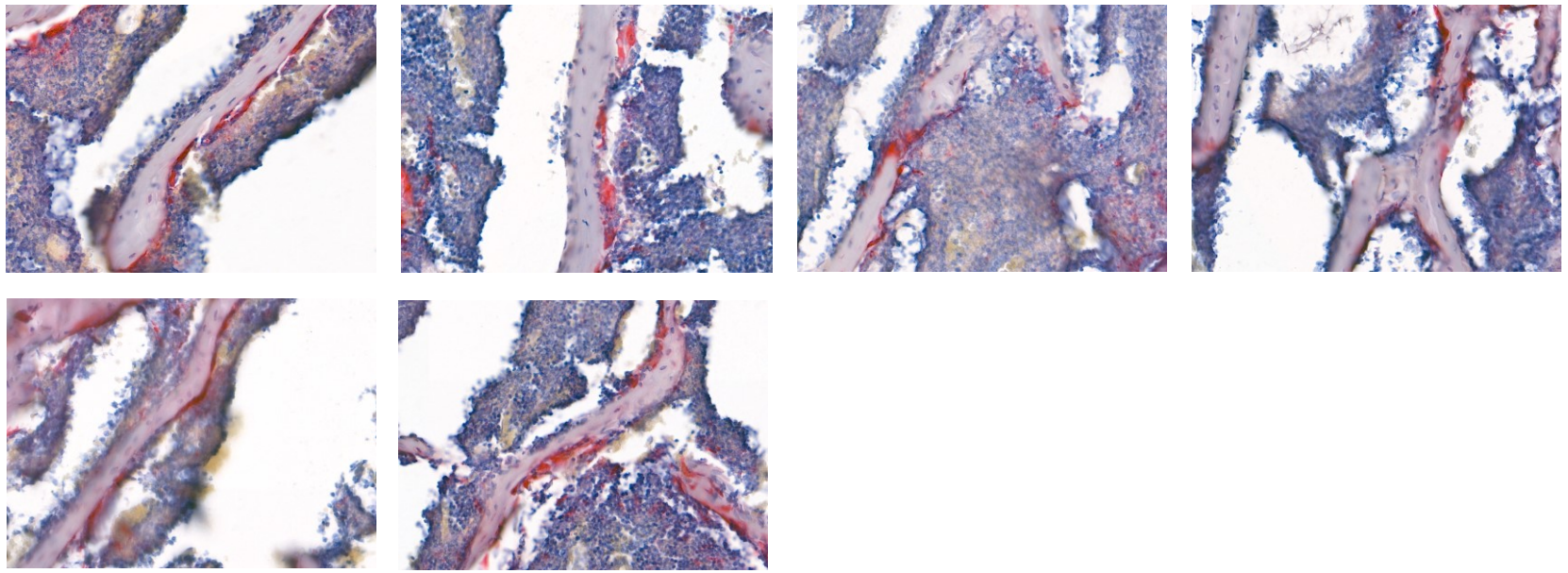


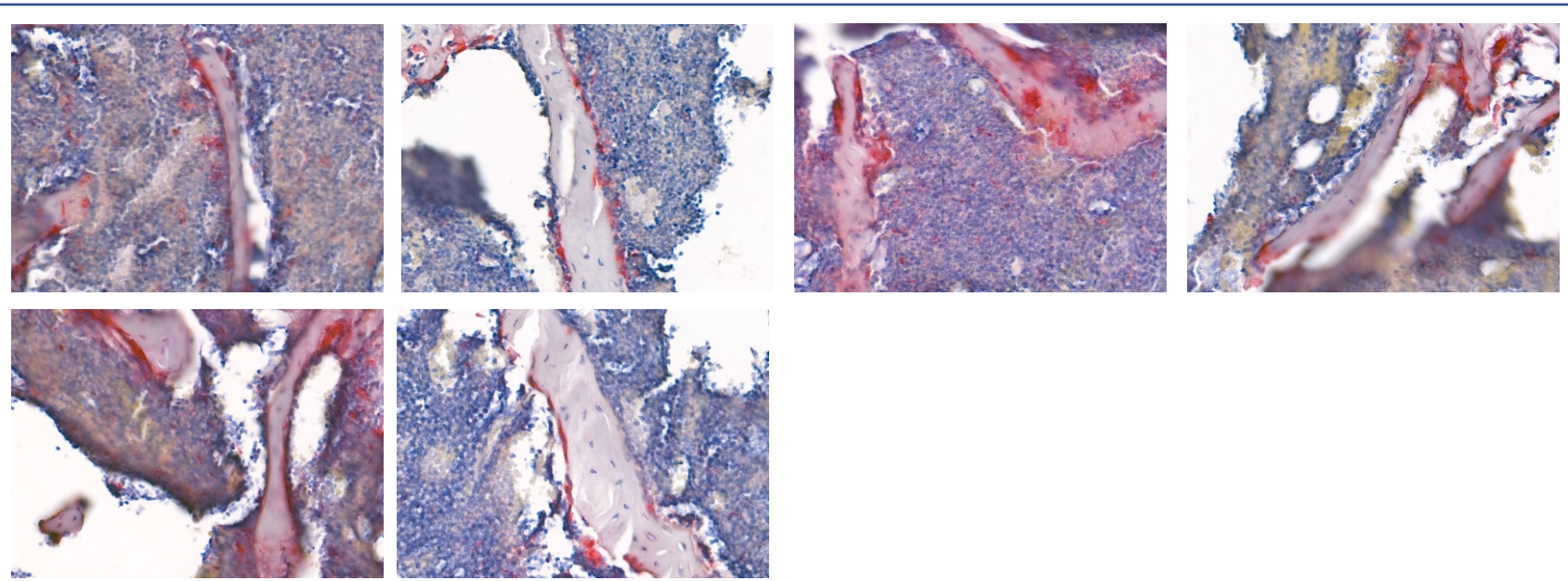

**Figure.4k** TRAP staining on paraffin-embedded femur sections in each group after corresponding sEVs treatment

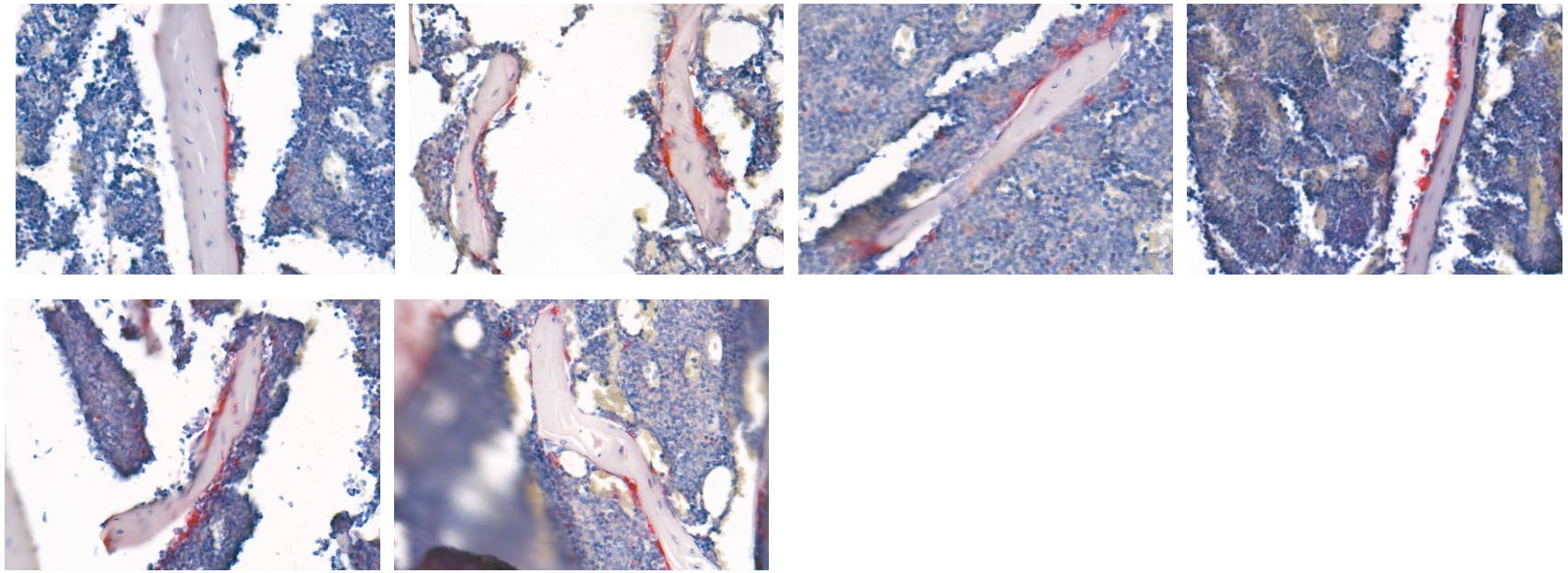

**Figure. 5b**

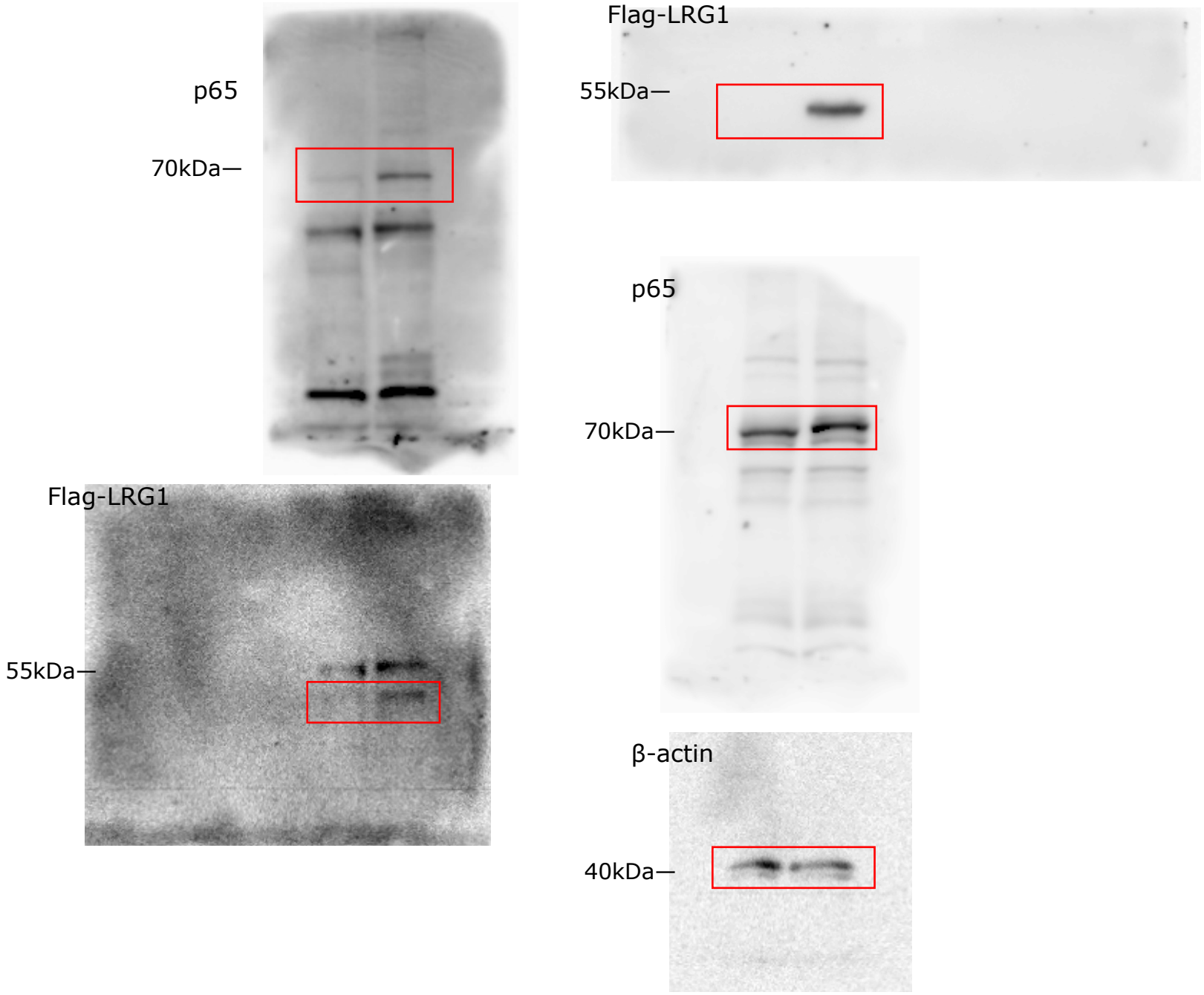
p65
70kDa—
Flag-LRG1
55kDa—
p65
70kDa—
Flag-LRG1
55kDa—
β-actin
40kDa—

**Figure. 5c**

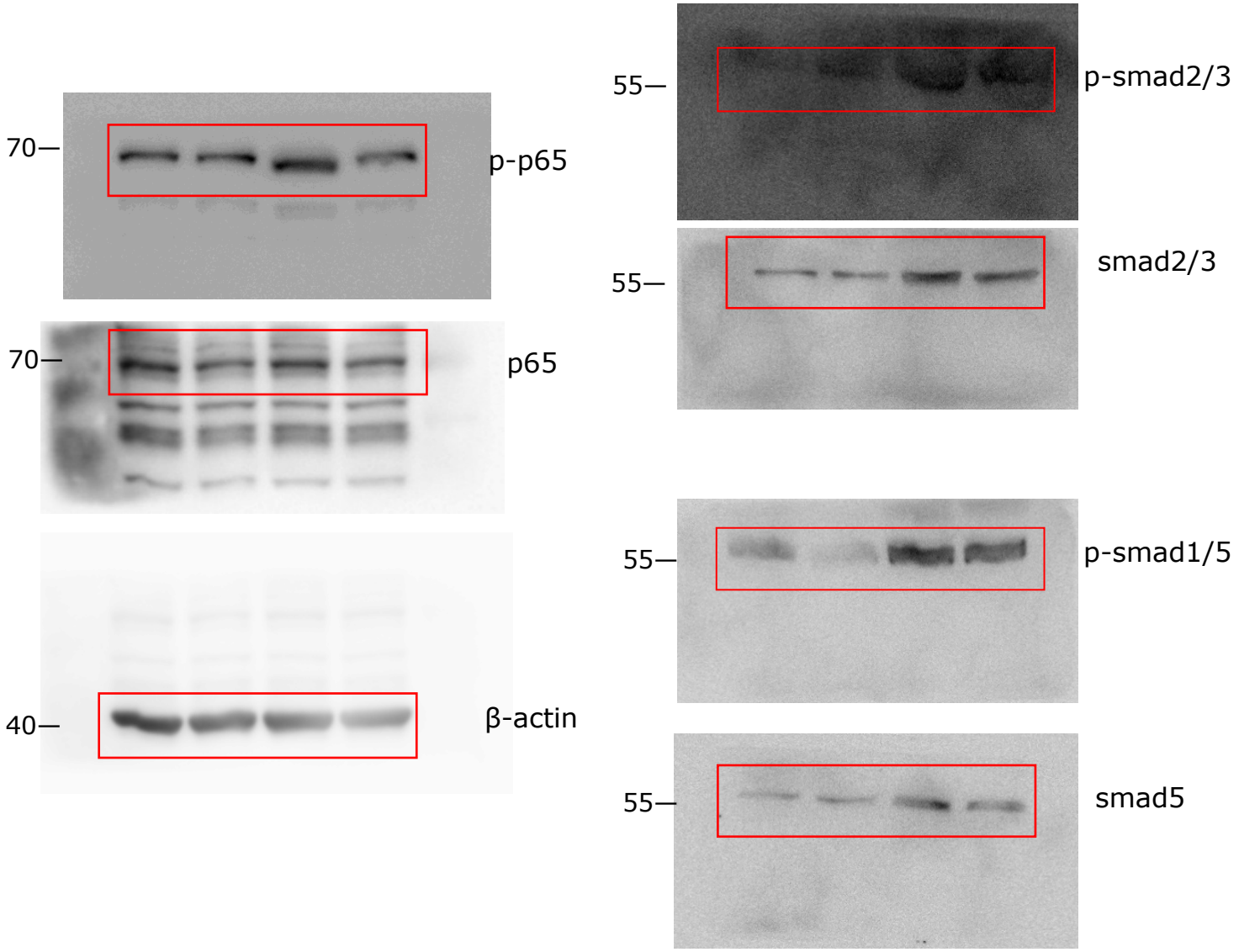
70—
p-p65
70—
p65
40—
β-actin
55—
p-smad2/3
55—
smad2/3
55—
p-smad1/5
55—
smad5

**Figure. 5f**

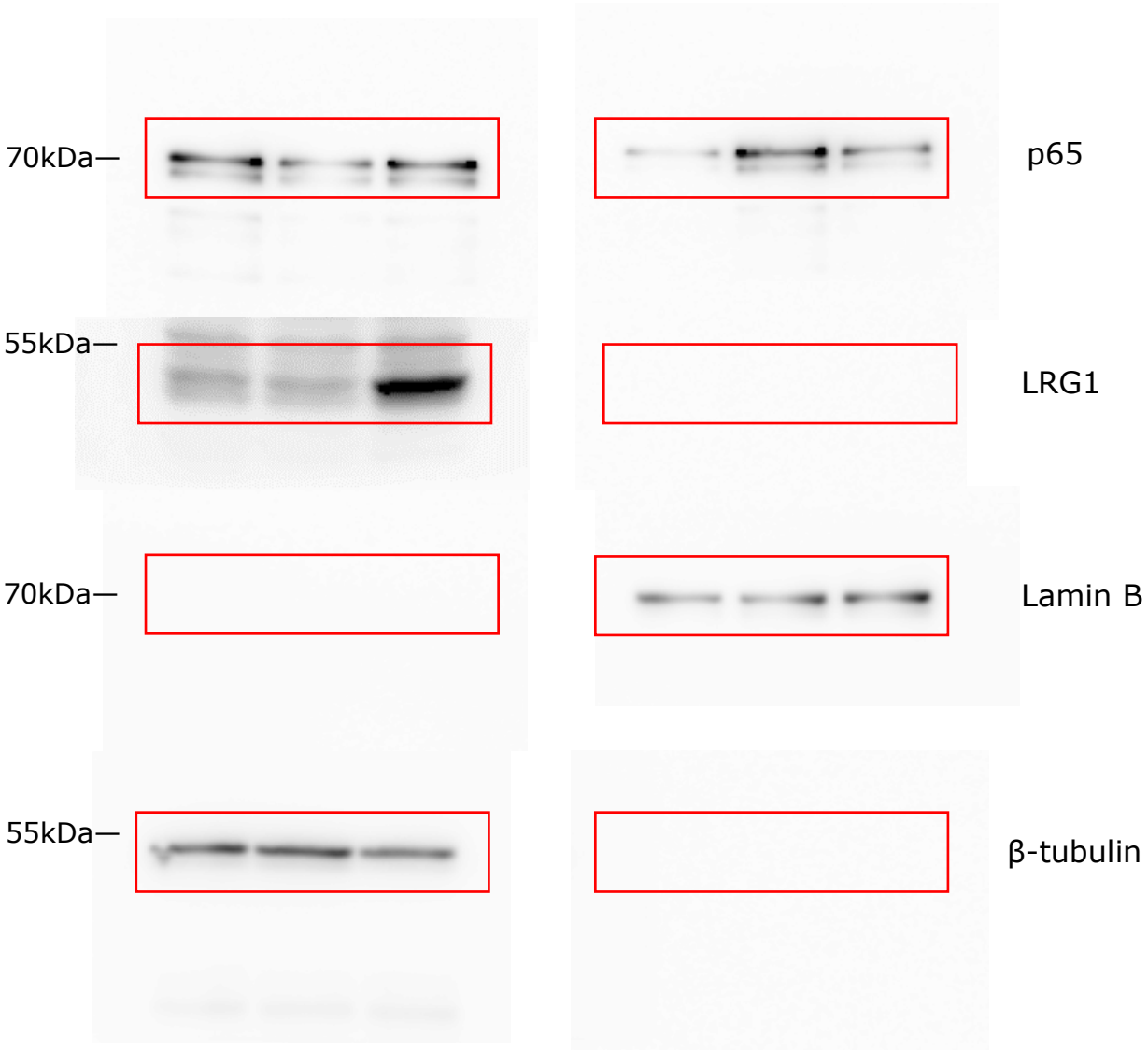

**Figure.5d** Immunofluorescence analysis of p65 (red) location in RANKL-induced BMDMs treated with LRG1-GFP-sEVs

CTRL

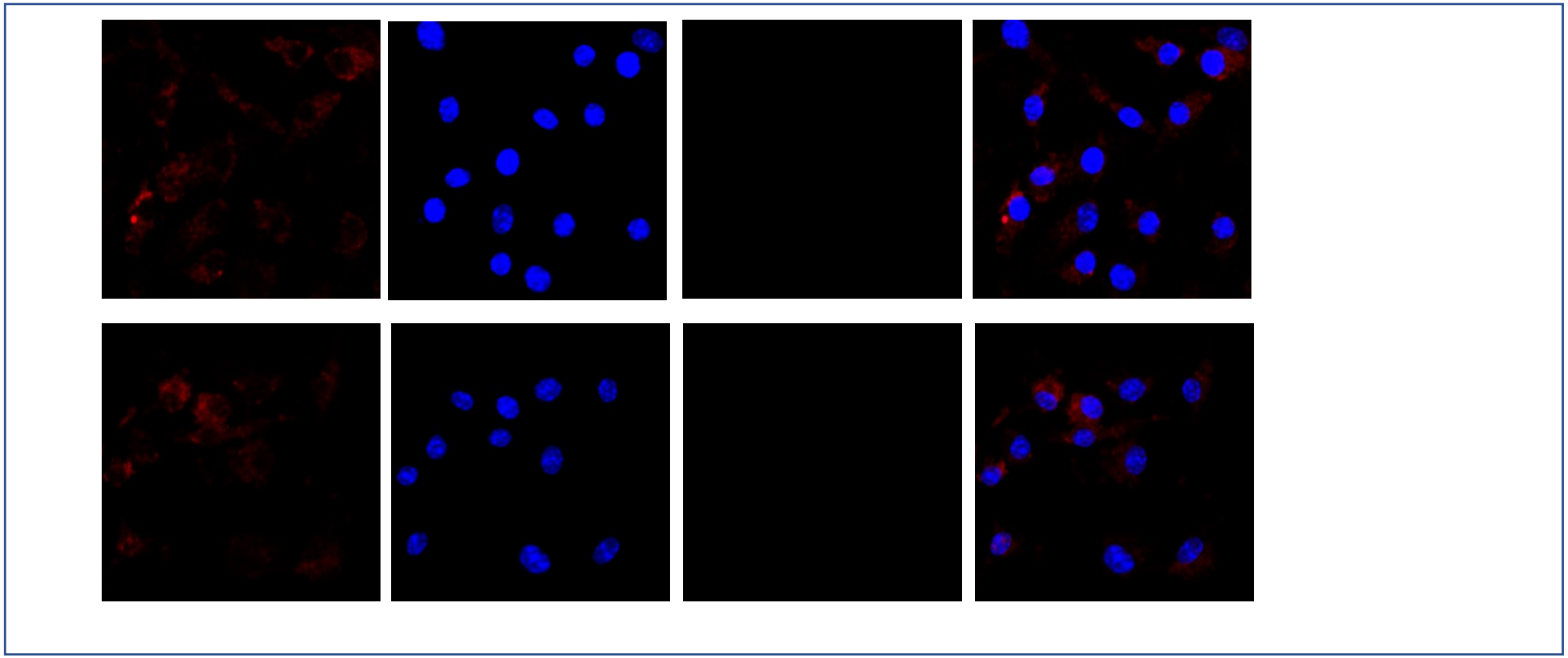

**Figure.5d**

RANKL

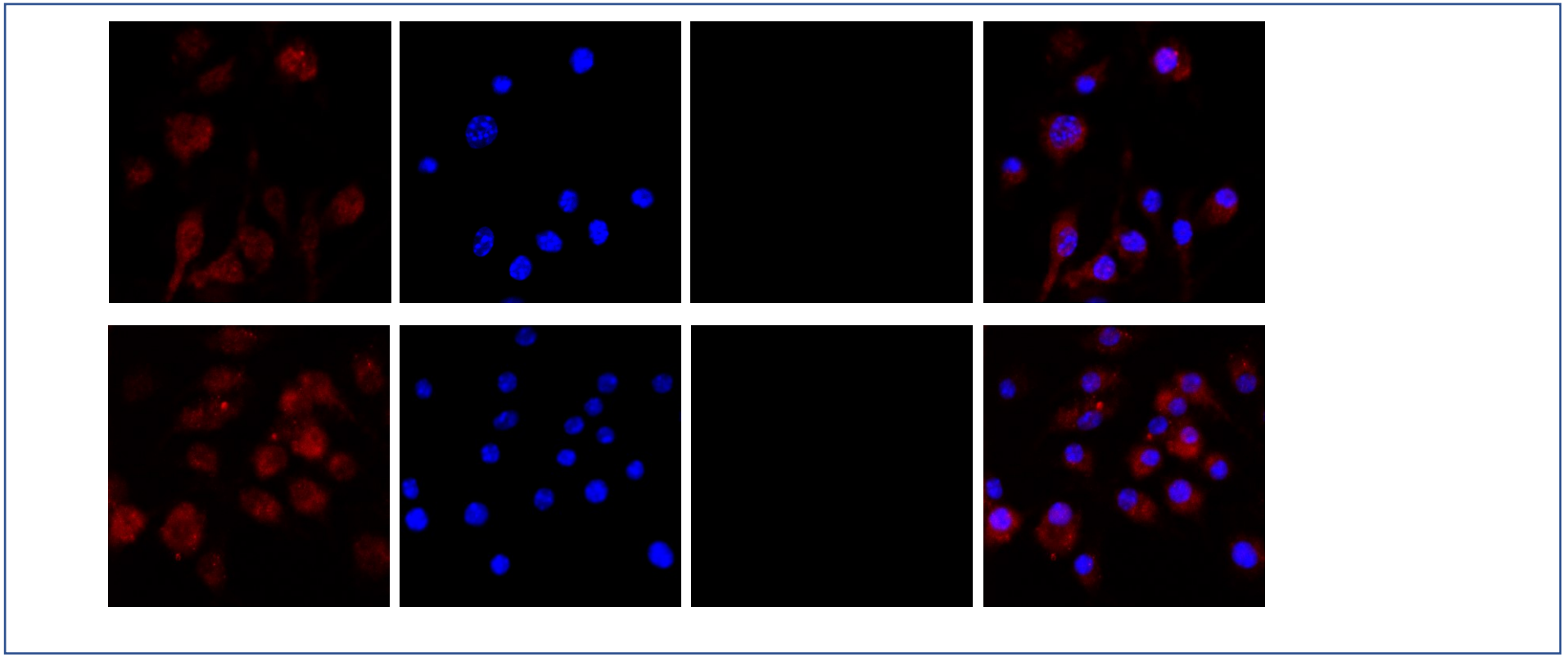

**Figure.5d**

RANKL+GPF-LRG1-sEVs

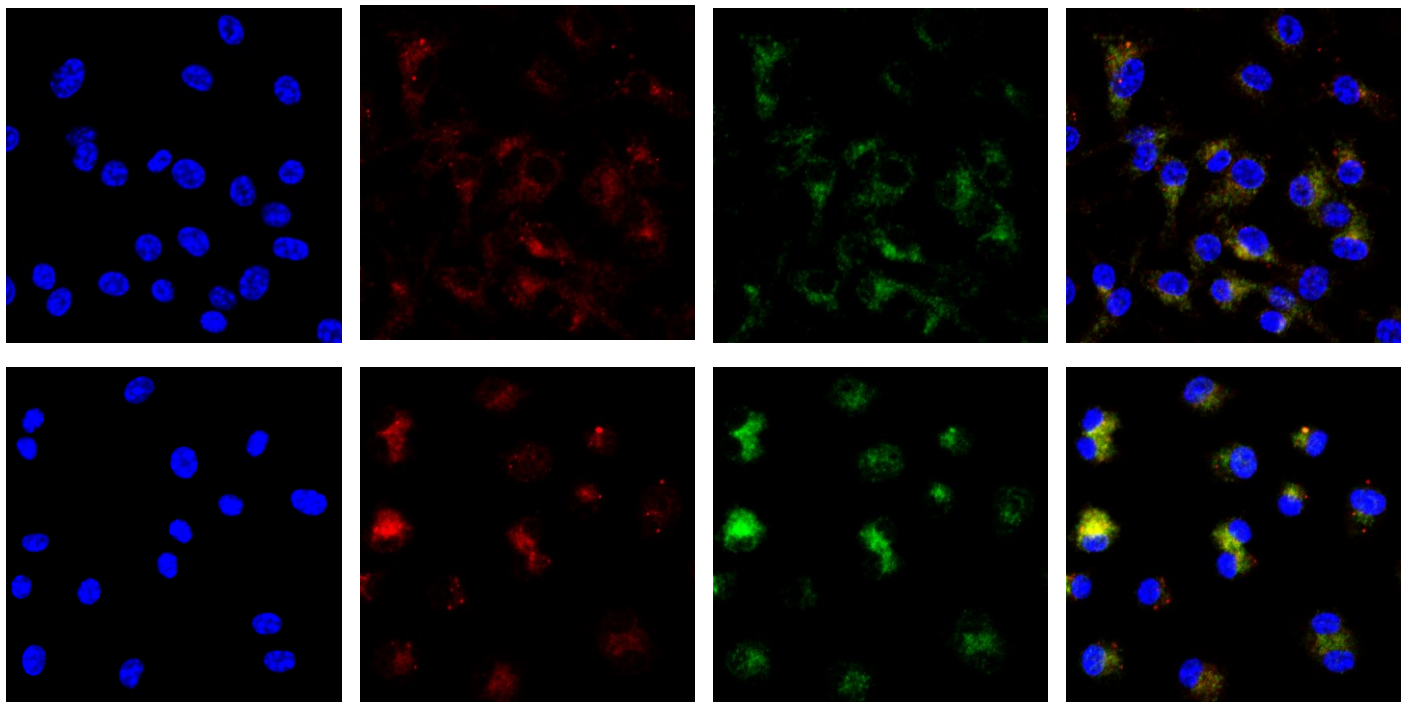

**Figure.5g** immunofluorescence images of primary BMDMs isolated from aged mice

Aged female mice Loxp

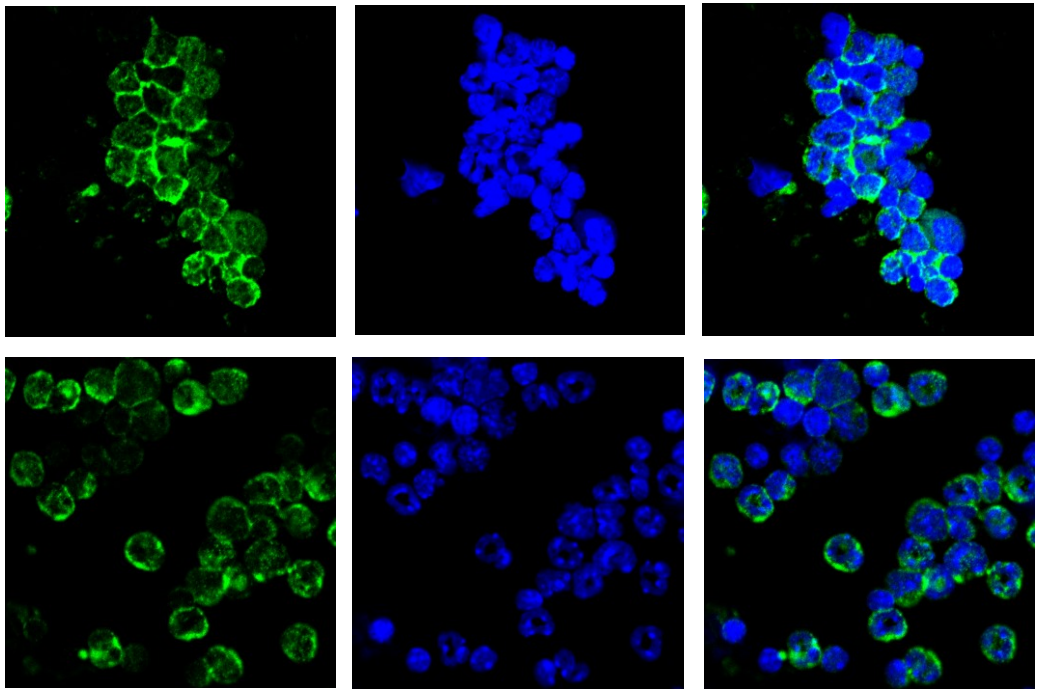

Aged female mice SIRT2-KOhep

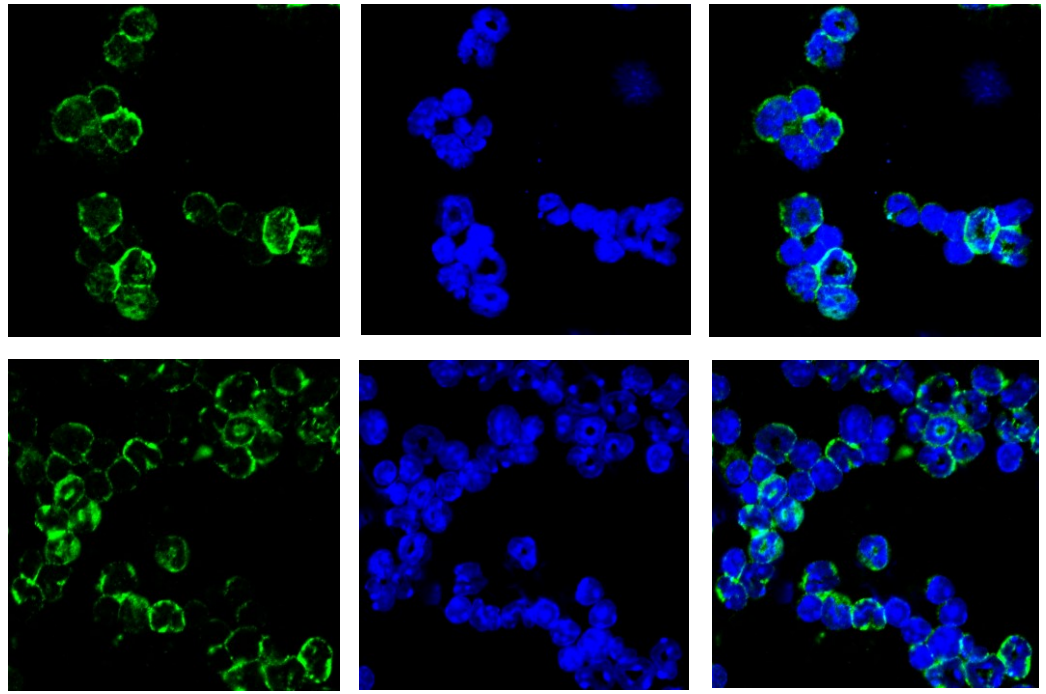

**Figure.5i** immunofluorescence images of primary BMDMs isolated from aged mice

Aged male mice Loxp

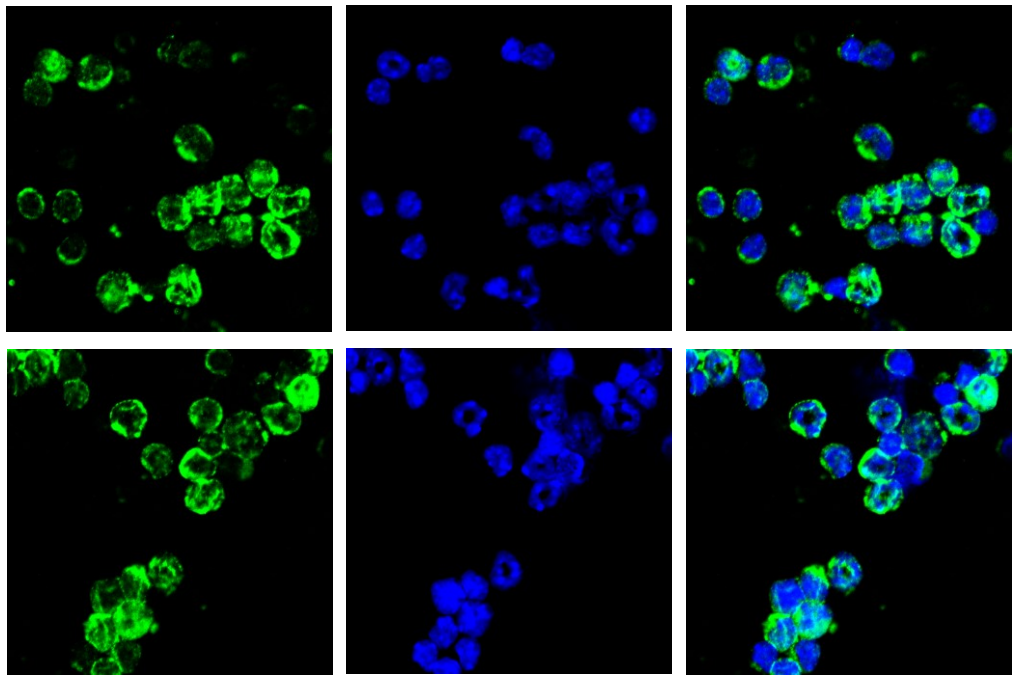

Aged male mice SIRT2-KOhep

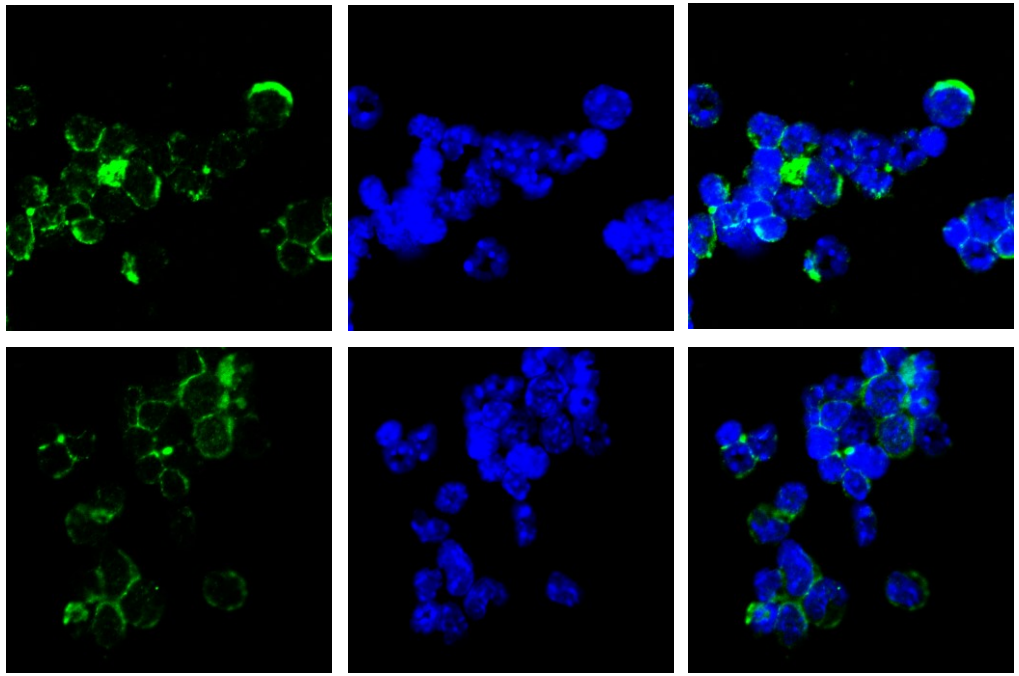

**Figure.5k** TRAP staining of osteoclasts treated with LRG1-sEVs and the inhibitors of p65 nuclear translocation

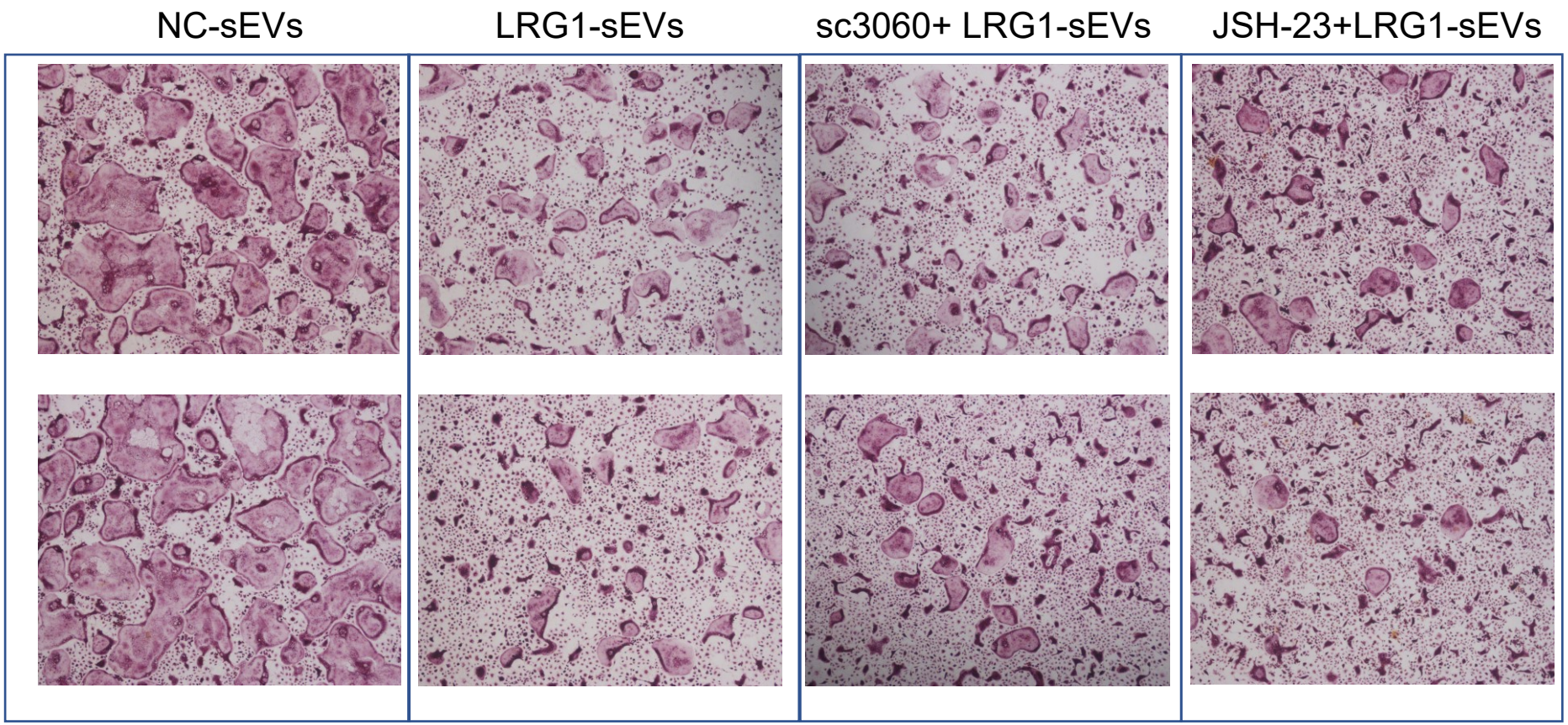

**Figure.5n** TRAP staining of RAW264.7 cells overexpressed p65 and treated with LRG1-sEVs

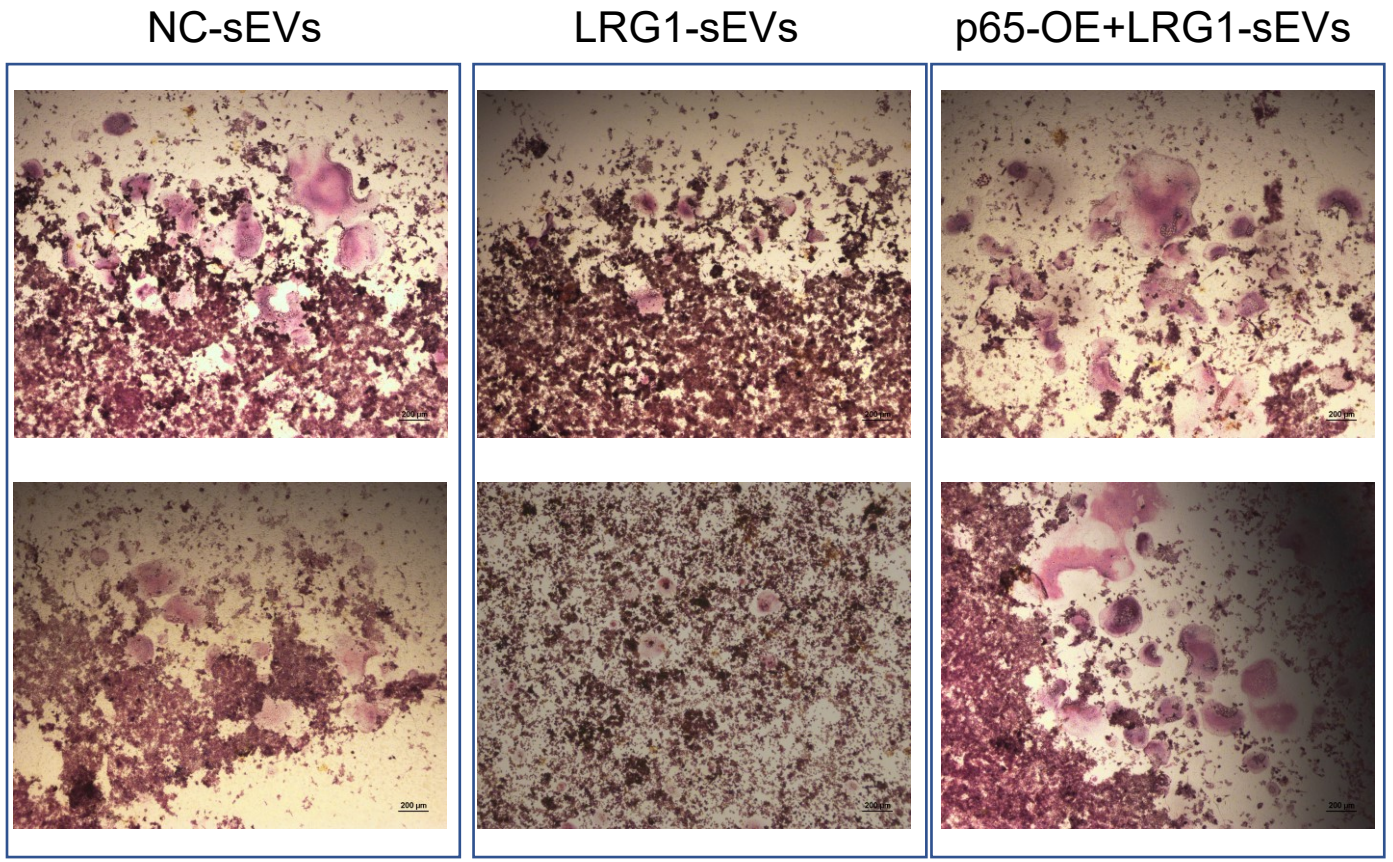

**Figure.6b**

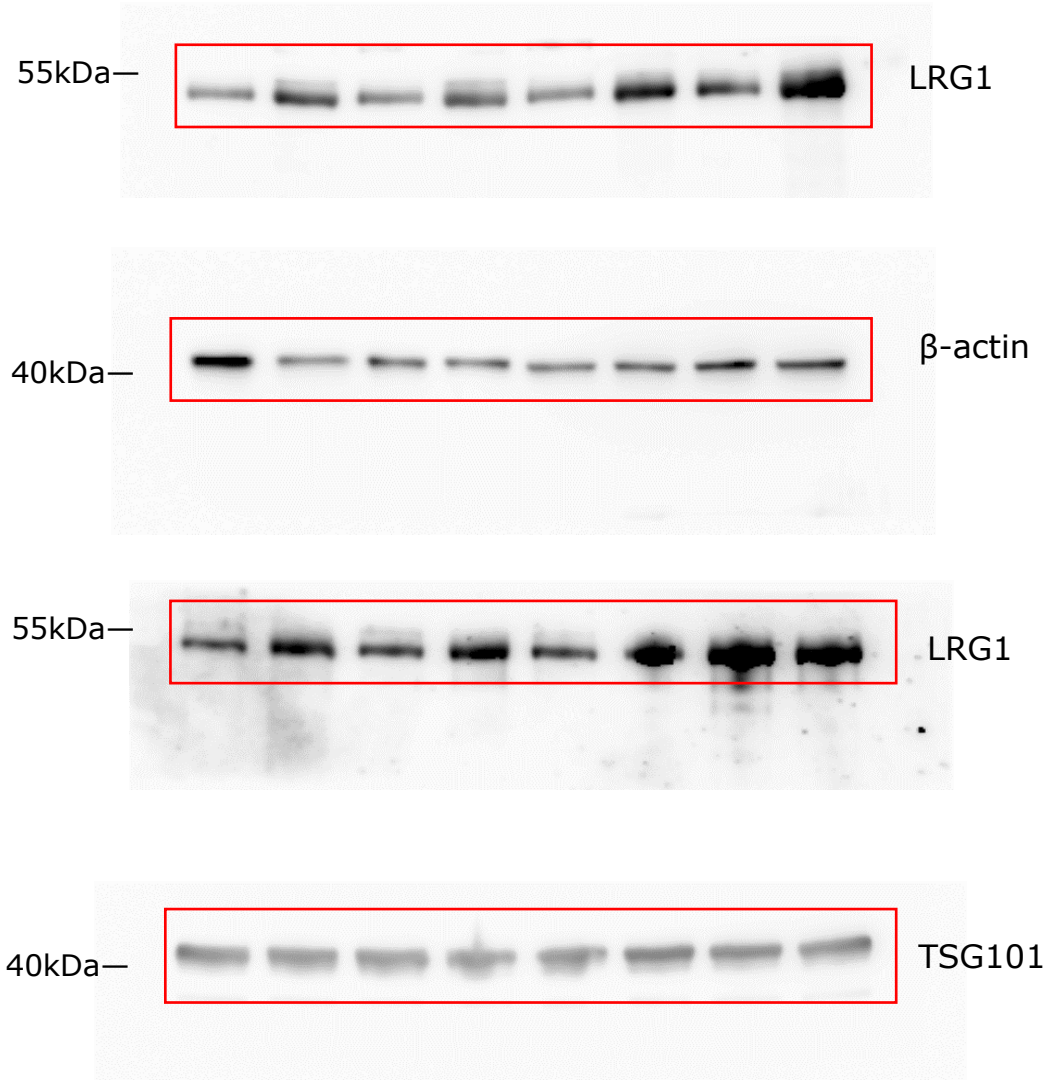

Figure.6c

sham

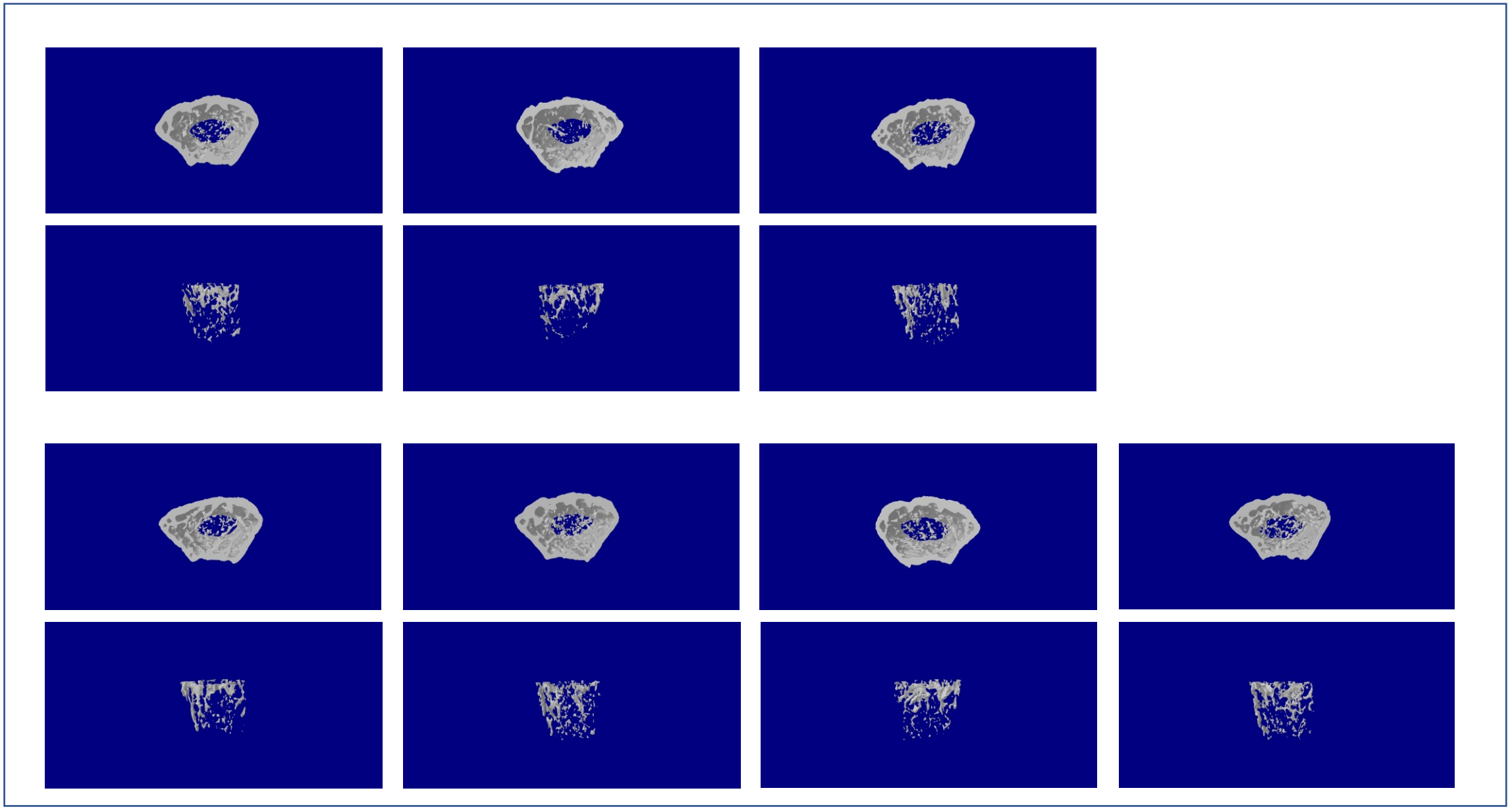

Figure.6c

OVX

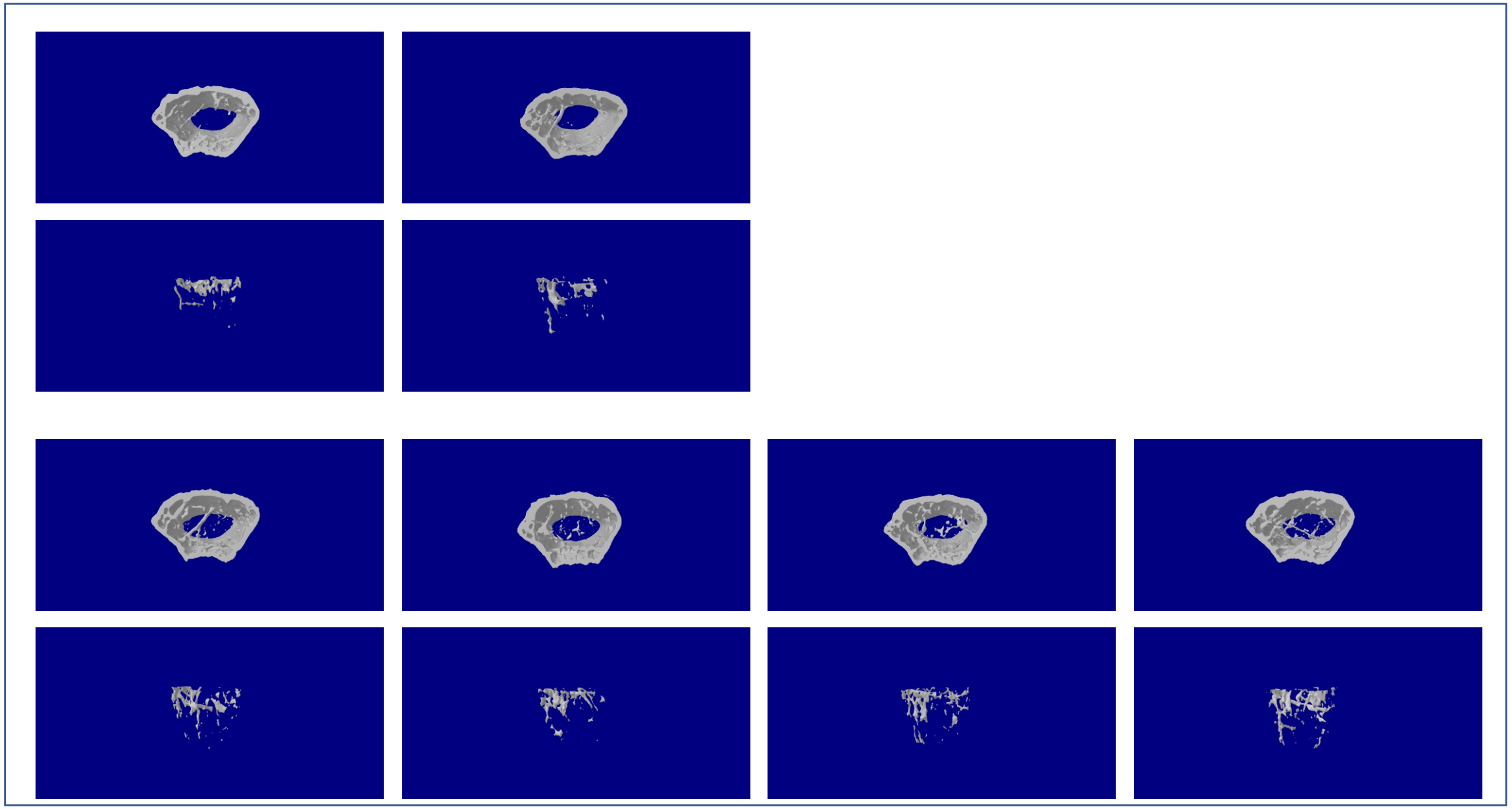

Figure.6c

OVX+AGK2

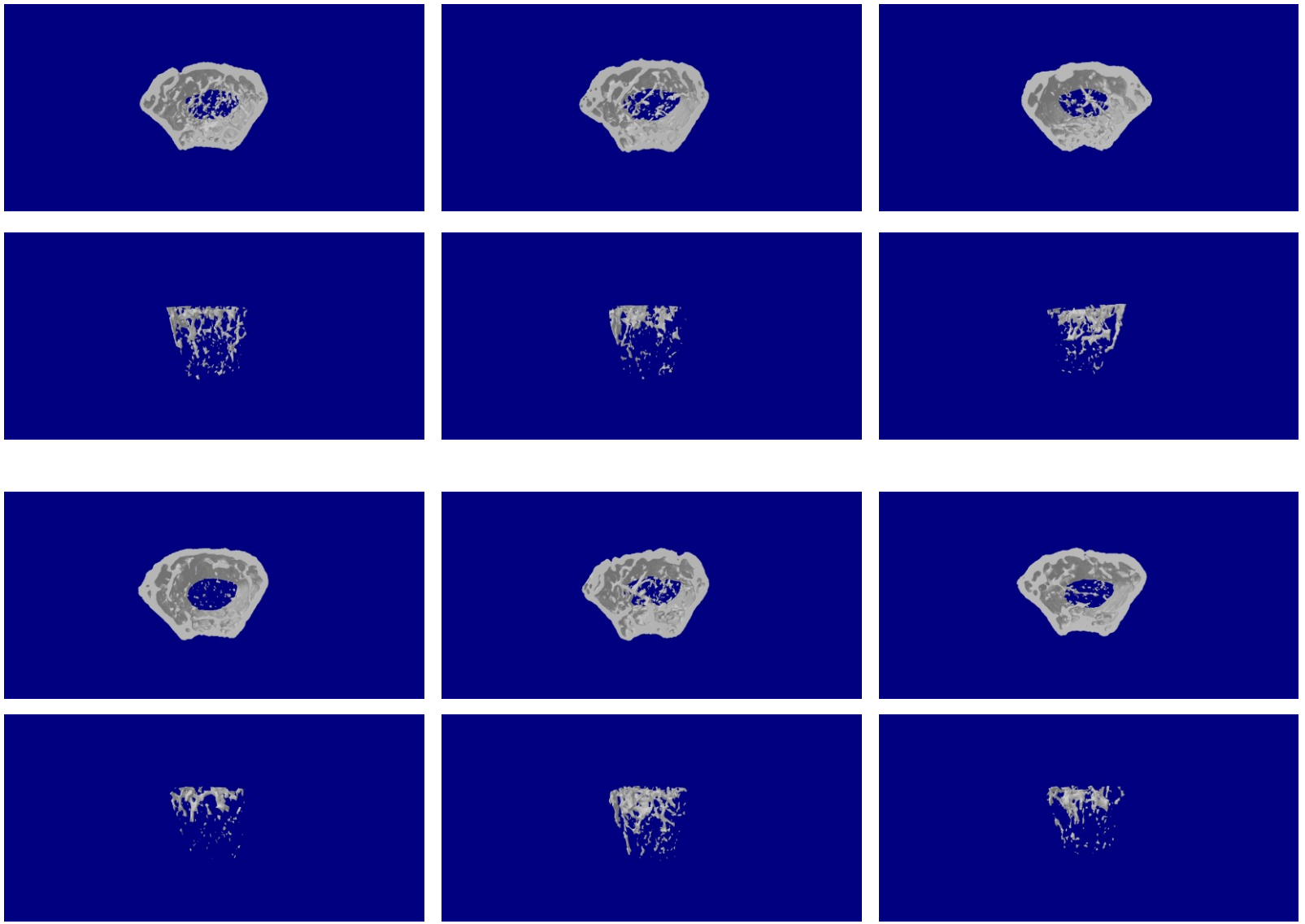

Figure.6e

OVX+Loxp

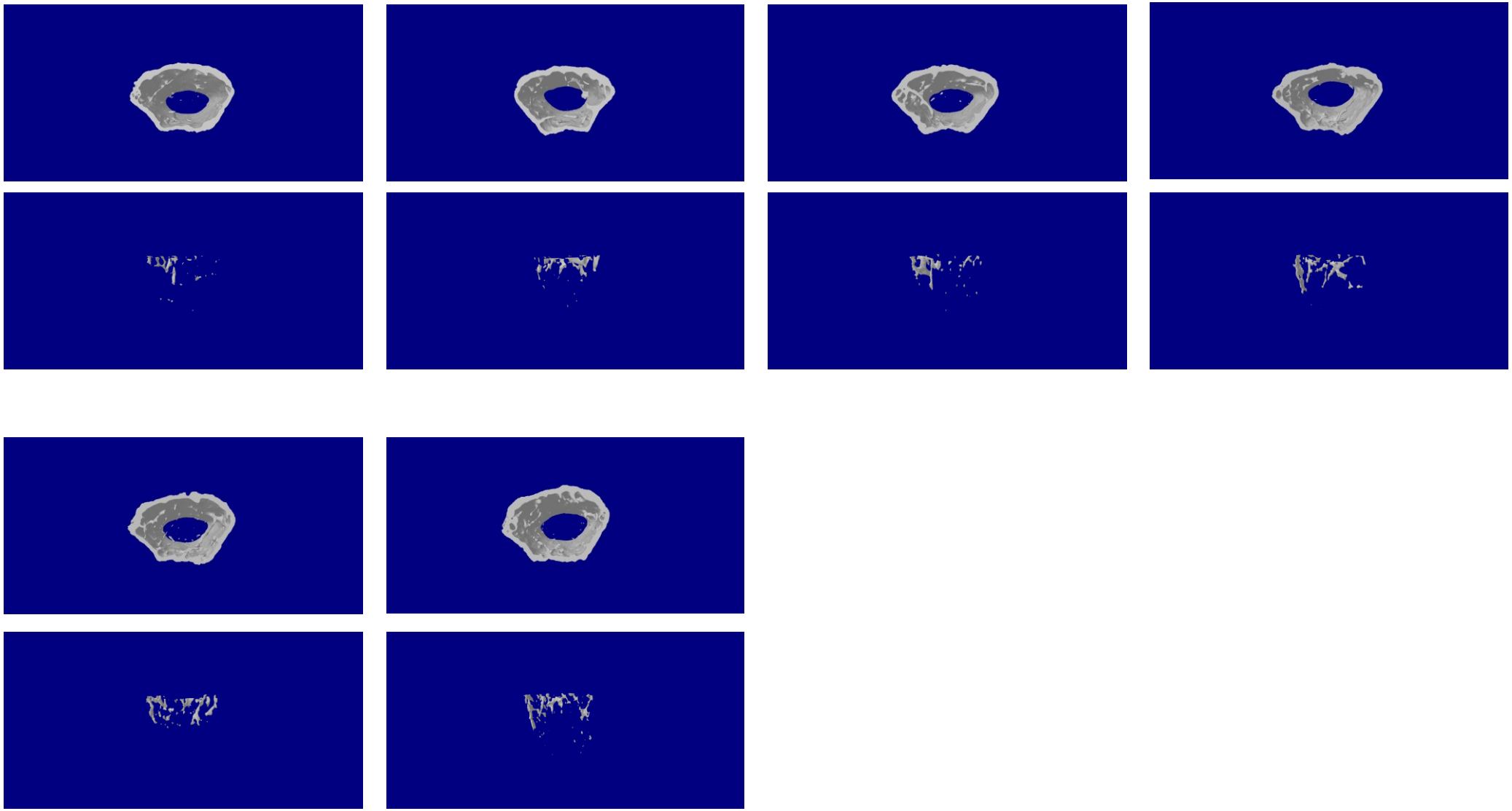

Figure.6e

OVX+SIRT2-KOhep

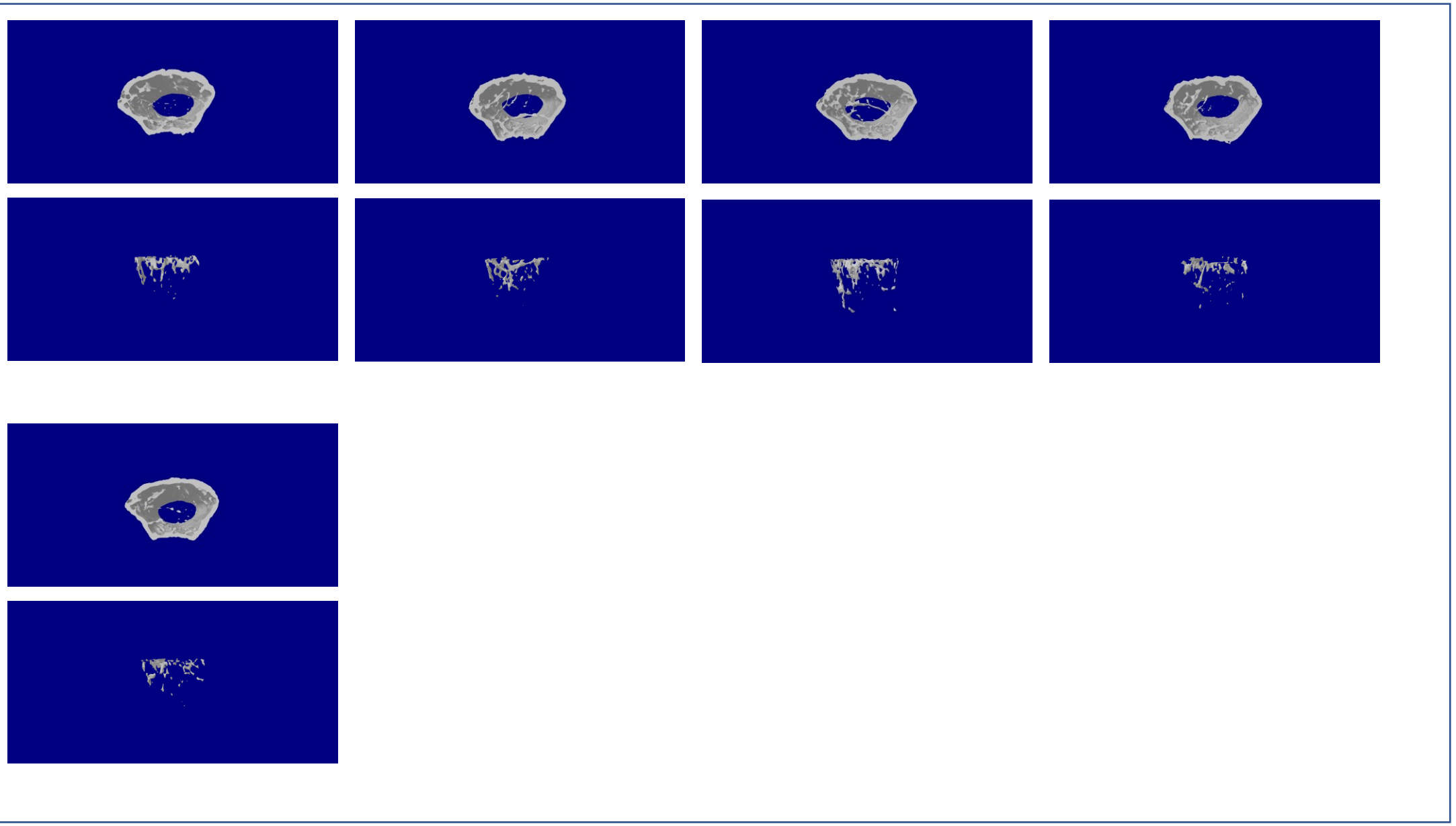

Figure.6e

OVX+SIRT2-Kohep+AGK2

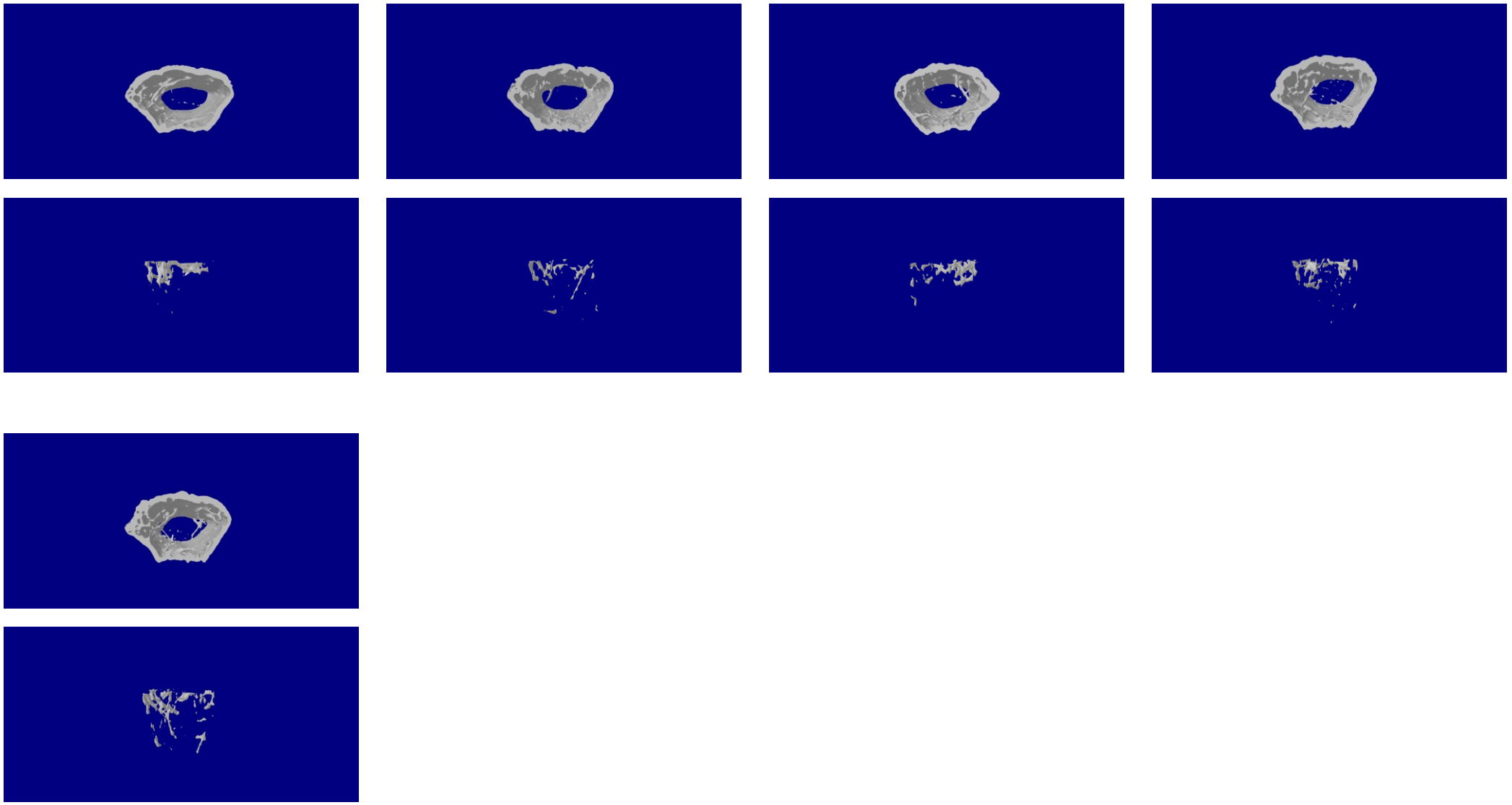

**Figure.7b** TRAP staining images of human PBMCs cultured with RANKL and sEVs

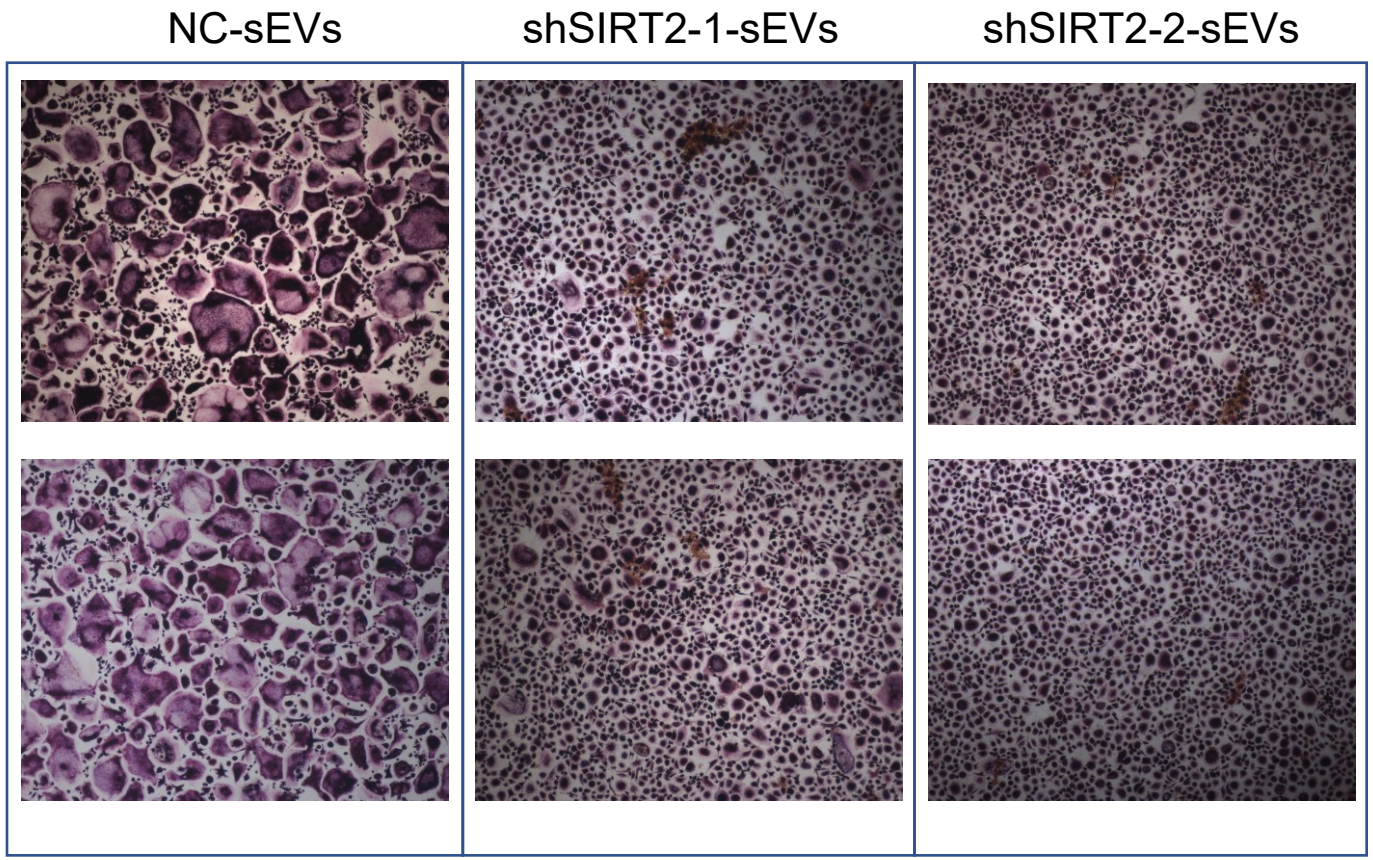

**Figure.7f** TRAP staining images of human PBMCs cultured with RANKL and sEVs

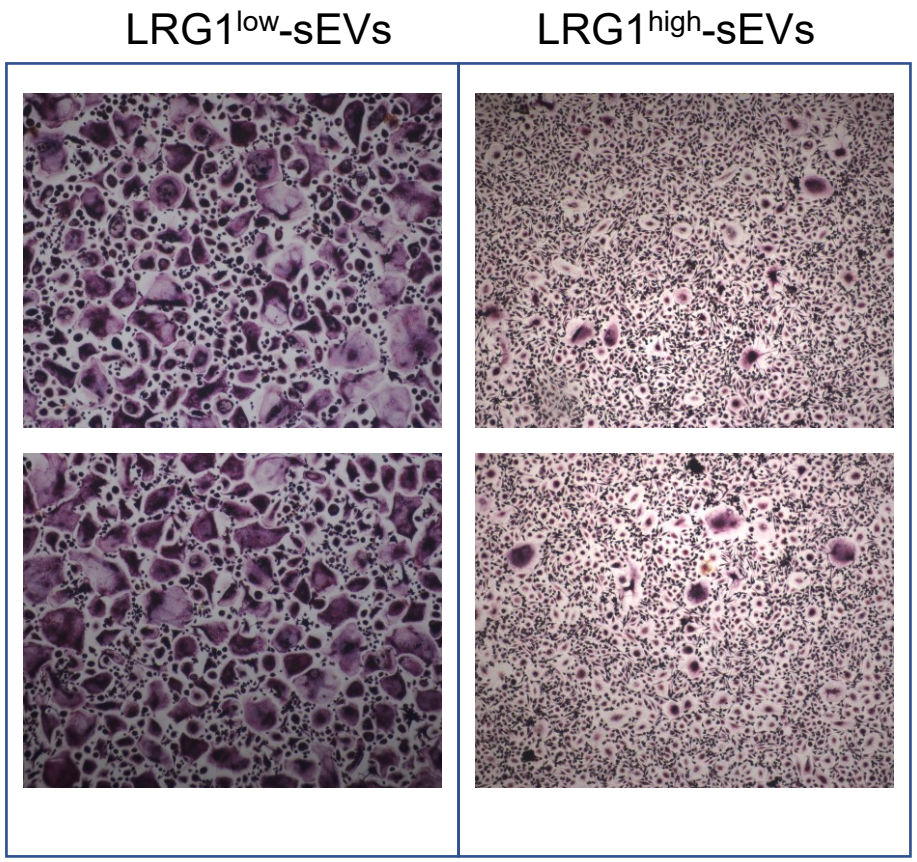

**Figure.7j** TRAP staining images of PBMCs cultured with RANKL and sEVs-LRG1 or denosumab

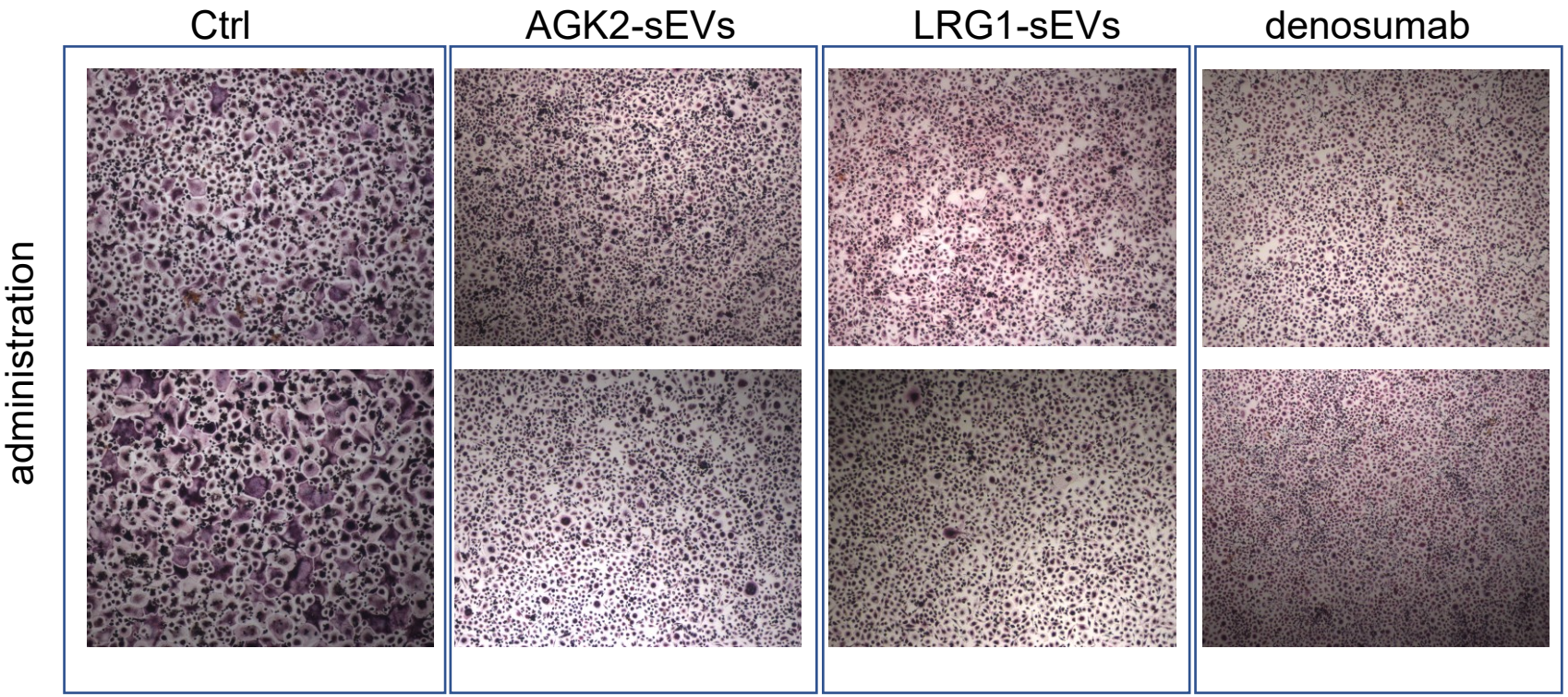

**Figure.7j** TRAP staining images of PBMCs cultured with RANKL and sEVs-LRG1 or denosumab

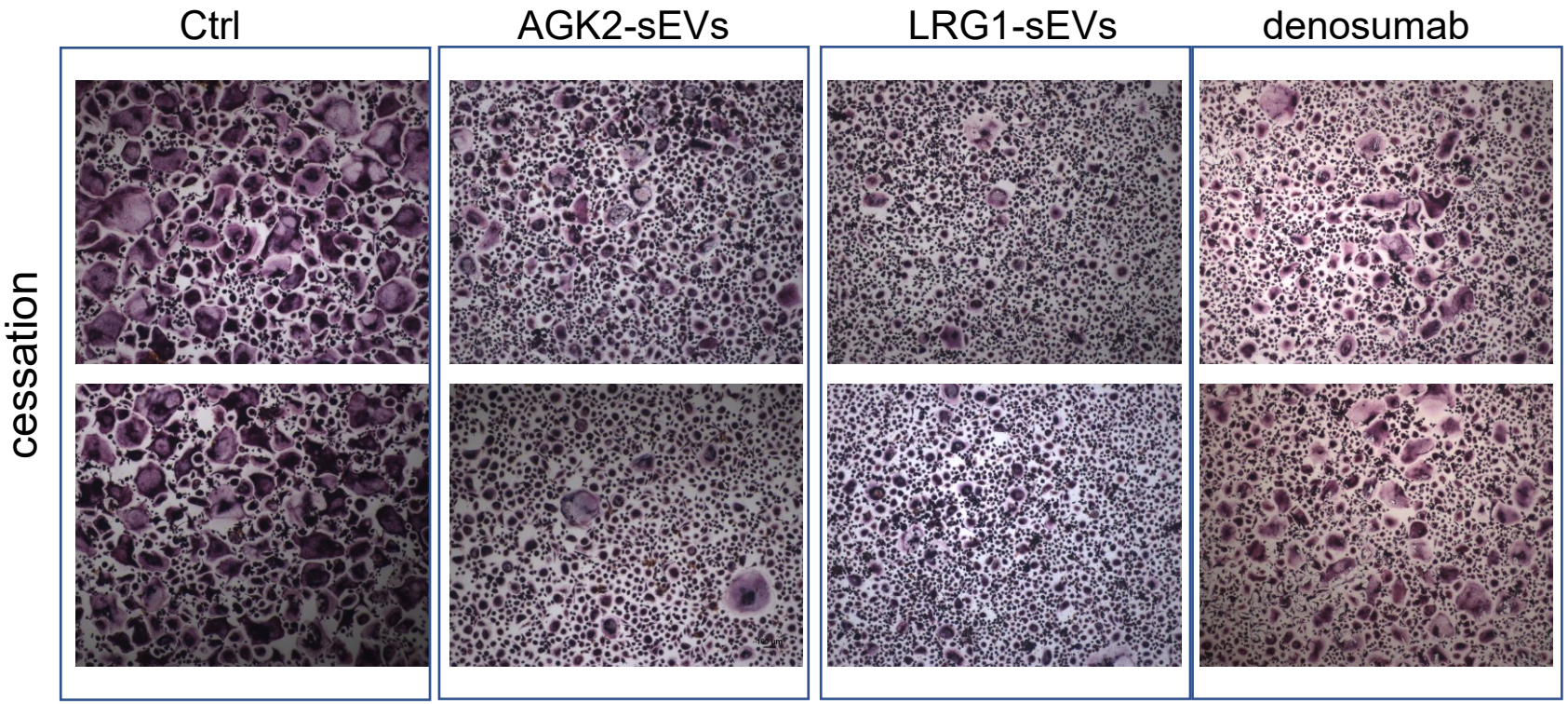

**Figure7I** IHC images of SIRT2 expression levels in human liver tissues

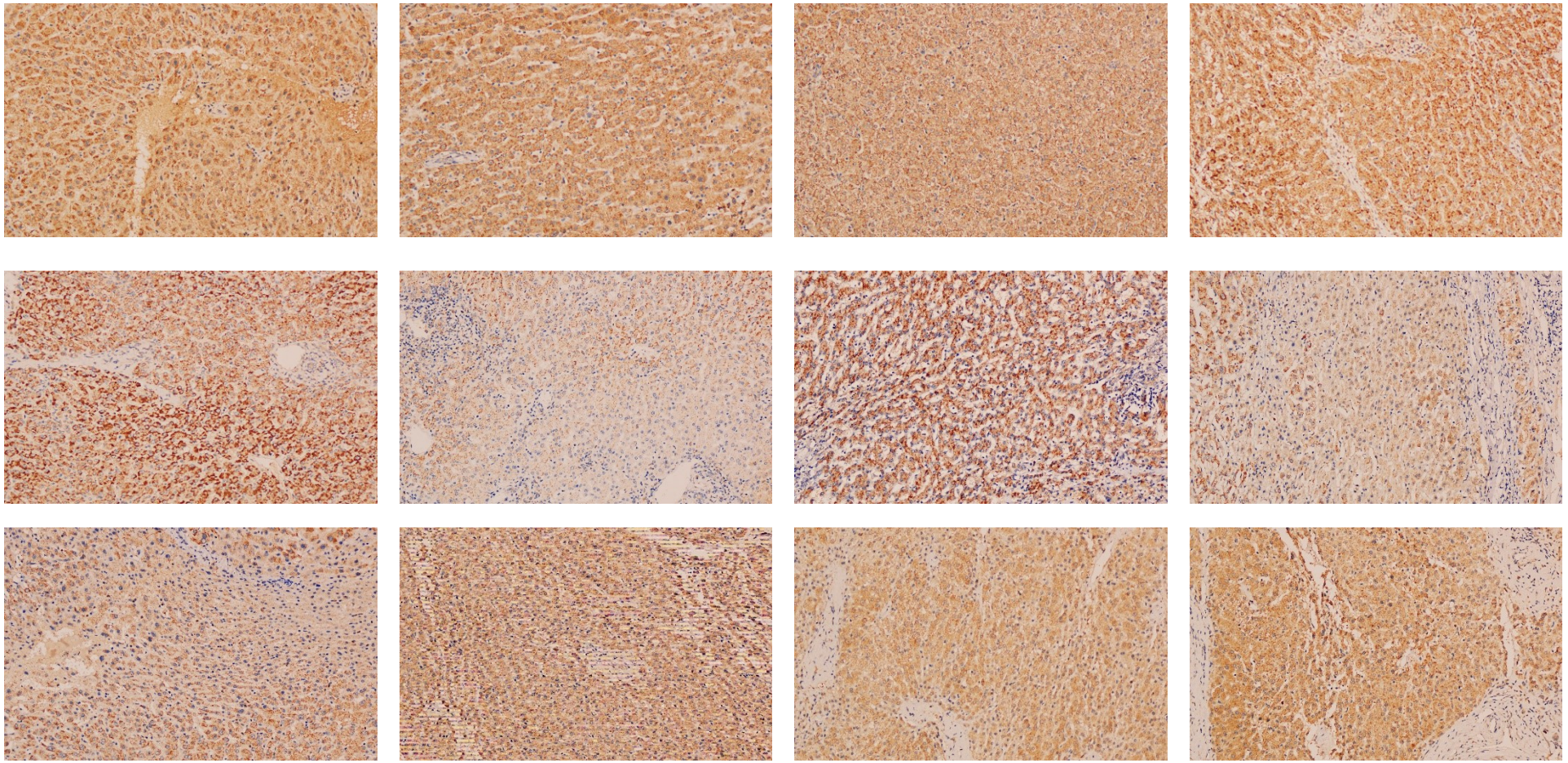

**Figure7I** IHC images of SIRT2 expression levels in human liver tissues

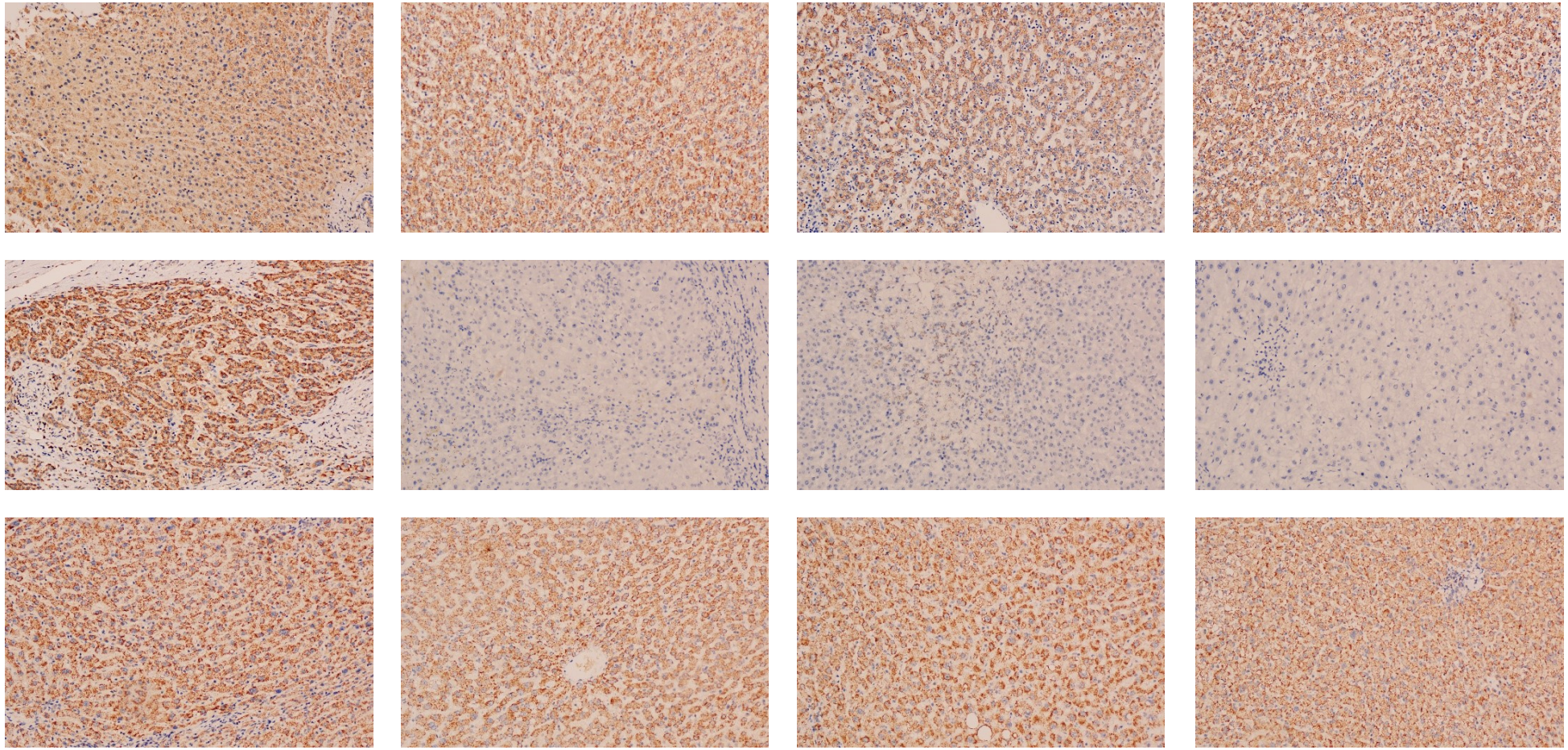

**Figure7I** IHC images of SIRT2 expression levels in human liver tissues

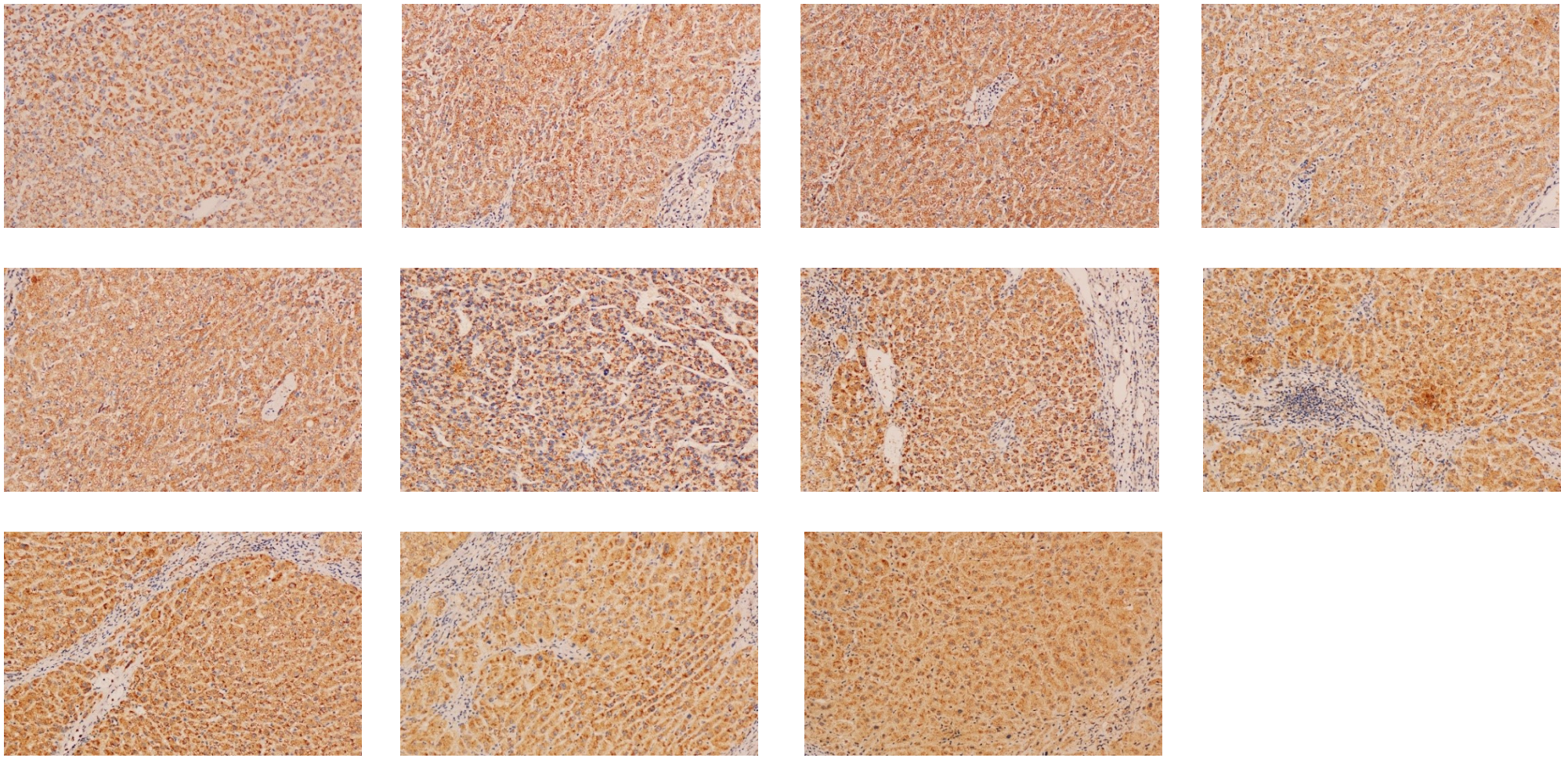

**Figure.7n** western blot analysis of the protein expression of plasma-sEVs-LRG1 from patients

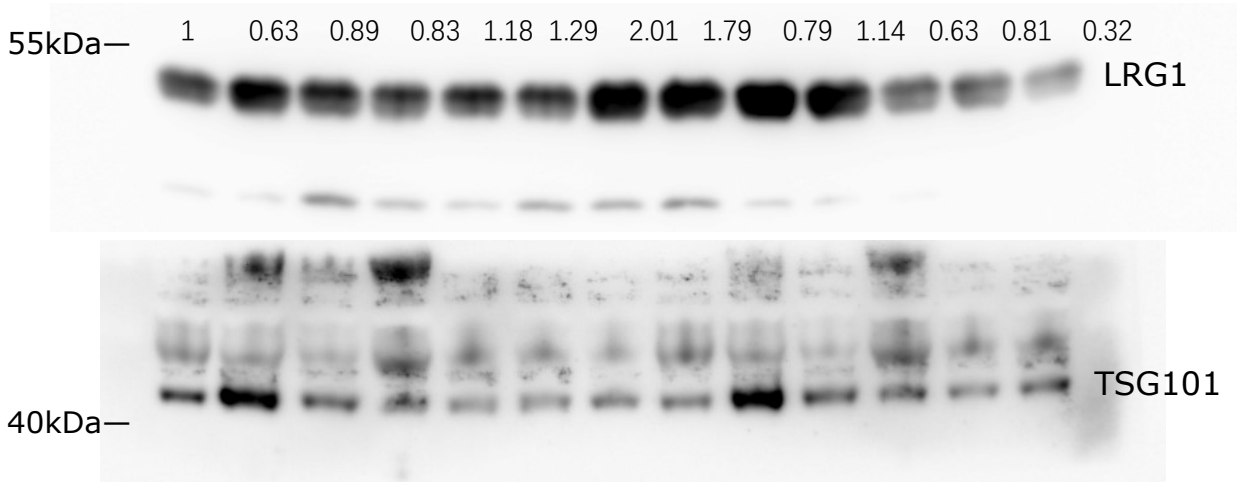

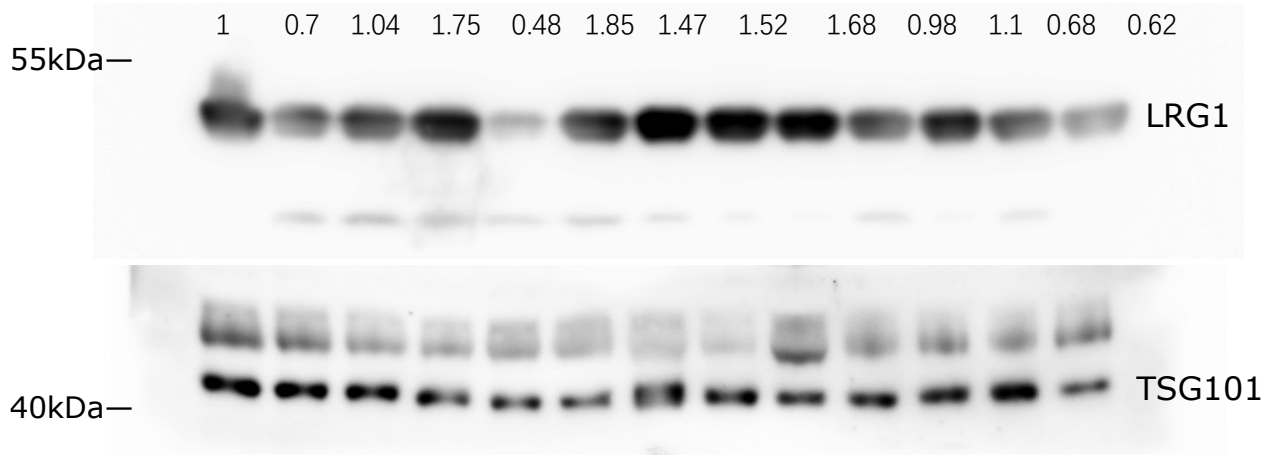
1
0.7
1.04
1.75
0.48
1.85
1.47
1.52
1.68
0.98
1.1
0.68
0.62
55kDa—
LRG1
40kDa—
TSG101

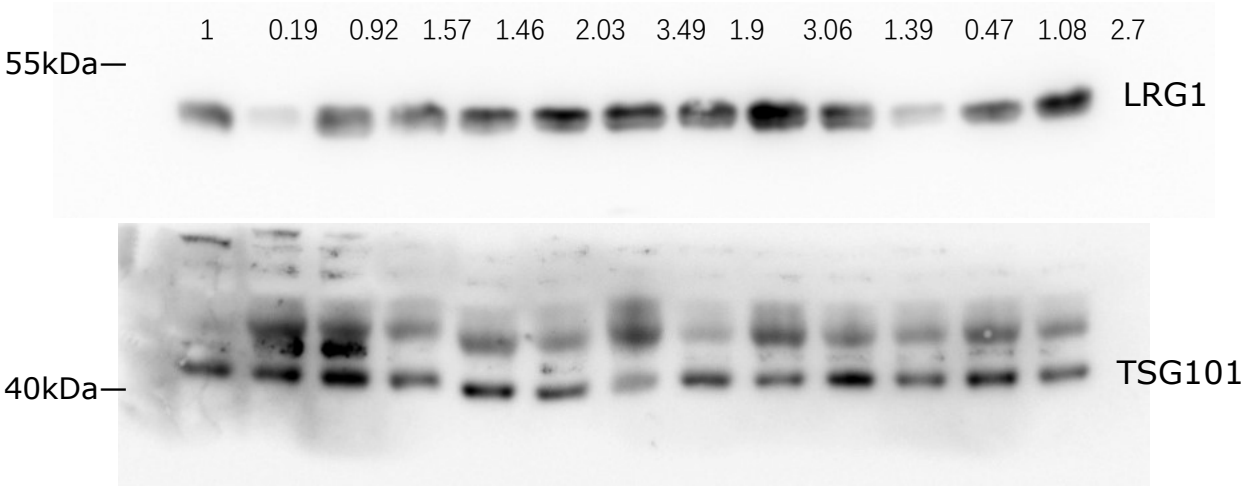
1 0.19 0.92 1.57 1.46 2.03 3.49 1.9 3.06 1.39 0.47 1.08 2.7
55kDa—
LRG1
40kDa—
TSG101

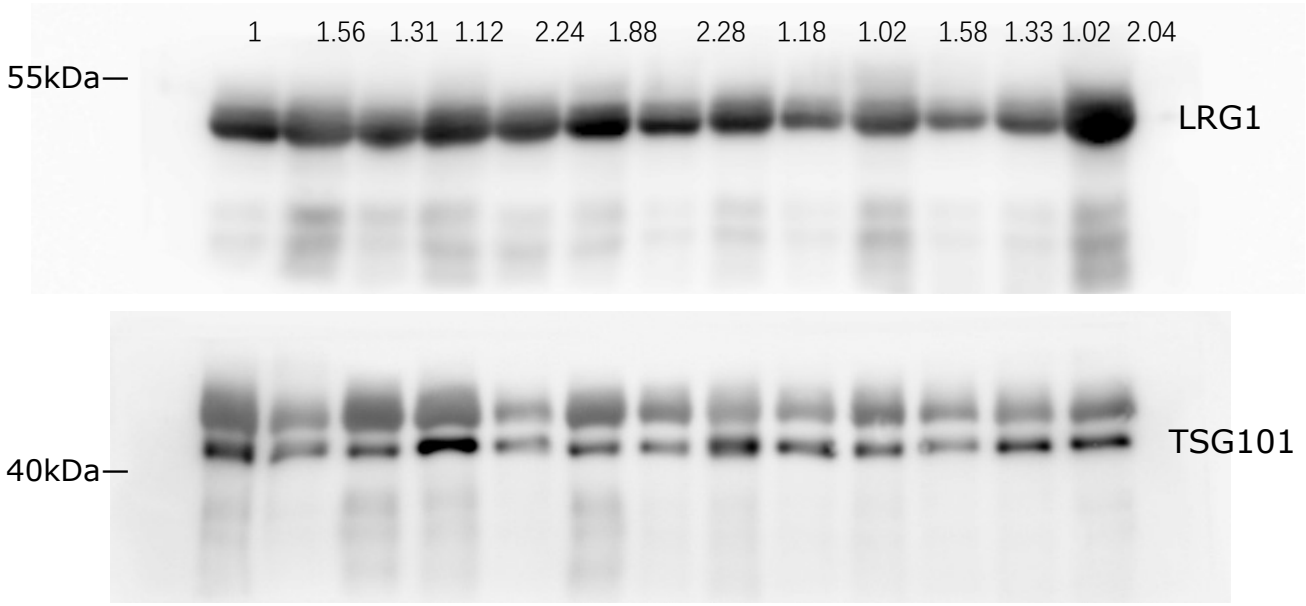
1
1.56
1.31
1.12
2.24
1.88
2.28
1.18
1.02
1.58
1.33
1.02
2.04
55kDa—
LRG1
40kDa—
TSG101

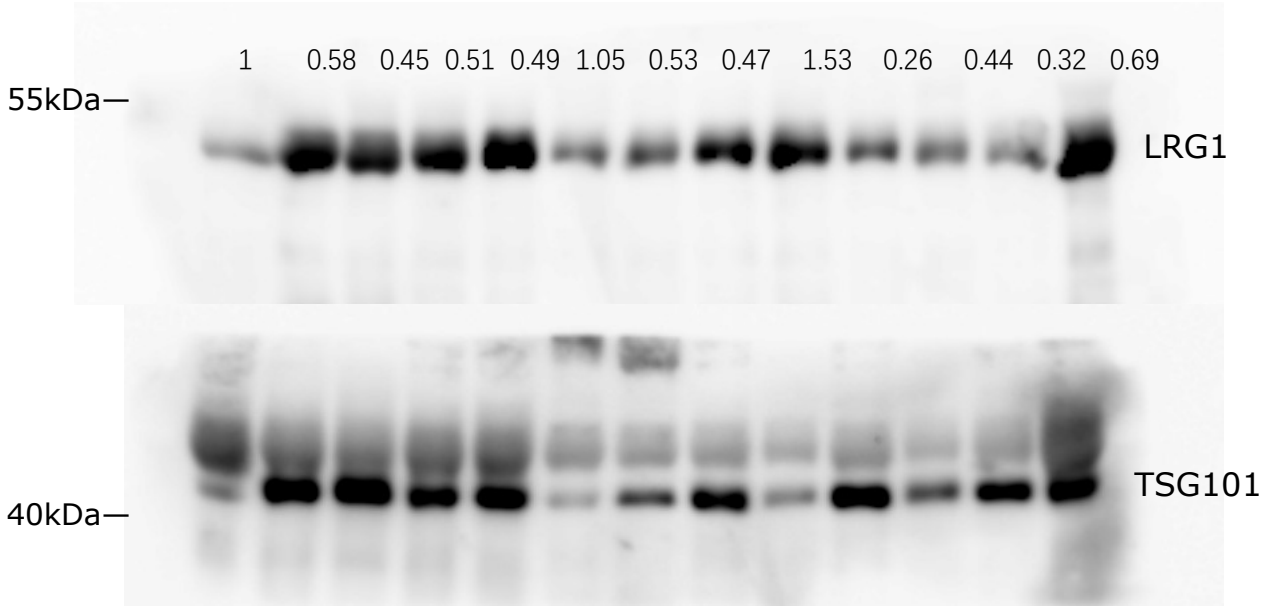
1
0.58
0.45
0.51
0.49
1.05
0.53
0.47
1.53
0.26
0.44
0.32
0.69
55kDa—
LRG1
40kDa—
TSG101

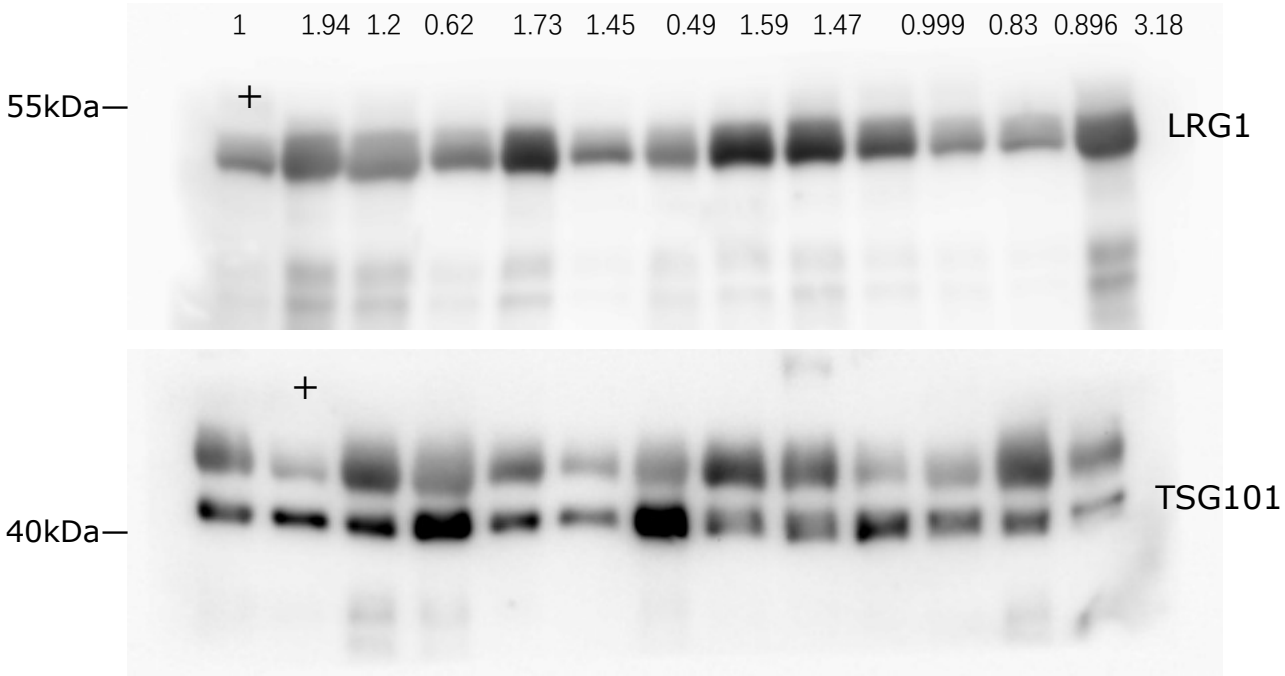
1 1.94 1.2 0.62 1.73 1.45 0.49 1.59 1.47 0.999 0.83 0.896 3.18
55kDa—
+
LRG1
+
40kDa—
TSG101

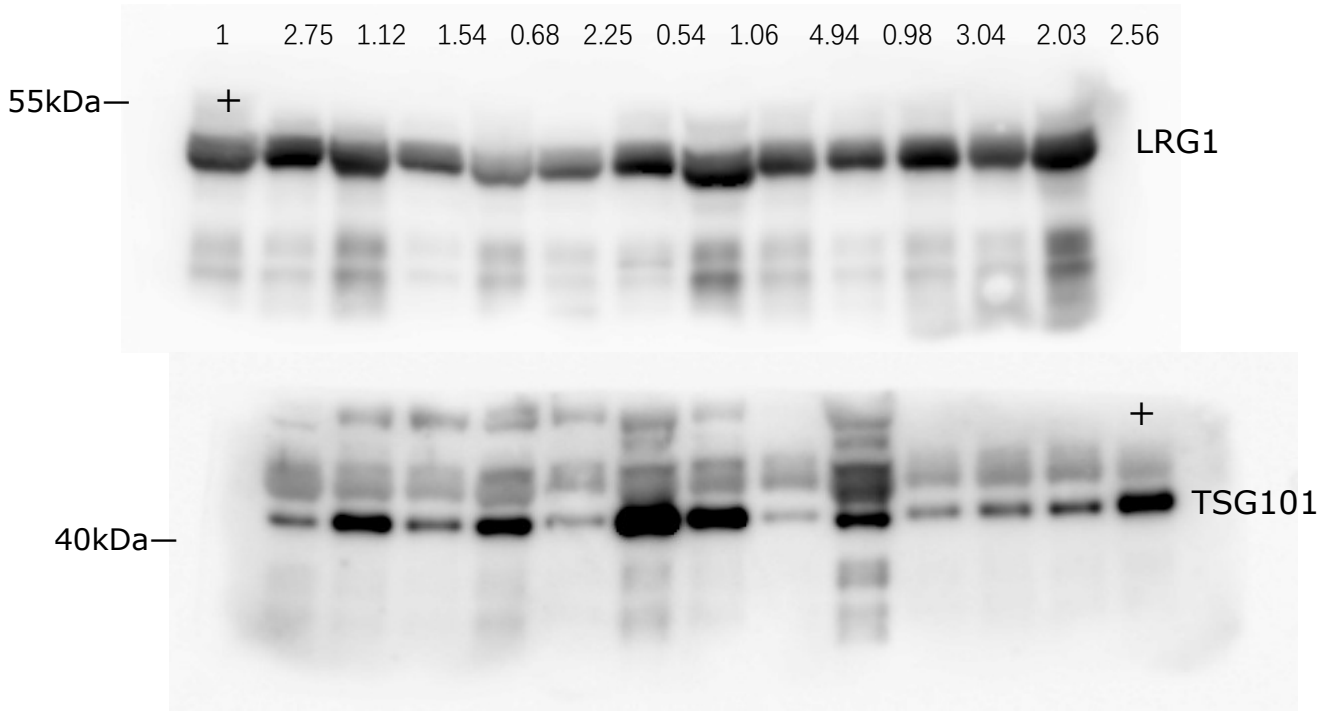
1
2.75
1.12
1.54
0.68
2.25
0.54
1.06
4.94
0.98
3.04
2.03
2.56
55kDa—
+
LRG1
+
40kDa—
TSG101

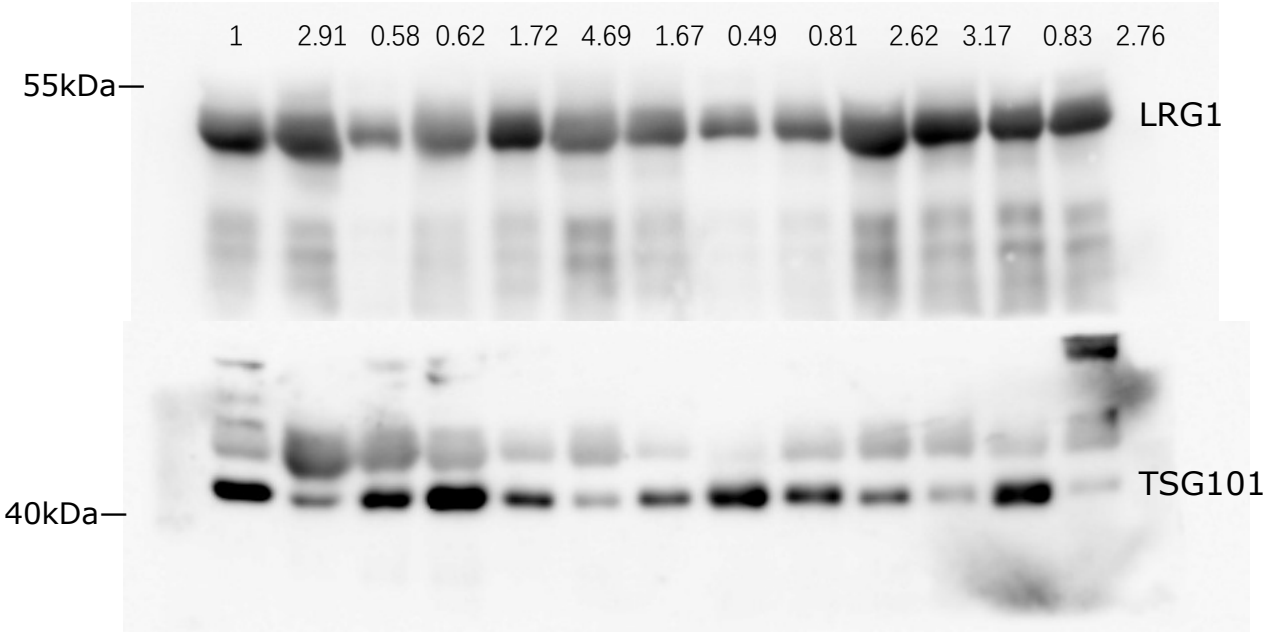
1
2.91
0.58
0.62
1.72
4.69
1.67
0.49
0.81
2.62
3.17
0.83
2.76
55kDa—
LRG1
40kDa—
TSG101

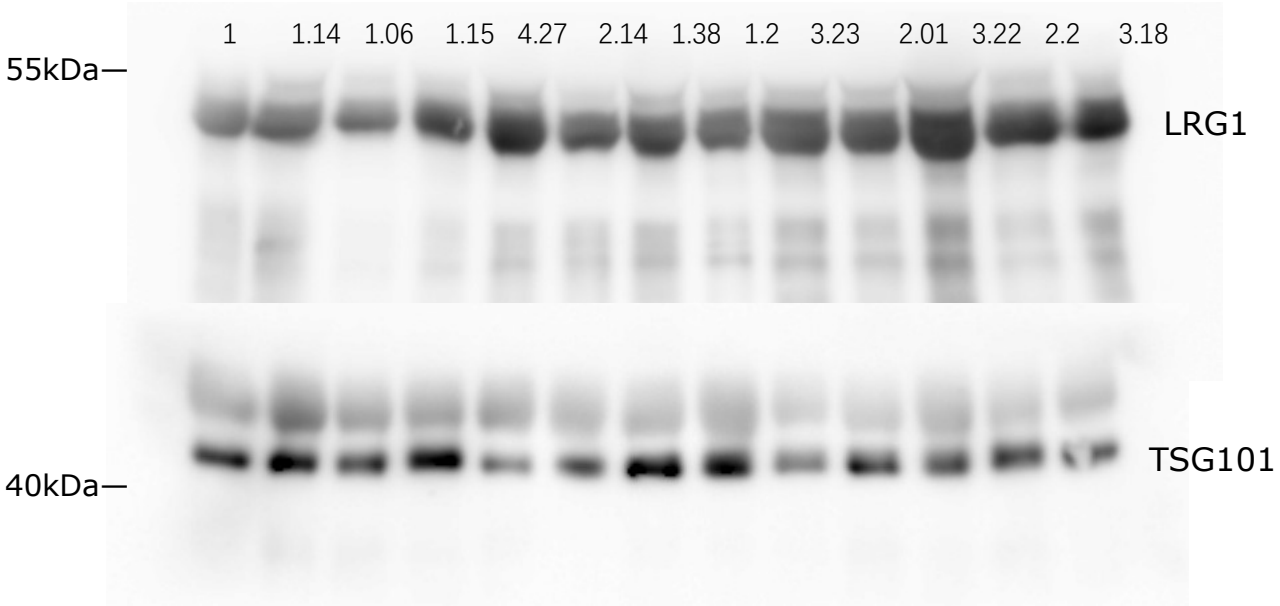
1
1.14
1.06
1.15
4.27
2.14
1.38
1.2
3.23
2.01
3.22
2.2
3.18
55kDa—
LRG1
40kDa—
TSG101

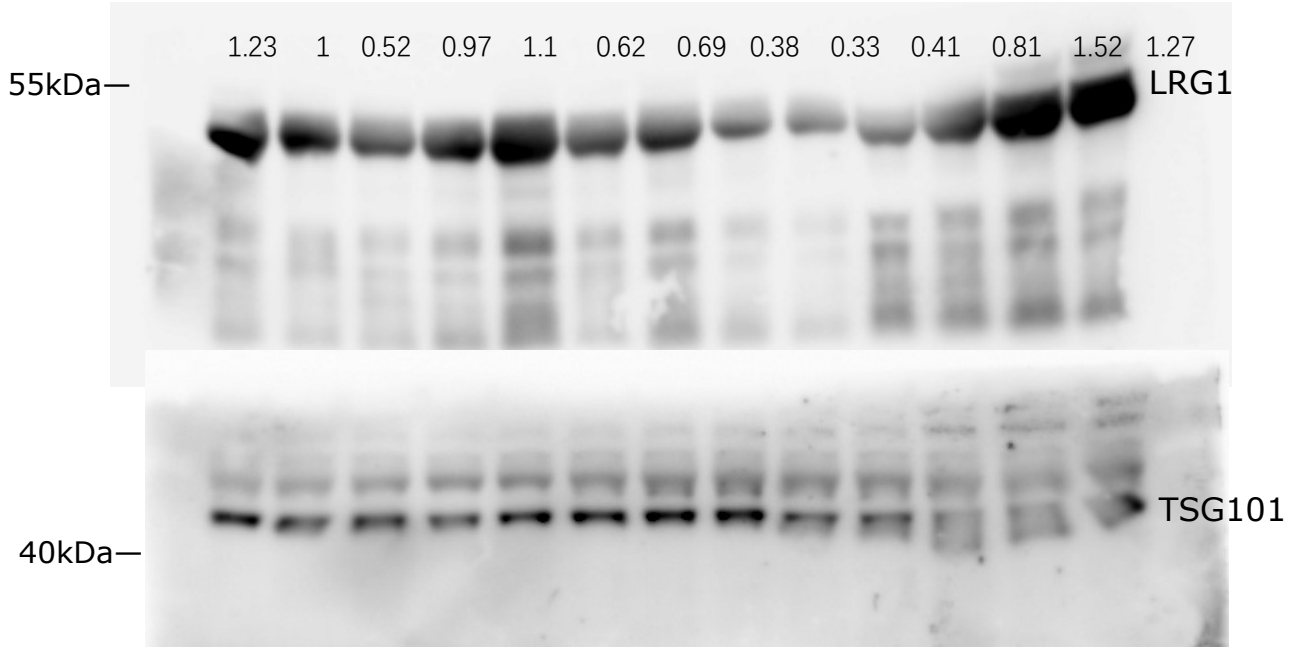
1.23
1
0.52
0.97
1.1
0.62
0.69
0.38
0.33
0.41
0.81
1.52
1.27
55kDa—
LRG1
40kDa—
TSG101

**Extended Data Fig.1b**

Young female mice

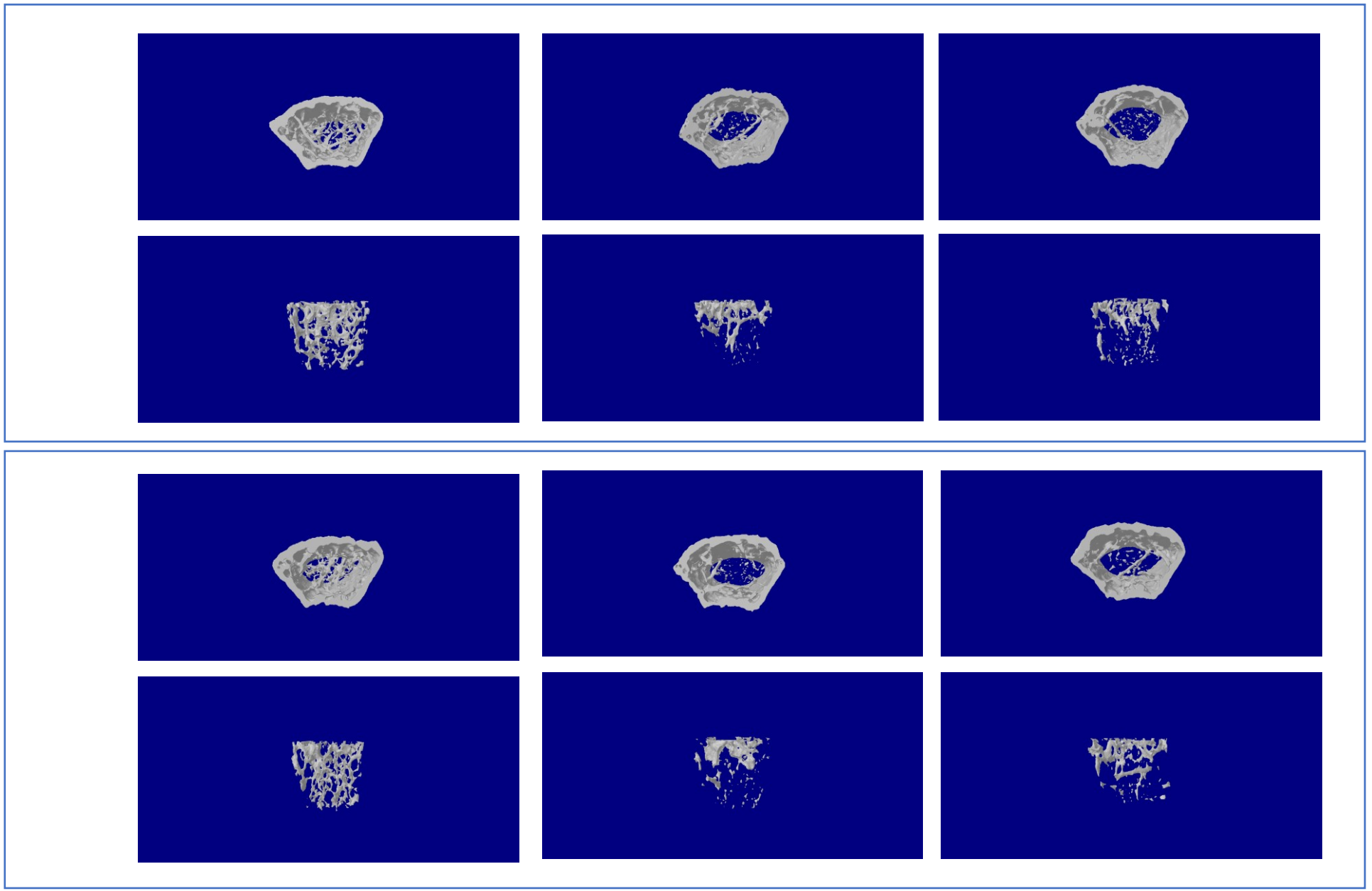

**Extended Data Fig.1e**

Young male mice-Loxp

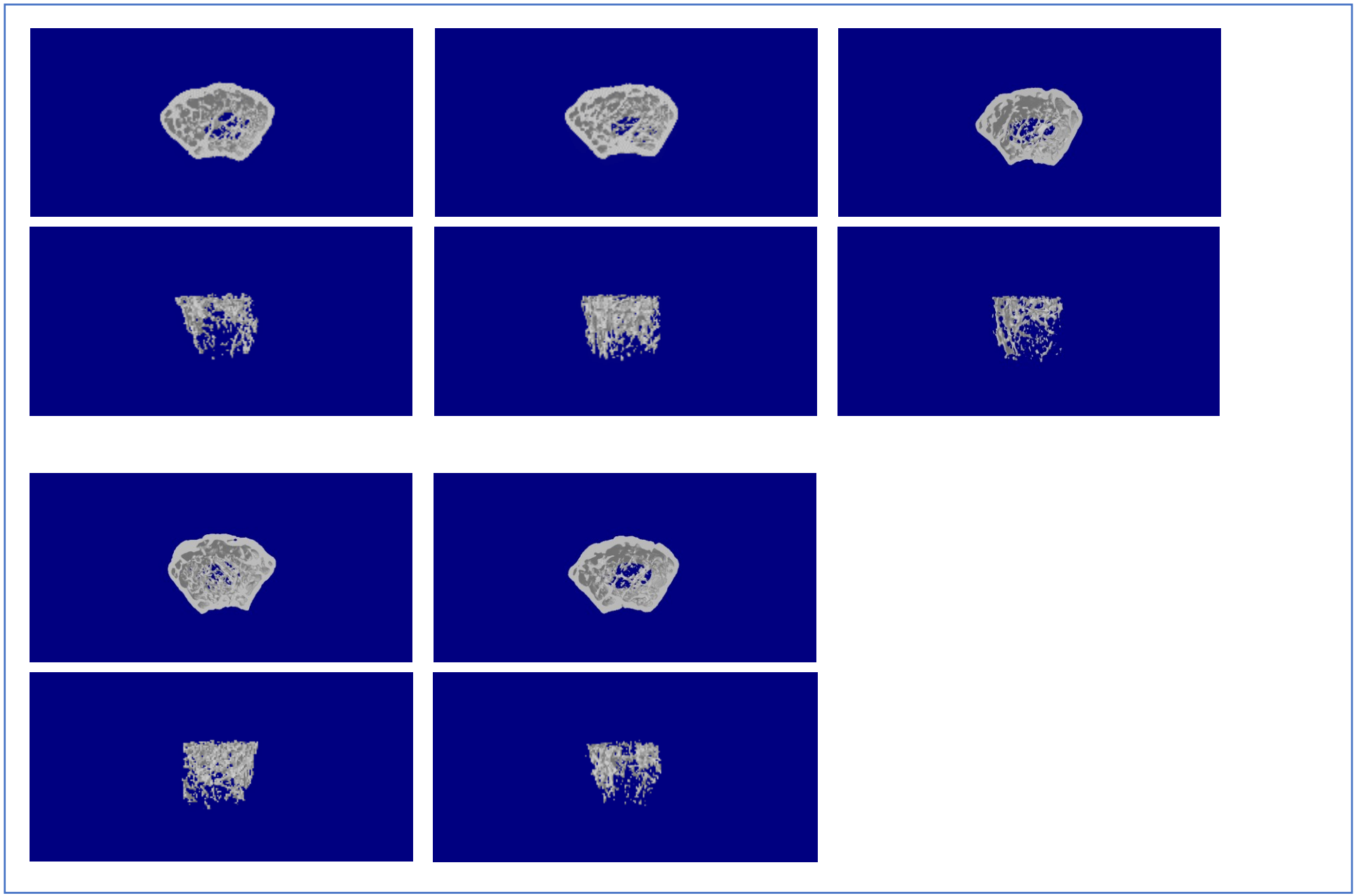

**Extended Data Fig.1e**

Young male mice-SIRT2-KO$^{hep}$

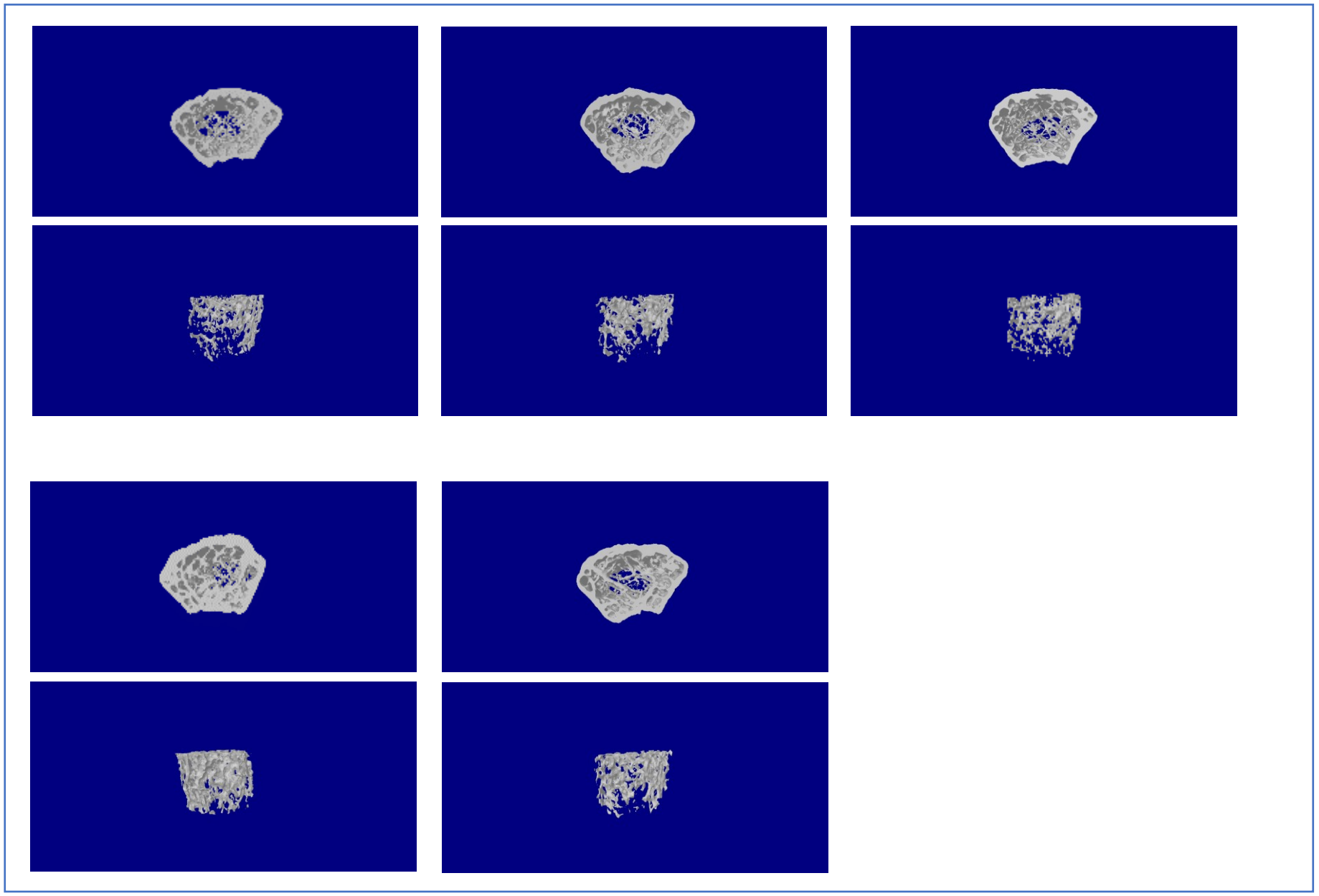

**Extended Data Fig.1i** H&E staining on paraffin-embedded femur sections in aged mice

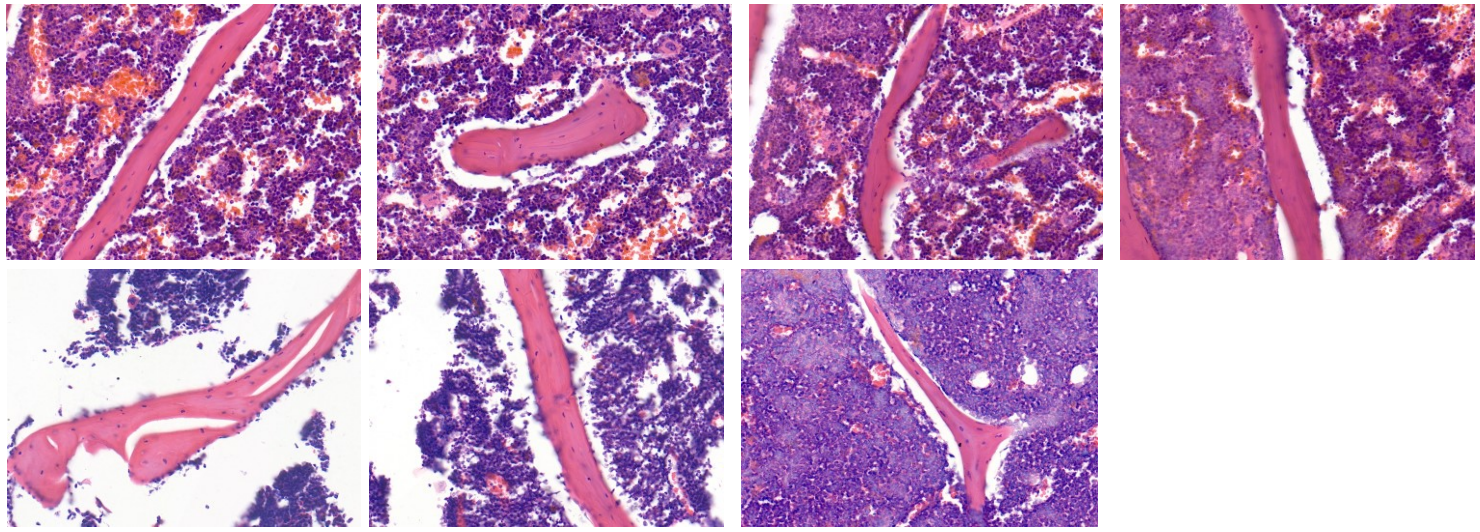

aged female mice
-Loxp

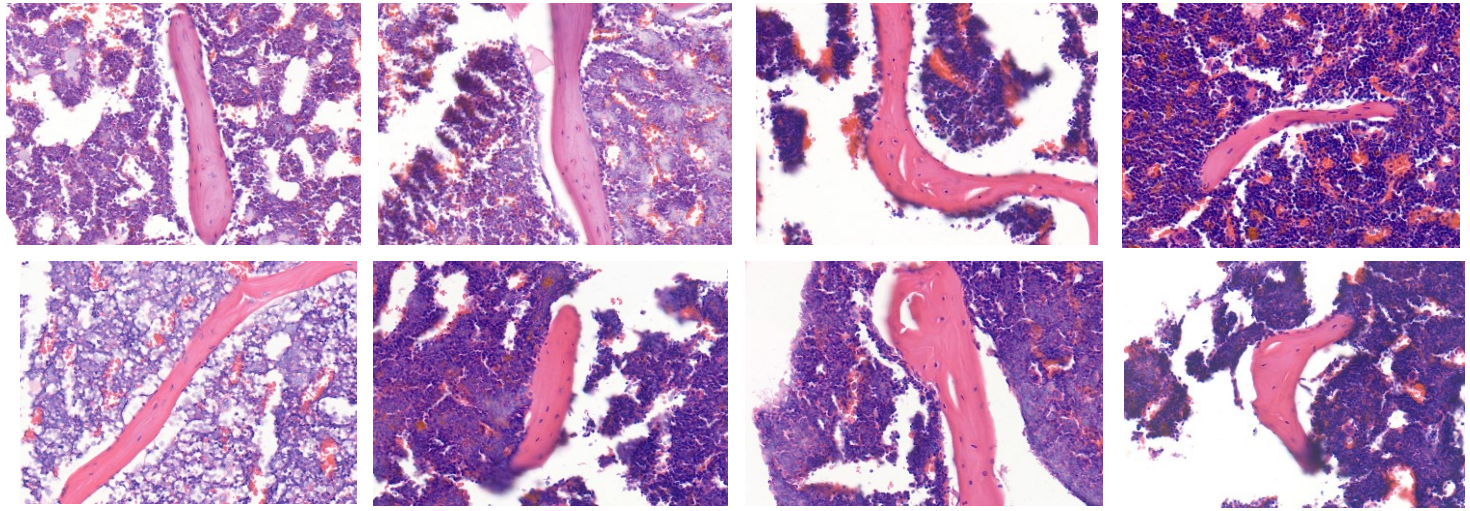

Aged female mice
-SIRT2-KO$^{hep}$

**Extended Data Fig.1m** H&E staining on paraffin-embedded femur sections in aged mice

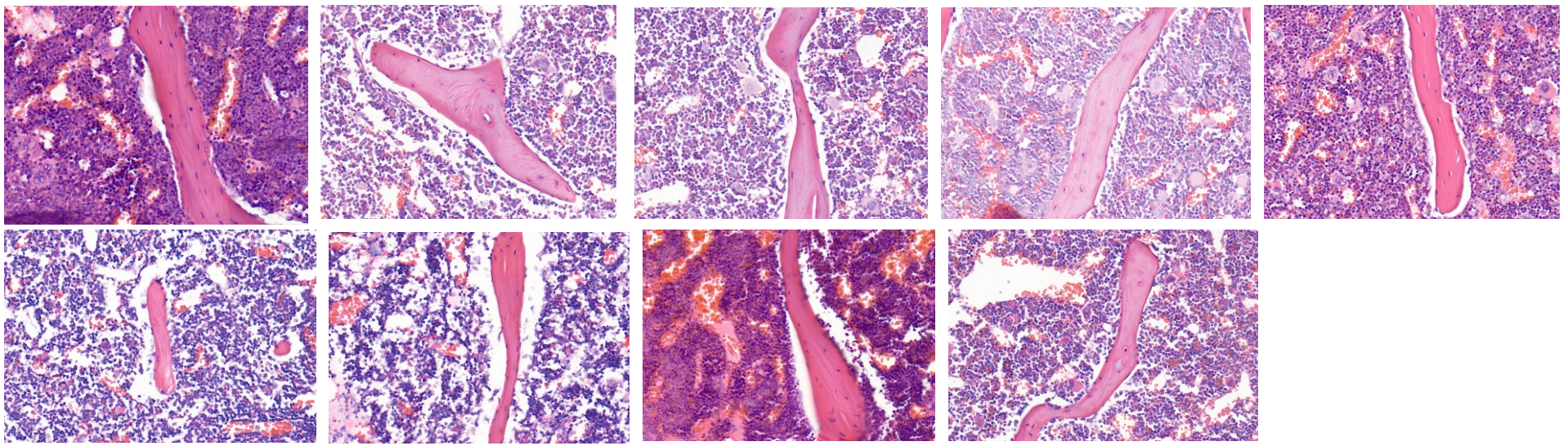

aged male mice
-Loxp

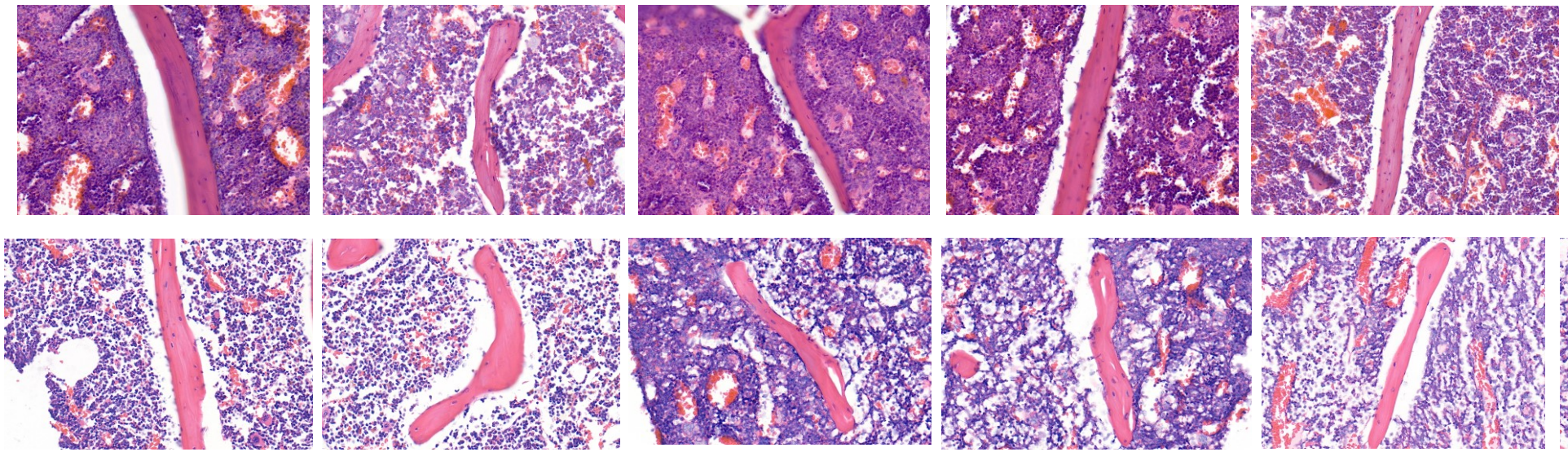

Aged male mice
-SIRT2-KO$^{hep}$

**Extended data fig.2a** ALP and ARS staining after osteogenesis from BM-MSCs treated with plasma

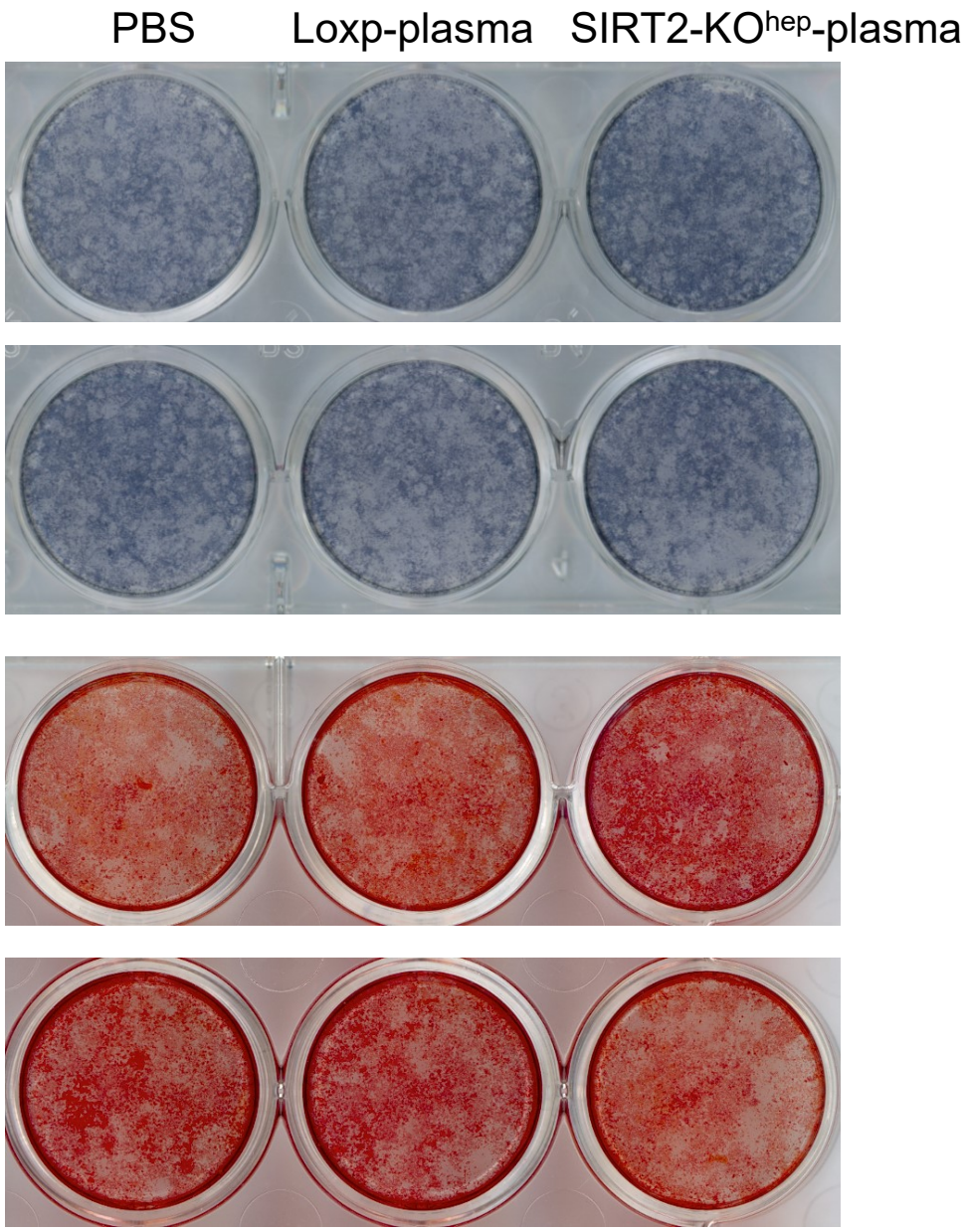

**Extended data Fig.4a** TRAP staining images of osteoclasts treated with the sEVs derived from AML12 hepatocytes

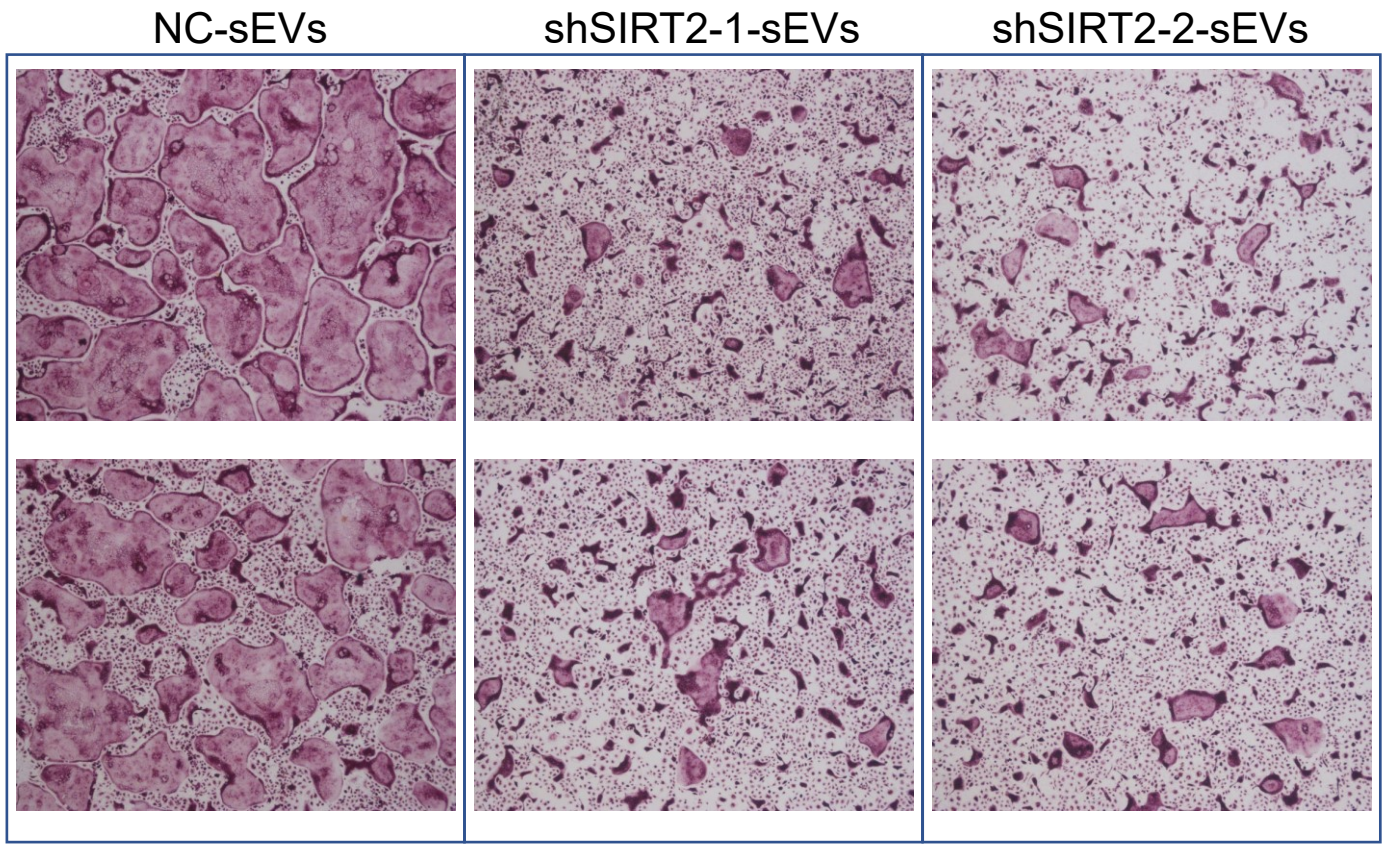

**Extended Data Fig.6a** TRAP staining on paraffin-embedded femur sections in young mice

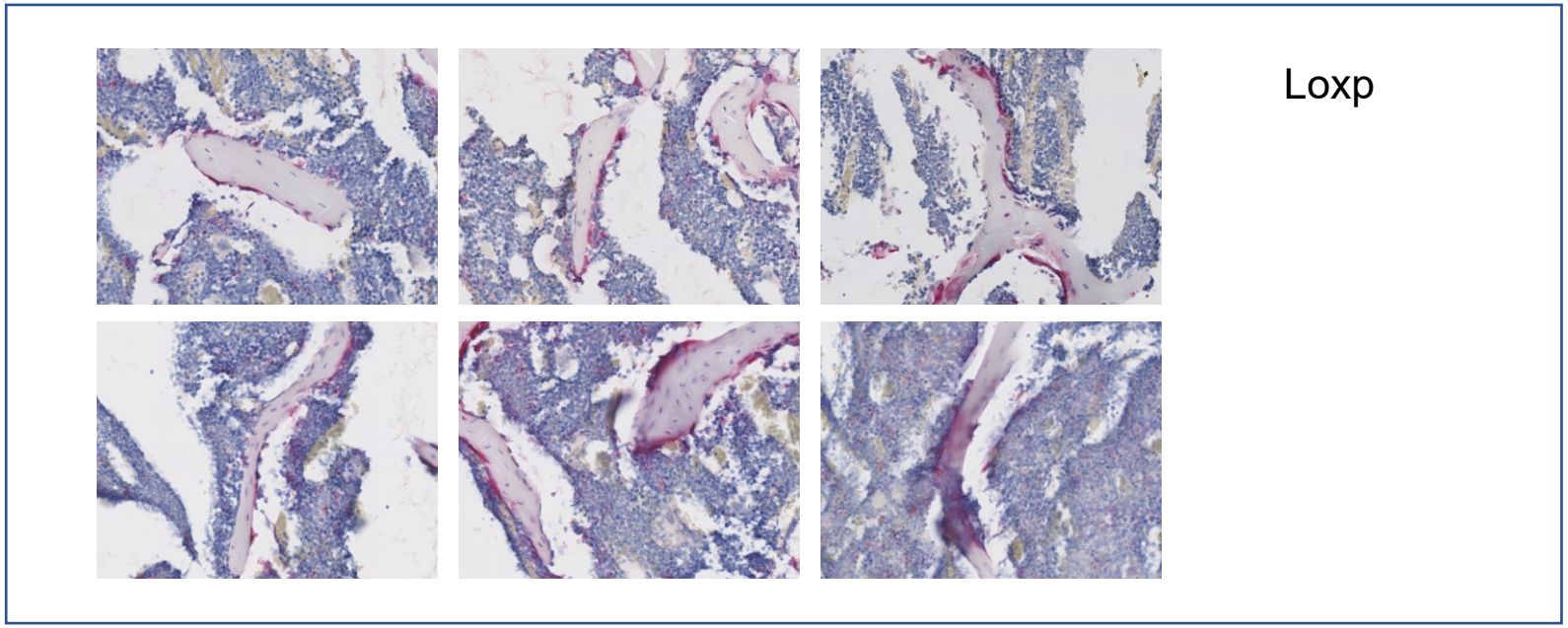


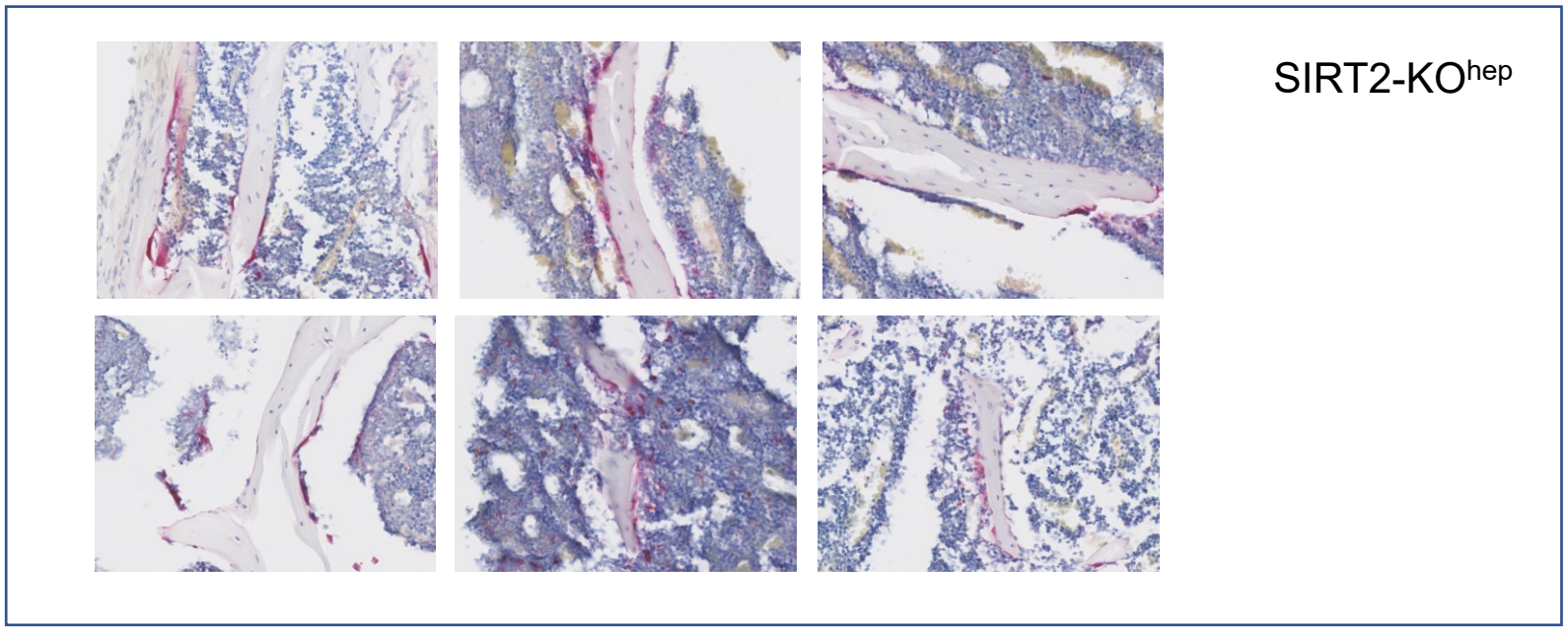

**Extended Data Fig.6c** immunofluorescence images of murine femurs in young mice

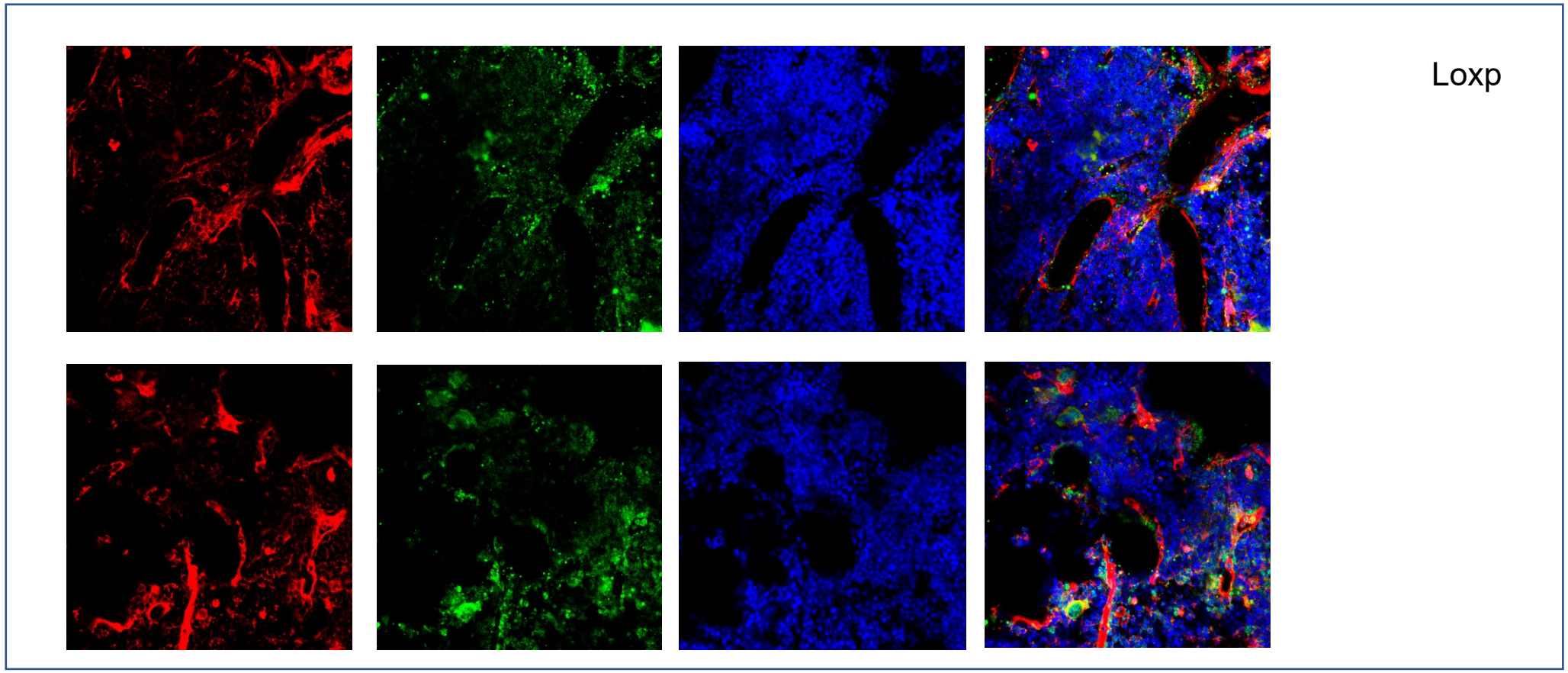

**Extended Data Fig.6c** immunofluorescence images of murine femurs in young mice

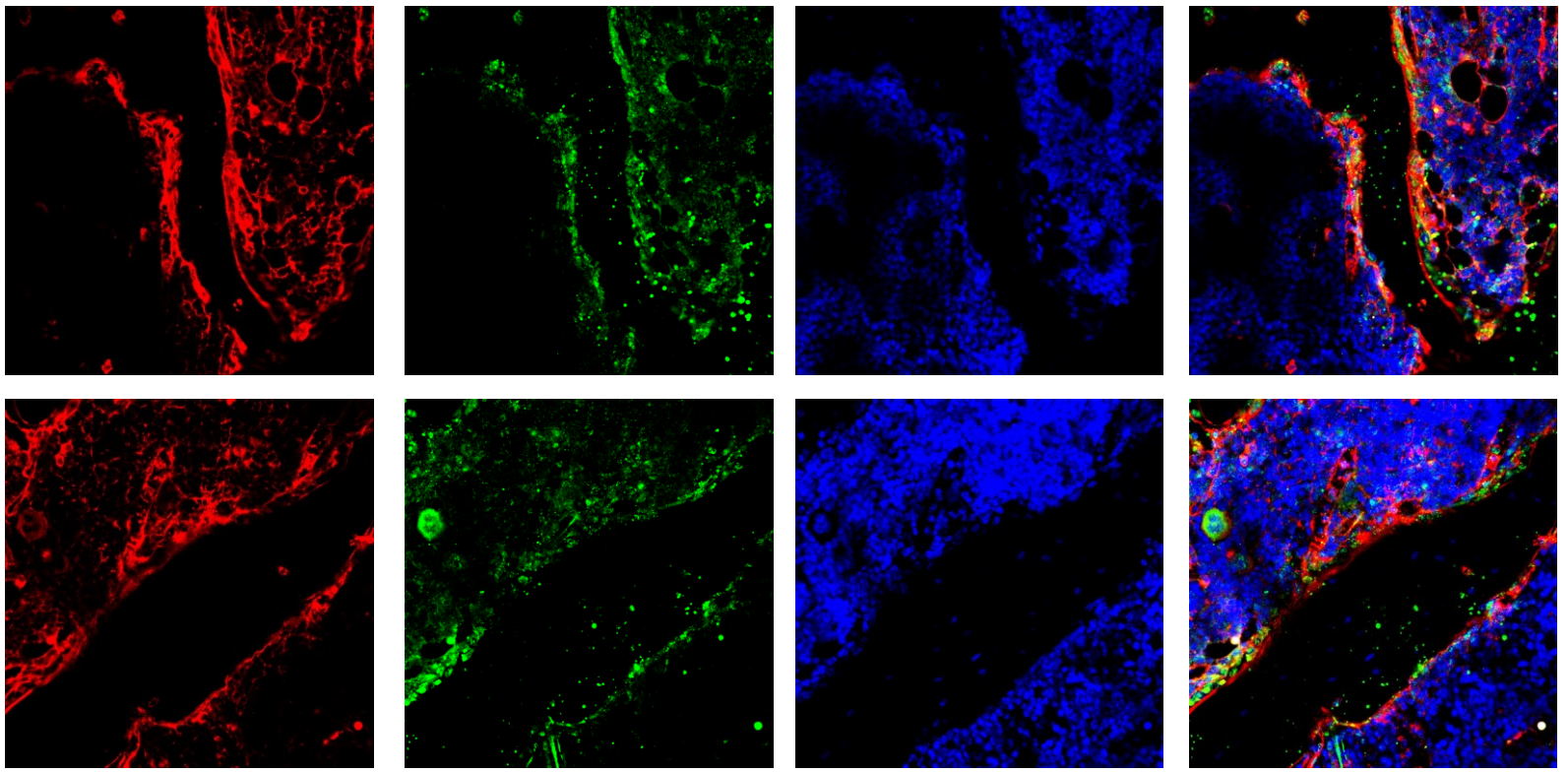

SIRT2-KO$^{hep}$

**Extended Data Fig.7d** IHC detection of CD31 in the paraffin-embedded bone section of distal femur of aged mice

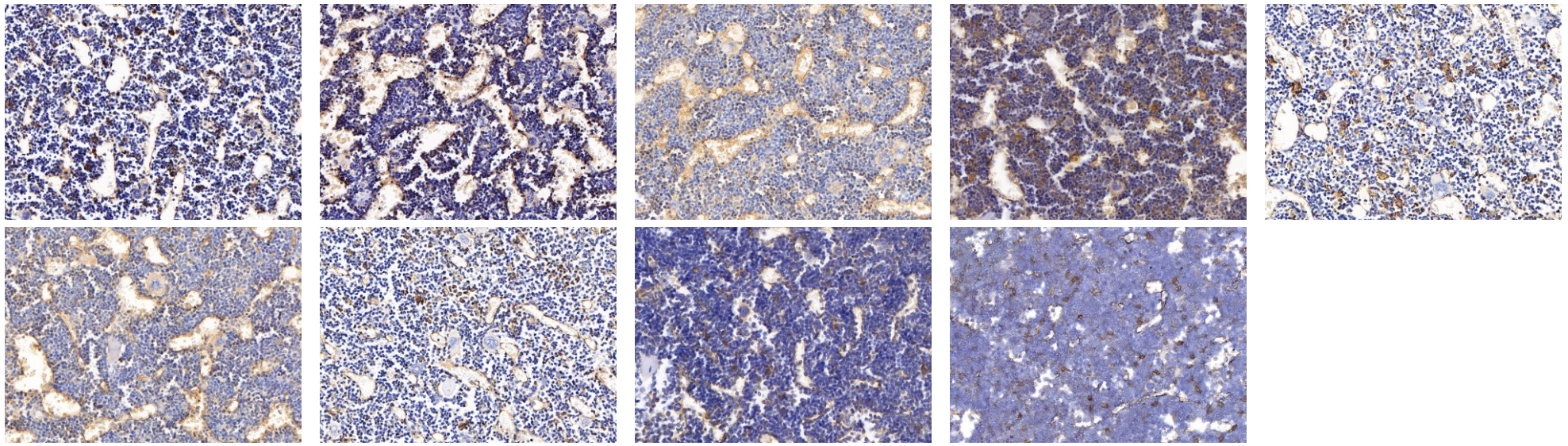


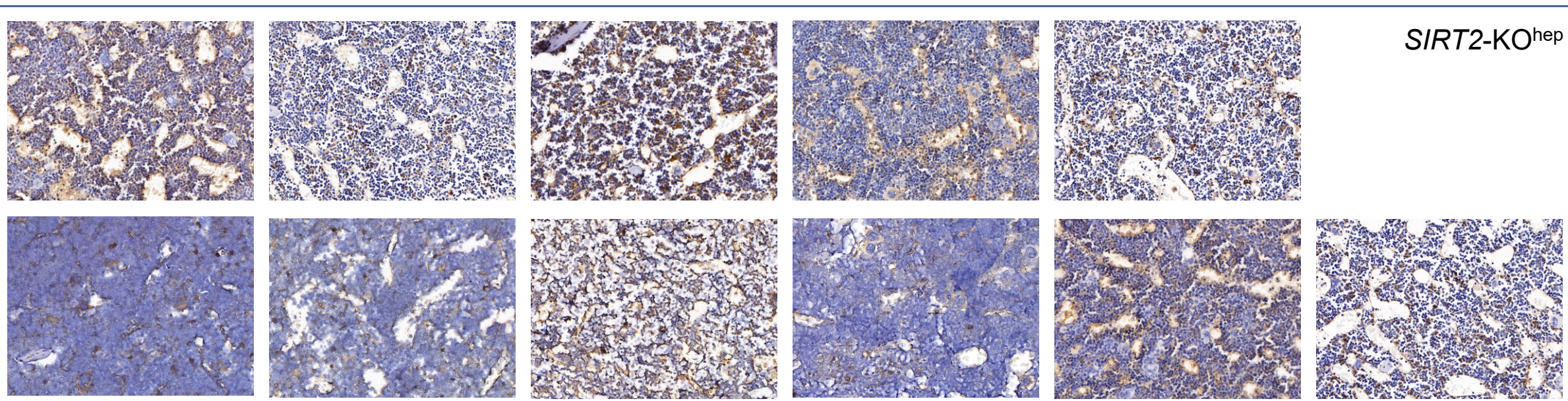

**Extended data fig.8a** TRAP staining images of BMDMs treated with RANKL and AGK2

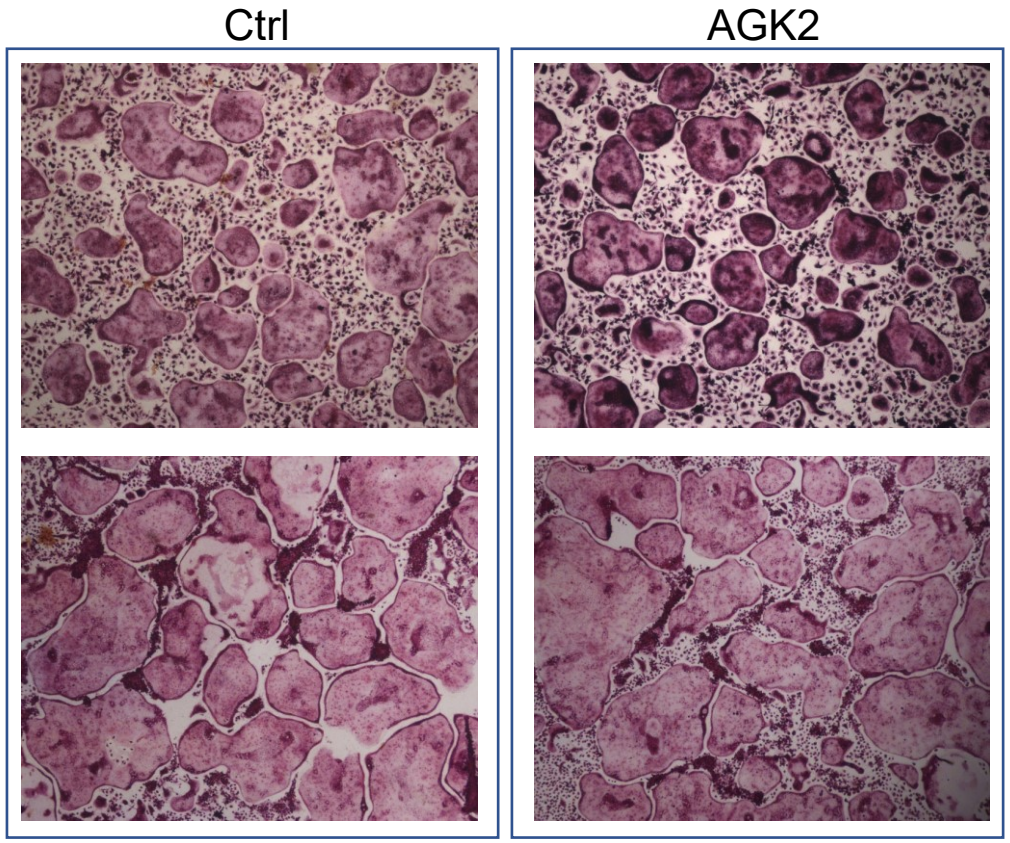

**Extended data fig.9e**

## aged female mice loxp

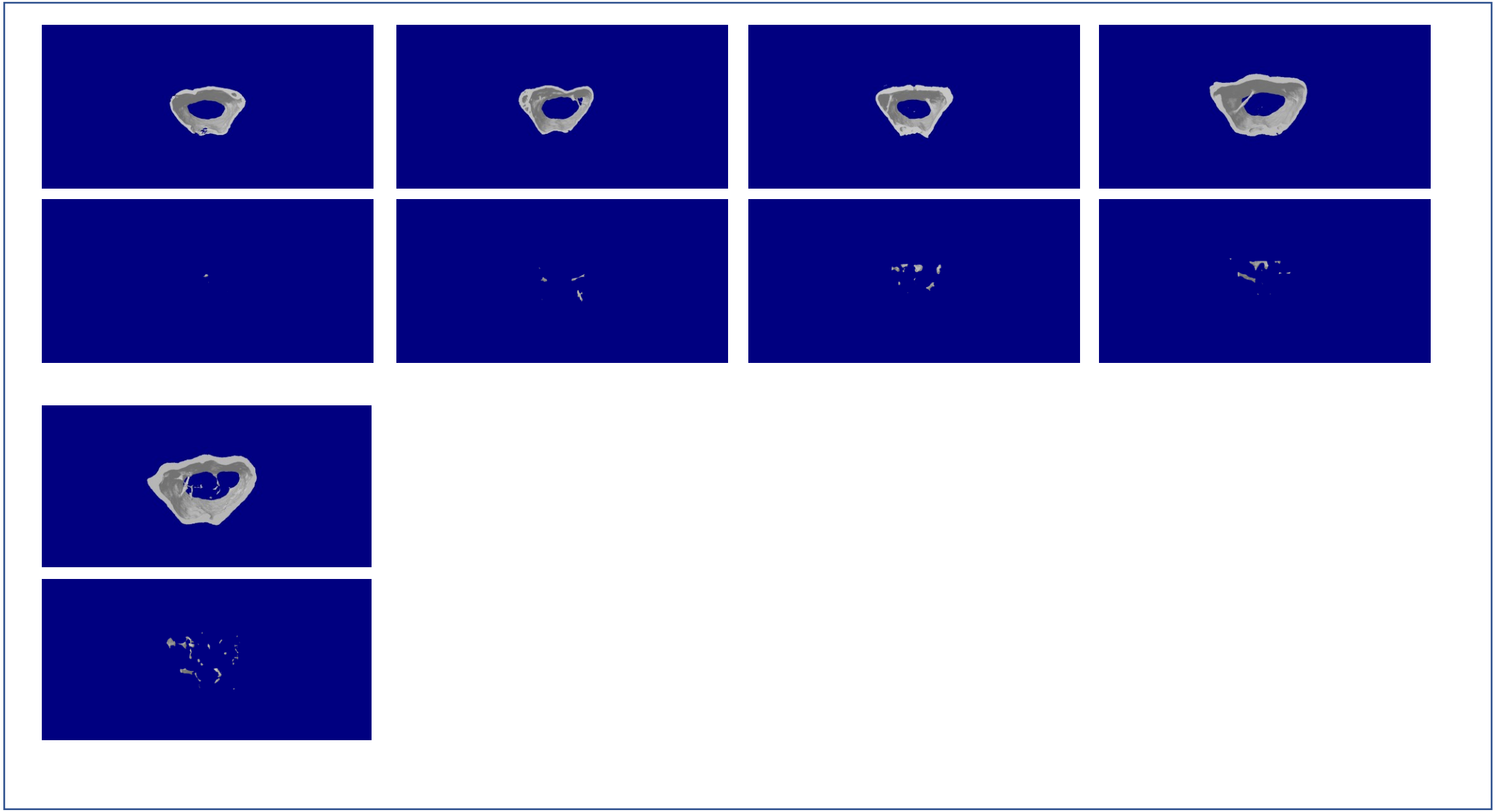

**Extended data fig.9e**

**aged female mice SIRT2-KO$^{lyz}$**

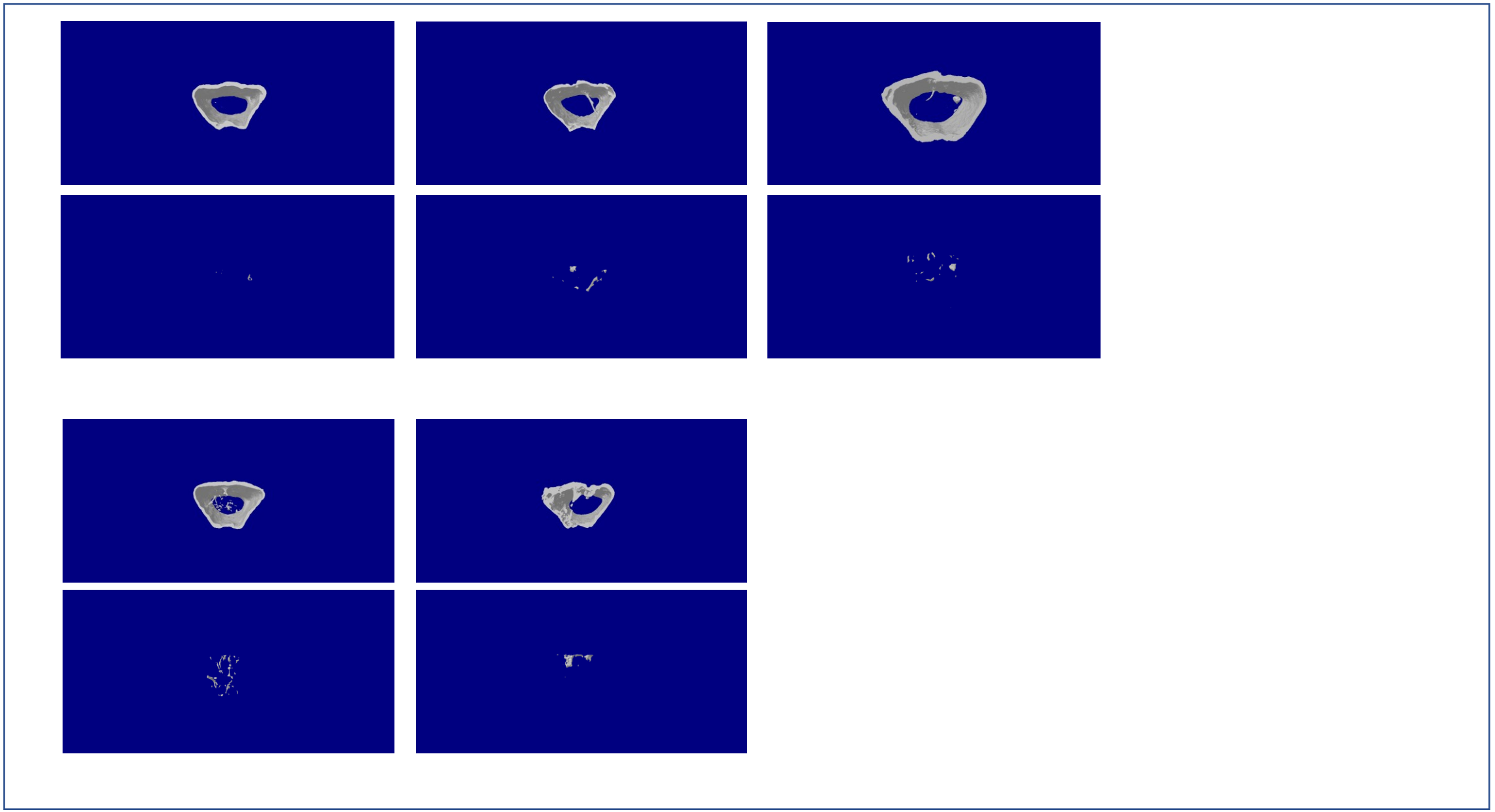

**Extended data fig.9g**

## aged male mice loxp

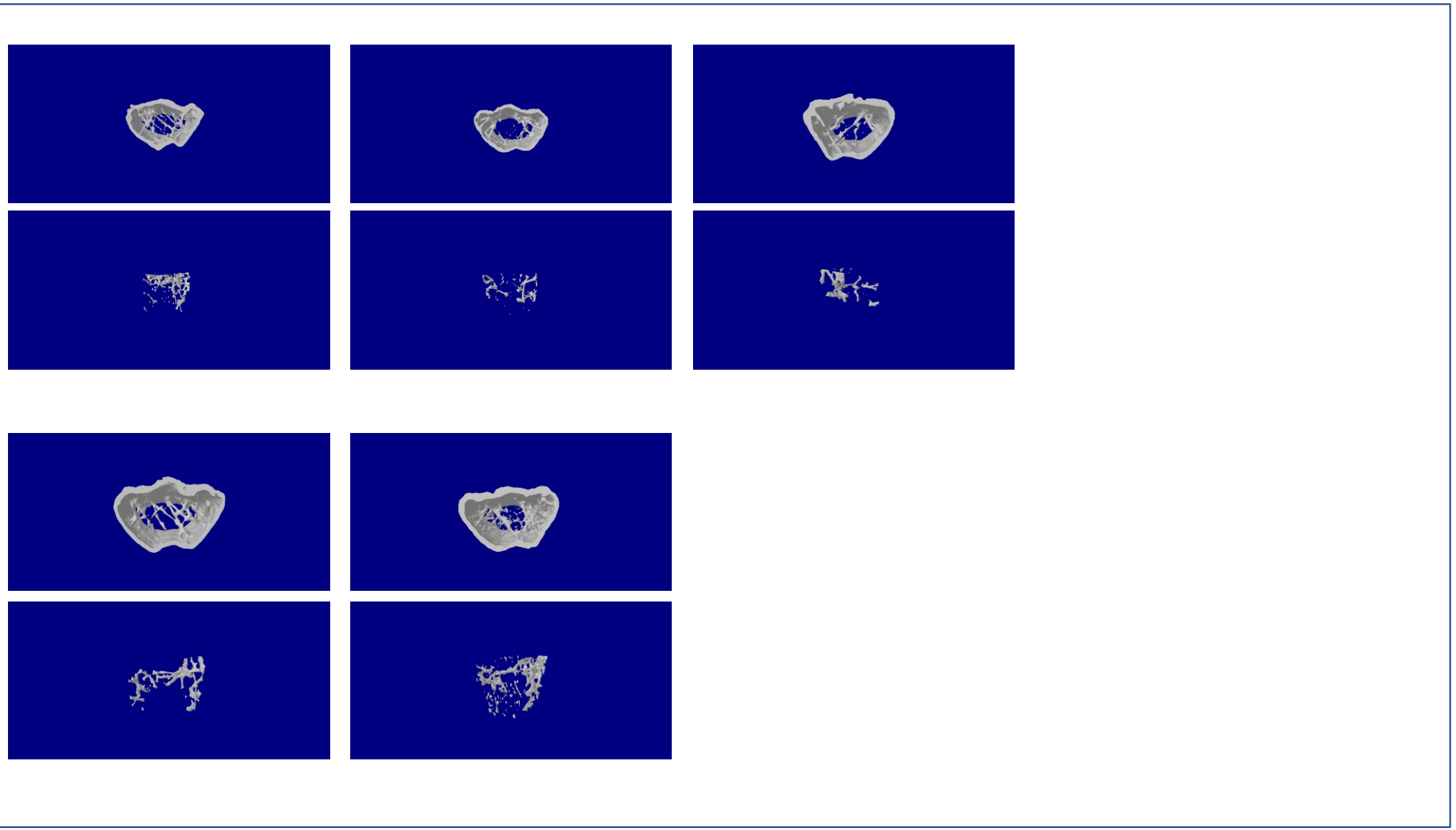

**Extended data fig.9g**

**aged male mice SIRT2-KOlyz**

**Extended data fig.9i**

## OVX loxp

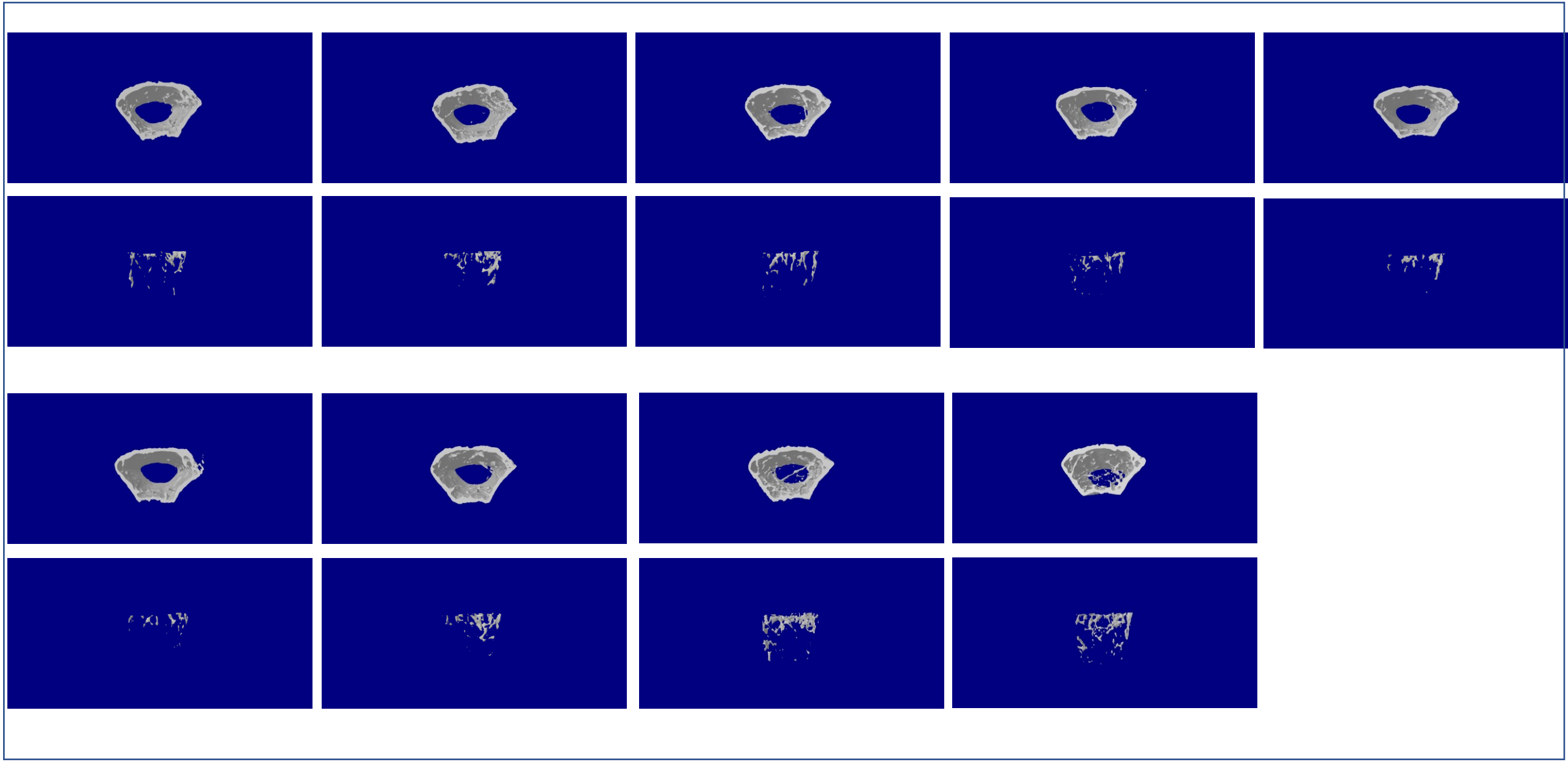

**Extended data fig.9i**

## OVX SIRT2-KOlyz

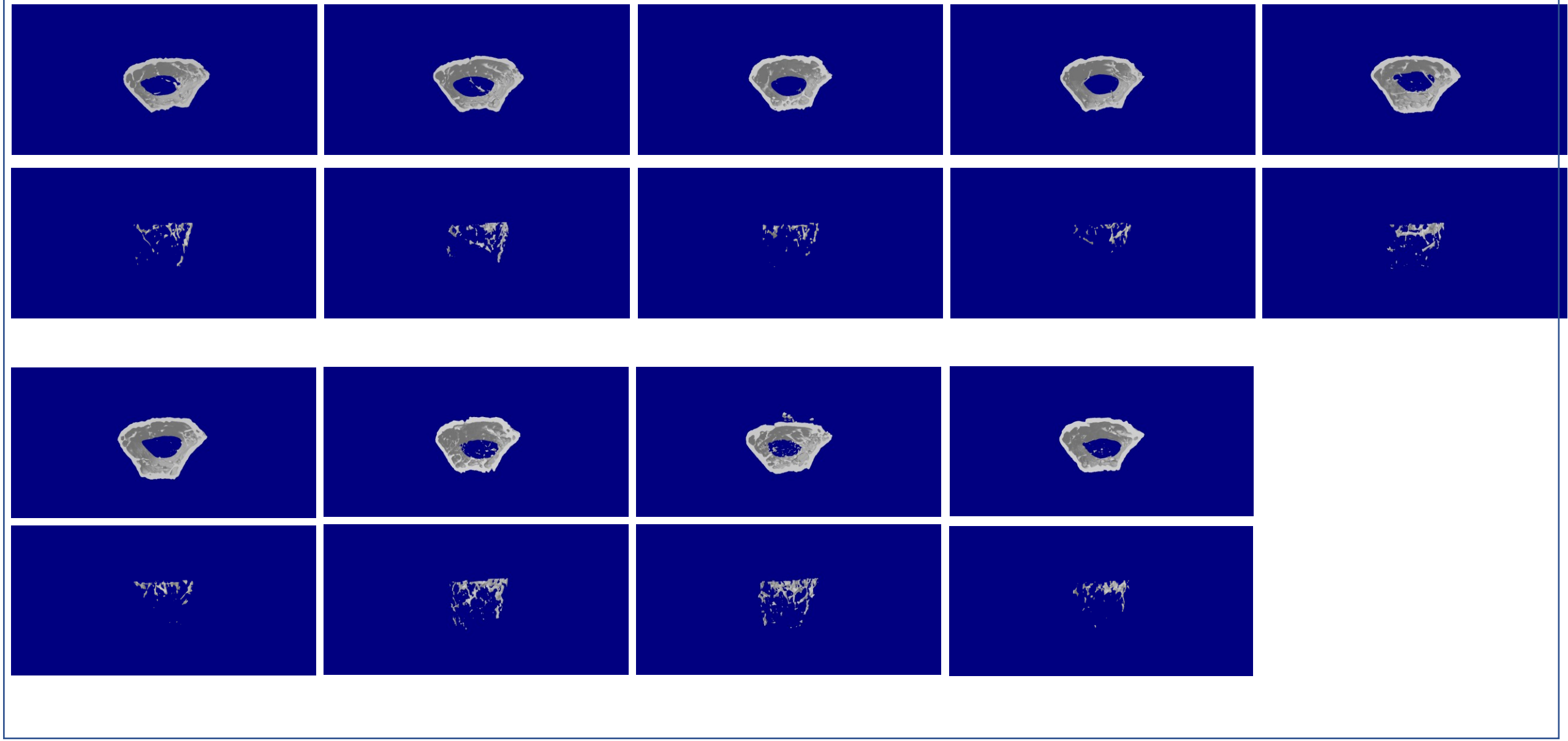

**Extended data fig.9k** BMDMs were isolated from LoxP and SIRT2-KOlyz mice and cultured with RANKL to generate osteoclasts.

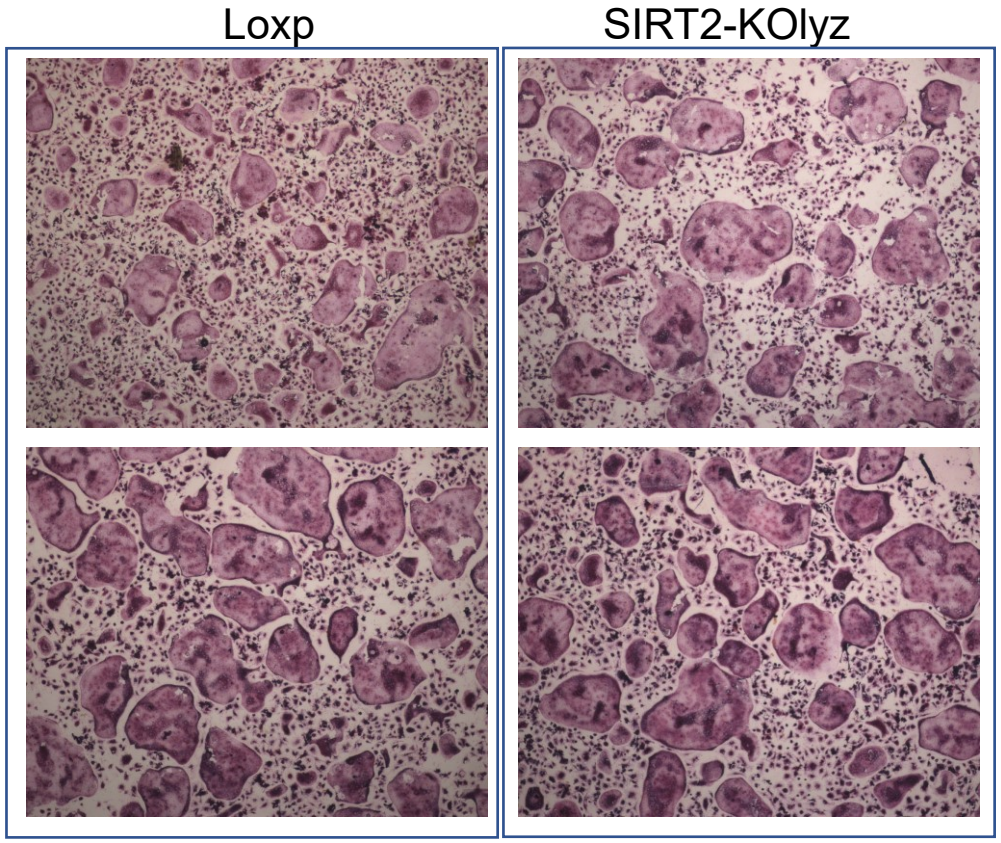

**Extended data fig.9n** BMDMs were isolated from LoxP and SIRT2-KOlyz mice and cultured with RANKL to generate osteoclasts.

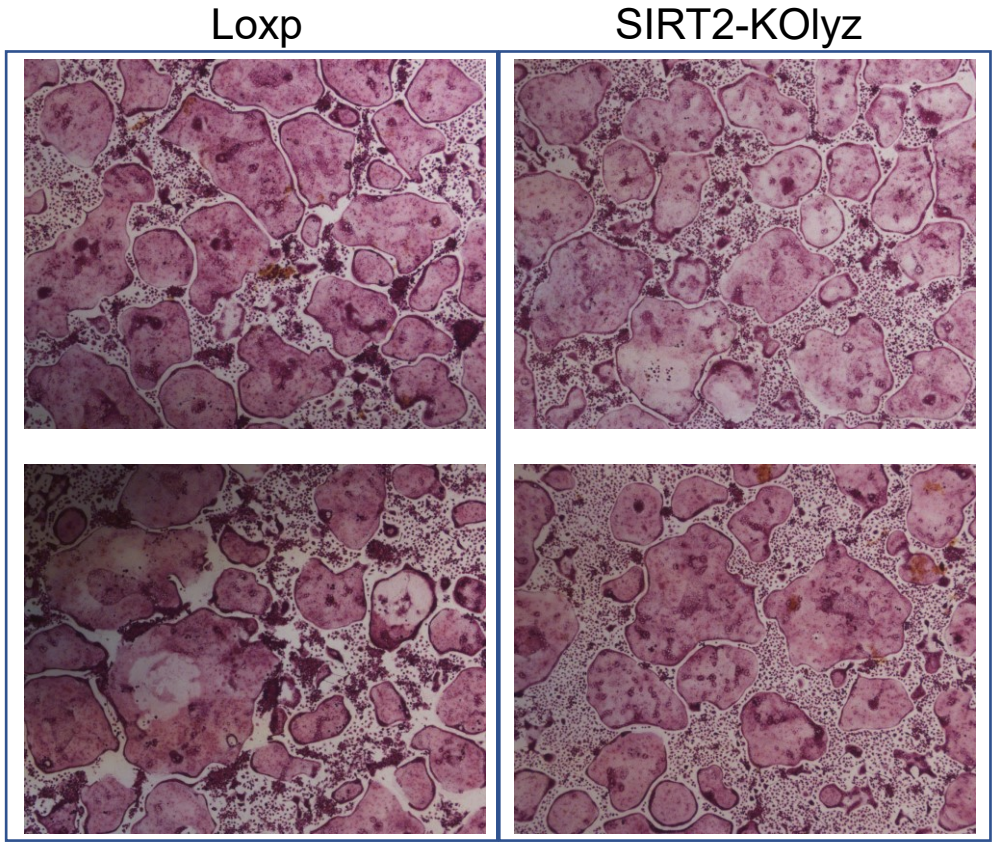

**Extended data fig.10** TRAP staining images of human PBMCs cultured with RANKL and sEVs from HepG2 cells treated with control or AGK2